Transfer and Development Lengths of Fully Bonded ½-Inch Prestressing Strand in Standard AASHTO Type I Pretensioned High Performance Lightweight Concrete (HPLC) Beams

by

Robert Thomas Kolozs, B.S.E

Thesis

Presented to the Faculty of the Graduate School of

The University of Texas at Austin

in Partial Fulfillment

of the Requirements

for the Degree of

Master of Science in Engineering

The University of Texas at Austin

May 2000

Transfer and Development Lengths of Fully Bonded ½-Inch Prestressing Strand in Standard AASHTO Type I Pretensioned High Performance Lightweight Concrete (HPLC) Beams

Approved by
Supervising Committee:

Ned H. Burns, Supervisor

John E. Breen, Supervisor

Dedication

To Erzsebet and Bertalan

… and Shadow

Acknowledgements

No project is possible without the support and financial backing of the sponsors. I would like to thank the Texas Department of Transportation for funding this project and Tom Rummel and Mary Lou Ralls for their support.

The extensive knowledge and insight provided by the co-supervisors for this research project was invaluable in the completion of this thesis. Dr. Ned H. Burns continually provided support in the decision-making processes of all aspects of the work: from manufacture, to testing, to writing of this thesis. Dr. John E. Breen was helpful in injecting his unique brand of insight into the different aspects of this project. I am especially thankful to both professors for their timeliness and effort in helping me prepare this thesis.

I owe my project partner some mention, whether it be thanks or something else I not quite sure. Heffington, we were doomed from the start, but ended up causing enough mayhem in the lab for all the graduate students combined. I guess I'll thank him for letting me embarrass him for my own amusement. -ℛ

The completion of this thesis would not have been possible without the help of my fellow graduate students at FSEL. Despite payment of only donuts and coffee, they worked hours and hours at a blistering hot prestressing plant. I am also grateful to all those who helped cast decks. A message to Thatcher: I hope you continue the *tradition of excellence* that Heffington and I have set before you.

Everyone else not mentioned, I'm out of room – Thanks.

May 5, 2000

Abstract

Transfer and Development Lengths of Fully Bonded ½-in Diameter Prestressing Strand in Standard AASHTO Type I High Performance Lightweight Concrete (HPLC) Beams

Robert Thomas Kolozs, M.S.E.

The University of Texas at Austin, 2000

Supervisors: Ned H. Burns and John E. Breen

The use of high performance lightweight concrete in Texas highway bridges could lead to a significant reduction in the dead load. Compressive strengths of 6,000 – 8,000 psi (41.4 – 55.2 MPa) can be achieved while maintaining a unit weight of 120 lb/ft^3 (18.9 kN/m^3). The behavior of ½-in (12.7-mm) prestressing strand in Standard AASHTO Type I beams is necessary to determine the feasibility of these HPLC bridges. Specimens were tested for transfer length, which indicated that ACI and AASHTO equations for the transfer length were not conservative for the HPLC. Development length testing indicated that the ACI and AASHTO equations for this value are conservative for the HPLC. The flexural behavior of the composite beams was similar to normal weight concrete beams tested.

Table of Contents

List of Tables

List of Figures

Chapter 1: Introduction

1.1 BACKGROUND

The use of lightweight aggregate concrete in the state of Texas is limited. The main use of structural lightweight concrete in Texas has been in pretensioned prestressed concrete double-T parking garage beams. This widespread application has proven the effectiveness of the material and the economy of its use. Another use has been in bridge deck slabs [16]. Part of the reason for the limited use of lightweight concrete is that less is known about the properties and behavior of the material than for normal weight concrete. Proper use, knowledge, and experience with the material are necessary for an effective design. Despite this, the state of California and the country of Norway have found success in the use of lightweight concrete in other structural applications including bridges [12,24,31,37,42]. The Texas Department of Transportation (TxDOT) is interested in expanding the application of lightweight concrete in Texas to prestressed concrete bridges.

The typical Texas bridge is constructed of normal weight pretensioned prestressed concrete girders with AASHTO Standard cross sections and a composite normal weight concrete deck, as shown in Figure 1.1. This system has proved extremely cost effective in Texas where the average cost of a bridge of this type is approximately 30 US$/sf [11]. Another possible application with this type of bridge system is the use of precast pretensioned concrete deck panels, which are approximately half the thickness of the composite deck. These panels

span the distance between beams and effectively remove the need for much of the typical formwork added to the precast prestressed girders for placing the deck concrete. This has led to better time efficiency in the construction of bridges, which also reduces cost.

Figure 1.1: Typical AASHTO Girder Bridge

Some or all of these bridge components can be produced in lightweight concrete with a unit weight at or below 120 lb/ft^3 (18.9 kN/m^3). Lightweight concrete mixes can be designed to yield compressive strengths between 6,000 – 10,000 psi (41.4 – 69.0 MPa), which is usually referred to a high strength lightweight concrete (HSLC) [47]. Fly ash has been used to augment the durability of HSLC and this is usually referred to as high performance lightweight concrete (HPLC) [22]. The strengths for HPLC equal or exceed the strength that is common in most normal weight prestressed concrete bridges, 6,000 psi (41.4 MPa). Therefore, compressive strength is not a consideration in the use of HPLC in bridges.

The main reason for using HPLC in the design of structural components in a typical prestressed concrete bridge is the reduction in dead load. Almost all the

dead load for a bridge comes from the weight of the beams, deck panels, and deck slab. Use of HPLC in these components, while maintaining the same compressive strength as normal weight concrete and lowering the weight of the concrete from 150 lb/ft^3 (23.6 kN/m^3) to 120 lb/ft^3 (18.9 kN/m^3), could lead to a significant reduction in dead load [44]. With the dead load reduced and the load capacity of the girder relatively unchanged, more of the load capacity of the girder can be used to carry live load. These factors could lead longer spans or reduce the number of girders needed in a bridge [47].

1.2 OBJECTIVES

TxDOT commissioned this research project to examine the feasibility of using HPLC in Texas bridges. Specifically, TxDOT was interested in the development of two HPLC mix designs and the performance of ½-in (12.7-mm) prestressing strands in Standard AASHTO Type I pretensioned HPLC beams. This required the exploration of several factors before a final judgment could be made on the effectiveness of the use of HPLC in this application. Therefore, this research project encompasses several different components. These components include:

Task 1) Literature Search

Task 2) Past Use of Lightweight Concrete Mix Designs

Task 3) Development of Lightweight Concrete Mix Designs

Task 4) Materials Research and Testing

Task 5) Full-Scale Testing of Type A Beams with Decks

Task 6) Prestress Loss and Evaluation of Beam Behavior, Handling of Beams, and Final Report

The overall objective of the study is to determine whether lightweight concrete is a feasible material for use in Texas highway bridges. This will be accomplished by completion of all the tasks in the research project.

1.3 SCOPE

The scope of this thesis includes Tasks 1 and 5 as listed above. A literature search was performed on topics relating to the past use of lightweight concrete in structural applications. Other topics researched included transfer and development length of prestressing strand in concrete, flexural testing of lightweight prestressed concrete beams, and the use of prestressed deck panels in bridges. In addition to the literature search, the manufacture and specifications of the beams and the deck panels is also discussed. Transfer length and development length instrumentation and testing are also included in this thesis. This included full scale testing of AASHTO Type I precast pretensioned prestressed concrete beams with composite slabs. This thesis does not include design recommendations for design because all the testing for this TxDOT project is not included in the scope of this thesis.

All the elements of this research project will be synthesized in the final report where recommendations on whether HPLC is feasible for pretensioned beams and components in Texas bridges will be made.

1.4 ORGANIZATION

This thesis is organized into 6 chapters. The first chapter gives a basic overview of the objectives of the thesis. The second chapter presents background information regarding transfer and development length and gives a literature review of the material relevant to the thesis. The third chapter includes details of the design basis for the HPLC beams and panels. A summary of the material properties of the concretes used for this project is also included. Manufacture of the components in a commercial casting yard is also discussed. The fourth chapter discusses transfer length and gives the results of testing for this measurable quantity using two methods: concrete strain measurement and strand draw-in. Full-scale load testing for determining the development length of the strand is presented in Chapter 5. Discussion of each chapter's test results is included in that chapter to give a concise package of all the information obtained for a topic. The last chapter gives summary and conclusions for the topics discussed in this thesis. The appendices follow and give all pertinent data obtained in this portion of the research study.

1.5 NOTATION

The notation used in this thesis is consistent throughout the work. The symbols used in formulas are not necessarily the same as those used in all the literature, since the symbols tend to vary between publications. When a new symbol is used in the text, it will be defined in that section. If that symbol is used again it may not necessarily be redefined. For reference, all notation used throughout this thesis is defined in Appendix A.

The mixes developed for this research project are technically labeled high performance lightweight concrete (HPLC) due to their combination of strength and durability. At times, the general term "lightweight concrete" is used in this thesis. When this term is used in reference to the lightweight concrete used in this research project, it should be taken to mean HPLC.

The primary units used throughout this thesis are U.S. Customary units. Metric conversions are given along with the U.S. units in parenthesis. Conversions from U.S. Customary to Metric units are given in Appendix B.

Chapter 2: Background and Literature Review

2.1 INTRODUCTION

This chapter includes background information relating to lightweight concrete and the bond characteristics of prestressing strand. A review of the pertinent literature associated with the topics discussed in this thesis is also presented.

2.2 BACKGROUND

This project dealt with two main topics: the structural use of high performance lightweight concrete (HPLC) in bridge girders and more specifically, the bond behavior of prestressing strand in HPLC. There has been extensive research performed on both these topics but a complete review of the literature on these topics is not given in detail. Many excellent sources are sited that will lead the reader to extensive information about structurally relevant properties of lightweight concrete and bond behavior. These references can be reviewed if more information is required than is summarized here.

2.2.1 Lightweight Concrete

A discussion of the properties and behavior of high performance lightweight concrete is not appropriate for the scope of this thesis. The theory and background research relating to this topic for this project can be found in a thesis prepared by Heffington [22].

2.2.2 Bond Behavior

When a pretensioned concrete beam is fabricated without the aid of anchorages, the forces that develop the compressive stress in the concrete depend completely on the bond between the pretensioned strands and the concrete. These forces are also responsible for developing the ultimate tensile strength of the prestressing strand during flexural failure of the beam. A bond failure occurs when the bond forces are less than the force applied by the stand which induces slip of the prestressing strands relative to the concrete. There are three bond mechanisms that act between the concrete and strand to transfer the stress in the steel to the concrete: a) Hoyer effect, b) adhesion, and c) mechanical interlock.

The Hoyer effect is the tendency of the prestressing strand to increase in diameter as the stress in the strand decreases at release [23]. Initially, when the strand is in air and is being stressed to its initial prestress, f_{pi}, its diameter will decrease due to Poisson's ratio effect. When the strand is released from the temporary end anchorages after the concrete cast around the stressed strands has cured, the strand not contained within the concrete will increase in diameter and resume its original size. However, the strand embedded in the concrete varies from zero stress at the very outer edge of the concrete to a constant stress at a distance located along the strand inside the concrete. This constant stress is known as the effective prestress, f_{se}, and the distance at which it occurs is the transfer length, L_t. Therefore, the maximum strand increase in diameter occurs at the inner edge of the concrete, where the stress is zero. The increase in diameter then gradually decreases in diameter as the stress in the strand increases over the

transfer length. The increased diameter of the strand acts like a wedge, preventing the strand from pulling into the concrete. The concrete acts against this wedging effect, transferring the stress from the strand to the concrete. This mechanism is the Hoyer effect and is displayed in Figure 2.1. The Hoyer effect is the greatest contributing factor to the bond at release of the initial prestress compared to the other two bond mechanisms.
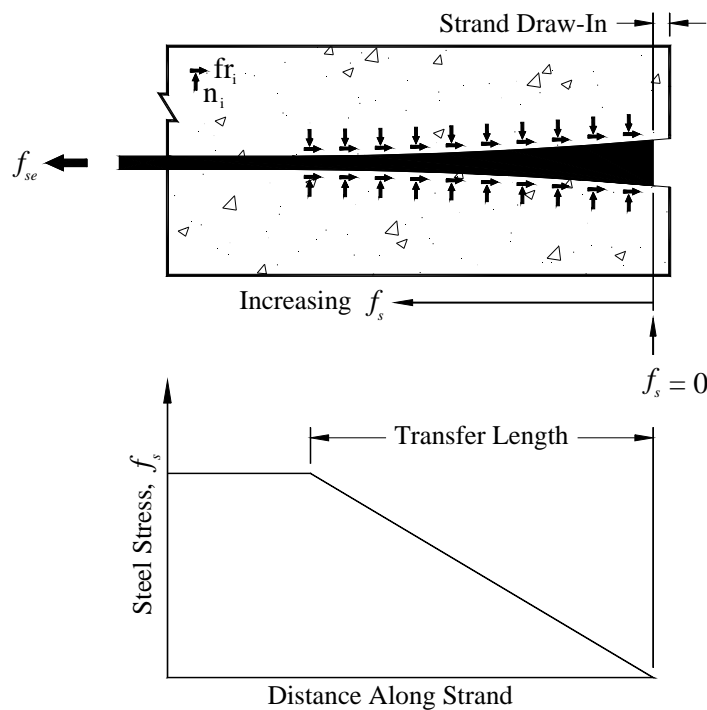
Figure 2.1: Diagram of Hoyer Effect [38]

Adhesion is another mechanism that aids in transferring the stress in the prestressing steel to the concrete. It is the chemical mechanism by which the concrete bonds to the strands [38]. This bond acts only to a certain degree. There is a point at which the bond stress is greater than the critical adhesion stress and a local bond failure between the strand and concrete occurs. Adhesion aids bond in

9

areas where slip of the strand does not occur relative to the concrete. This mechanism contributes the least in developing bond stresses in the concrete compared with Hoyer effect and mechanical interlock.

Mechanical interlock is the last mechanism by which the strand transfers stress to the concrete. This mechanism only occurs in twisted strand and is due to the tendency of the strand to want to unwind due to increased stress levels [38]. Since the concrete cast around the strand has hardened, it conforms exactly to the stressed shape of the strand. Therefore, the concrete resists the unwinding or pull-out of the strand, increasing the amount of stress that can be transferred to the concrete. Mechanical interlock provides the greatest amount of bond stress when the stress in the strand is increased beyond the transfer stresses. For example, this occurs when there is cracking of the concrete at the location of the strands, which indicates elongation and increased stress in the strands, but the strands are prevented from unwinding by the surrounding concrete.

2.2.2.1 Definitions

There are two types of bond stresses (transfer and flexural) and three types of bond lengths (transfer, flexural bond, and development) that describe the behavior of bond in prestressed concrete. The embedment length is a term that relates to the development length.

The bond stresses are responsible for developing increases in strand stress over the transfer and development lengths along the beam. The *transfer bond stresses* are defined as the stresses developed in the concrete due to bond mechanisms that result in the increase from zero stress in the steel and concrete at

the free end of the member to the effective prestress in the steel at the transfer length. The main bond mechanism that contributes to this change in stress is Hoyer effect [38]. The *flexural bond stresses* are stresses in the concrete due to bond mechanisms required to increase the stress in the steel from effective prestress to the ultimate stress occurring in the strand, f_{pu}, as bending moment develops up to the ultimate moment, M_u. The main bond mechanism that influences these stresses is mechanical interlock.

There are different distances along the concrete over which the transfer and flexural bond stresses are developed as defined by the ACI 318 Code [2], as shown in Figure 2.2. The *transfer length*, L_t, is associated with the transfer bond stresses and is defined as the distance from the end of the concrete to the point where the stress in the prestressing steel is constant. This constant stress in the steel referred to as the effective prestress after losses, f_{se}. The *flexural bond length*, L_{fb}, is the distance from the end of the transfer length zone to a point at which the ultimate stress in the strand can be developed. The *development length*, L_d, is the distance from the end of the concrete to the point at which the ultimate tensile stress in the steel can be developed without bond failure. The development length is also considered the addition of the transfer and flexural bond lengths.

The *embedment length*, L_e, is a term used to describe the bonded length of the tendon from where the stress is zero to the critical section. Depending on the applied load, the critical section usually occurs at the point of maximum moment. The embedment length is important because it defines whether a bond failure ($L_e < L_d$) or a flexural failure ($L_e > L_d$) will occur in the beam. A bond failure occurs

11

when the bond forces are less than the forces imparted to the concrete by the strand, thereby allowing slip of the strand relative to the concrete. Flexural failure occurs when the bond forces are equal to the strand forces, thereby allowing the strand to reach its ultimate tensile strength.
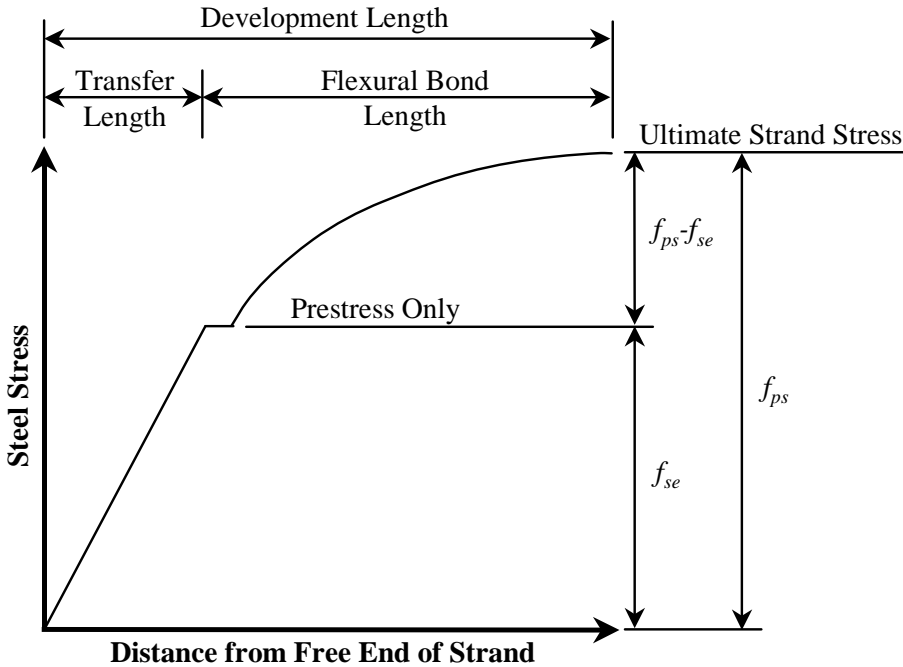
Figure 2.2: Variation of Steel Stress [2]

2.3 LITERATURE REVIEW

This section details the literature reviewed for this project on a variety of subjects that pertained to the research involved in this study including the testing of normal weight and lightweight concrete beams.

2.3.1 Use of Lightweight Concrete

2.3.1.1 Zia, P. – [47]

This study indicated that commercially available HSLC using natural sand as the fines was available in compressive strengths ranging from 5,000 – 7,000 psi (34.5 – 48.3 MPa). Also, by using fly ash and water reducing agents the compressive strength can be increased to 8,000 – 10,000 psi (55.2 – 69.0 MPa).

Calculations were performed by Zia to determine the amount of prestressing strand and the necessary concrete compressive strength for different span bridges using normal weight and lightweight concrete. For short and long span bridges, Zia showed that there was more than an 10% reduction in the amount of steel area required for completely lightweight concrete girders and slab bridges compared to normal weight concrete bridges using the same concrete compressive strength.

The study also indicates that given a certain concrete compressive strength, the maximum span distance of the girders is greatest for lightweight concrete bridges, although a limiting factor is the deflection limit under service load.

2.3.1.2 Yang, Y. & Holm, T. – [44]

This paper is a review of a T.Y. Lin report [18] and the progress made since its publication. The researchers found that replacement of normal weight concrete decks with lightweight concrete decks has increased the live load capacity of bridges studied in the report and also allowed increased deck widths.

13

It also indicates that the number of lightweight concrete bridges being built each year is increasing with over 500 major bridges now completed in North America.

The economic advantages of using lightweight concrete in bridges are also discussed. For example, the paper indicates that the dead load from self-weight for long span concrete bridges can be 85% of the total load applied to the structure. The use of lightweight concrete in place of normal weight concrete could reduce the total applied load of the structure by 25%. This economic benefit would favorably impact the cost of the piers and foundation due to the reduction of dead load.

The paper also indicates that there may be concerns about deflections of bridges using lightweight concrete, which has a lower modulus of elasticity than normal weight concrete. The problems presented by deflection can be alleviated by:

1) Pre-cambering

2) Providing additional cables to modify the stress diagram

3) Provide spaces for additional cables to be stressed one or two years after completion of the project

4) Using higher strength (say 30% higher) concrete for the bottom slab of the box section

2.3.1.3 Other Sources

The scope of this thesis does not include a complete review of the literature pertaining to the use of lightweight concrete. The few sources presented in this section are representative of the type of information that exists on the

feasibility of using lightweight concrete in bridges. Other sources can be found in the references and Heffington [22].

2.3.2 Testing of Lightweight Concrete Beams

2.3.2.1 Ahmad, S. & Barker, R. – [3]

This study consisted of six single reinforced (bottom strands only) HSLC beams with varied concrete compressive strength, 5,200 – 11,000 psi (35.9 – 75.8 MPa), and tensile steel content as a ratio of the balanced steel content (ρ/ρ_b), 0.18 – 0.54. The average unit dry weight for the lightweight concrete was 122 lb/ft^3 (19.2 kN/m^3). Their experimental results showed that the ultimate moment capacity exceeded the ACI predicted capacity by an average of 7% with a maximum of 12%. The following two conclusion of this study are pertinent to this research project:

1) The ACI-equivalent rectangular stress block provides accurate, conservative predictions of the ultimate flexural capacity of singly reinforced lightweight concrete members having a compressive strength not exceeding 11,000 psi (75.8 MPa) and a ρ/ρ_b not exceeding 0.54.

2) The ACI recommendation of 0.003 as the maximum usable concrete strain appears to be an acceptable lower bound for HSLC members with compressive strength not exceeding 11,000 psi (75.8 MPa) and ρ/ρ_b value less than 0.54.

15

2.3.2.2 Swamy, R. & Ibrahim, A. – [4]

This study examined the strength, cracking, and deformation characteristics of expanded slate (Solite) prestressed lightweight concrete beams. The cube compressive strength varied from 5,000 – 5,800 psi (34.5 – 40.0 MPa) and the unit weight varied from 105 – 108 lb/ft^3 (1,659 – 1,706 kg/m^3). The study found that the average ratio between the ultimate moment developed in the beam and the cracking moment was 1.70. They also found that the ultimate moment determined from Whitney's theory (Rectangular-Stress Block) overestimated the actual moment capacity by 5%. All failures for the beams were flexural in nature and ultimate capacity was reached by crushing of the compression concrete. The conclusions of this study were that the deflections under design loads of the Solite concrete was within parameters defined in the ACI Building Code. Also, that the prestressed beams showed adequate ductility and deflections prior to failure. They found that the strain distribution in the lightweight concrete beam were similar to that for normal weight concrete beams. Finally, they observed that the failure zone of the lightweight concrete beams was more extensive compared with that of normal weight concrete beams.

2.3.2.3 Mor, A. – [34]

This research study was used to determine the effects of condensed silica fume on the mechanical bond properties when used in HSLC. Normal weight and lightweight mixes were produced with and without adding silica fume. The lightweight mixes had densities between 126 – 130 lb/ft^3 (19.8 – 20.4 kN/m^3). All the mixes had 28-day compressive strengths above 9,000 psi (62.1 MPa).

16

Pullout tests were performed to determine the bond properties. The results of these tests led to the following conclusions:

1) Bond strength of normal weight concrete and lightweight concrete of similar high compressive strength without silica fume were similar.

2) Bond strength of HSLC with silica fume was about double that of every other concrete of same compressive strength at a slip of 0.01 in 0.0254 mm).

2.3.3 Use of Deck Panels

2.3.3.1 Bieschke, L., and Klingner, R. - [10]

The purpose of this study was to determine the effect of transverse strand extensions on the behavior of precast pretensioned panel bridges. Full scale static and dynamic testing was performed at FSEL on a three-girder (AASTHO Type II) bridge incorporating panels with and without transverse strand extensions. Normal weight concrete was used in the casting of the panels and beams. Placement of the panels on the girders had details similar to those described in Chapter 3 of this thesis.

The study found that AASHTO punching shear theory gave conservative estimates of the failure load at interior bridge deck locations and that it underestimated the failure at the middle areas of the deck overhang. Flexural yield-line theory gave conservative results for the behavior in both areas.

As to the behavior of the panels with and without the transverse strand extensions, the study found that this did not affect the overall or local behavior of the bridge. More importantly, the use of the fiberboard strips between the panels

and beam was found to be an important detail in performance of the composite section. When the panel is constructed with fiberboard strips, the panel can bear on the concrete that flows into this area after it has hardened. This prevents longitudinal cracking of the panel that might occur if the panel only bears on the fiberboard strip or concrete beam alone.

2.3.3.2 Barnoff, R. – [8]

This study discusses the use of precast prestressed concrete deck panels as a method of reducing the deterioration of concrete decks due to improper placement of the concrete, improper curing of the concrete, insufficient concrete cover over the reinforcing steel, excessive use of deicing agents, and cracking of the deck slab due to overloads. For this research project a bridge was constructed using removable wood forms, permanent steel forms, plain butt joints between adjacent panels, and keyed joints between adjacent panels. Design and overload load tests were then performed on the bridge.

The prestressed panels were constructed of normal weight concrete with a 3-in (76.2-mm) depth and were pretensioned with 7/16-in (11.1-mm) diameter 7-wire strand. Testing at service loads found that full composite action was developed between the beam and deck when panels were used. This composite action was also present at failure. Tests were also conducted on laboratory specimens.

The conclusions of the study were the following:

1) Bridge decks constructed with panels and a cast-in-place topping can be assumed to be continuous over the supporting beams.

18

2) The AASHTO formula used to compute moments in bridge decks is conservative when compared with experimental results measured from static loads.

3) The type of joint used between panels has no effect on the behavior of the deck.

2.3.4 Transfer and Development Length Studies

The behavior associated with the transfer and development length of prestressing strand in concrete is complex and dependent on many variables. The ACI 318 [2] and AASHTO [1] Codes along with many other sources only consider certain major factors affecting the transfer and development lengths. This section reviews the past and present literature pertaining to the models used for comparison of the test results in this research project.

2.3.4.1 Martin, L. & Scott, N. – [32]

The researchers in this study indicate that the values for transfer and development length in the ACI Code were determined from a study by Kaar and Magura [21]. All the tests that Kaar and Mangura performed were on normal weight concrete specimens. The researchers contended that in the Kaar and Magura study only one test beam failed as a result of bond failure. Also, the equations developed from these tests were based on final bond failure instead of first bond failure. There is a significant increase in load carrying capacity between these two events after first bond failure due to the contribution of mechanical interlock between the prestressing strand and the surrounding concrete. They

believe that first bond failure data should be used as an indication of development length bond failure.

They suggest that the transfer length should be equal to eighty times the strand diameter, d_b. For the development length they suggest that a bilinear curve be used to determine the calculated stress in the steel, f_{ps}. The equations they give for determining this value are given below in Eqn. 2.1 & 2.2.

$$L_e \leq 80 d_b \qquad f_{ps} \leq \frac{L_e}{80 d_b} \left(\frac{135}{d_b^{1/6}} + 31 \right) \qquad \textbf{Equation 2.1}$$

$$L_e \geq 80 d_b \qquad f_{ps} \leq \frac{135}{d_b^{1/6}} + \frac{0.39 L_e}{d_b} \qquad \textbf{Equation 2.2}$$

2.3.4.2 Mitchell, D., et. al. – [33]

This team of researchers examined the influence of concrete strength on the transfer and development length for pretensioned strand in normal weight concrete. They performed an experimental program that tested 22 precast pretensioned beams, varying the concrete compressive strength from 3,050 – 7,050 psi (21.0 – 48.6 MPa) at transfer and from 4,500 – 12,900 psi (31.0 – 88.9 MPa) for development length testing. They also expressed concern that the equations developed by Kaar and Hanson were not accurate.

To determine the transfer length they used the slope-intercept method. They used the equation developed by Zia and Mostafa [46] as the model for their equation. They concluded that the transfer length should be a function of the initial stress in the steel, f_{si}, and concrete compressive strength at transfer, f'_{ci}. The

square root factor in Eqn. 2.3 (units in ksi) is used as a correction factor to account for the influence of concrete strength at transfer.

$$L_t = \frac{f_{si}d_b}{3}\sqrt{\frac{3}{f'_{ci}}}$$ **Equation 2.3**

Beam tests showed that an increase in concrete compressive strength, f_c', also corresponded with an increase in the flexural bond length. They determined that the flexural bond length was a function of the effective prestress in the steel and the ultimate concrete compressive strength. Based on their tests and the transfer length equation that they developed, they formulated an equation for the development length given below as Eqn. 2.4 (units in ksi):

$$L_d = L_t + (f_{ps} - f_{se})d_b\sqrt{\frac{4.5}{f'_c}}$$ **Equation 2.4**

2.3.4.3 Russell, B. & Burns, N. – [39]

The researchers performed tests on 44 test specimens to determine transfer length. They also reviewed the results from past research involving transfer length studies. Their tests indicated that AASHTO type beam specimens had shorter transfer lengths than simple rectangular 1, 3, and 5 strand specimens. They also indicated that current codes do not take into account the effect of concrete strength on transfer length, where recent studies had shown that it was a factor. However, they said that an exact equation was not necessary for design of safe structures. Based on their testing and analysis of research data from several other research studies they developed an equation that would encompass all the values that had been presented in valid tests to give a safe approximation of the transfer length. This expression is given below as Eqn. 2.5 (units in ksi):

21

$$L_t = \frac{f_{se}}{2} d_b \qquad\qquad \textbf{Equation 2.5}$$

2.3.4.4 Balazs, G. – [6]

A theoretical approach can be taken to find a correlation between the amount of draw end at the free end of the strand, Δ_d, the initial strain in the strand, e_{si}, and the transfer length of the steel. The original equation formulated by Guyon is given below as Eqn. 2.6 [20].

$$L_t = \frac{\alpha \cdot \Delta_d}{\varepsilon_{si}} \qquad\qquad \textbf{Equation 2.6}$$

In this equation α is a term that accounts for either a constant load stress distribution, $\alpha=2$, or a linear load stress distribution, $\alpha=3$. Balazs states that Polish researchers had conducted tests which found this constant to equal 2.86 [47] while research performed by den Uijl obtained a value of 2.46 for α [5]. Balazs states that the problem with Guyon's equation is that the coefficient takes into account the assumed shape of the bond stress distribution. He develops an equation that did not have this problem (Eqn. 2.7). Here the value of b is dependent on strand diameter. When b is equal to 1/3, Eqn. 2.7 corresponds to $\alpha=3$ in Eqn. 2.6. When b=0, Eqn. 2.7 corresponds to $\alpha=2$ in Eqn. 2.6. For ½-in diameter strand Balazs suggests a value for b equal to 1/2.

$$L_t = \frac{2}{1-b} \frac{\Delta_d}{\varepsilon_{si}} \qquad\qquad \textbf{Equation 2.7}$$

Balazs also used the theory developed by Guyon and took into account the nonlinear nature of the phenomenon. Balazs offers two alternate equations (Eqn.

2.8 & Eqn. 2.9, units in mm & MPa) based on a nonlinear approach, where f'$_{ci}$ in initial compressive strength of the concrete.

$$L_t = \frac{111\Delta_d^{0.625}}{f_{ci}^{'0.15}\varepsilon_{si}^{0.4}}$$ **Equation 2.8**

$$L_t = \frac{3.5 f_{si}}{\sqrt{f_{ci}^{'}}\sqrt{\Delta_d}}$$ **Equation 2.9**

2.3.4.5 Zia, P. & Mostafa, T. – [46]

The researchers reviewed past studies, both theoretical and experimental, to determine the factors that affect transfer and flexural bond length. The factors they determined that affected transfer and flexural bond length were:

1) Type of steel (wire, strand)

2) Size of steel (diameter)

3) Steel stress level

4) Steel surface condition (i.e. clean or rusted)

5) Concrete compressive strength

6) Type of loading (static, repeated, impact)

7) Type of prestress release (gradual, sudden)

8) Confining reinforcement around steel (helix, stirrups)

9) Time-dependent effects

10) Consolidation and consistency of concrete around steel

11) Concrete cover around steel

Based on a review of previous experimental studies, they developed an equation that best approximated the transfer length. They indicated that the initial prestress, f$_{si}$, and not the effective prestress, was an important factor in

determining the transfer length (Eqn. 2.10). Also, the researchers believed that the initial compressive strength of the concrete at release was a factor.

$$L_t = 1.5\frac{f_{si}}{f'_{ci}}d_b - 4.6$$ **Equation 2.10**

To determine the flexural bond length the researchers looked at Hanson and Kaar's test data [21] and determined that the ultimate strength of the strands had occurred in beams at a shorter length before general bond failure occurred. They determined that the average bond stress was lower than what was implied by the ACI Code. They based their equation for flexural bond length on these facts. Combining this equation with the transfer length equation yielded the development length equation which is given as Eqn. 2.11:

$$L_d = L_t + 1.25(f_{pu} - f_{se})d_b$$ **Equation 2.11**

2.3.4.6 Buckner, C. – [13]

This report was commissioned by the FHWA to review the recent studies being completed at that time on transfer and development length, analyze the data, and formulate design equations and guidelines. The studies that Buckner examined were from such institutions as University of Tennessee at Knoxville, Florida Department of Transportation, University of Texas at Austin, Purdue University, Louisiana State University, and McGill University. He also reviewed past research. All the data for the study was for normal weight concrete.

For transfer length Buckner found that the largest factors affecting the transfer length was f_{si} and d_b, but Buckner also looked at individual contributions from other sources. When examining the correlation between the transfer length and the elastic modulus of the concrete on the data, Buckner formulated Equation

24

2.12. This was a unique evaluation that had not been suggested in the past studies. The equation was developed to best fit the data with some variation expected due to the pooling of different research studies and the fact that all variables affecting transfer length could not be controlled. Because the elastic modulus of concrete, E_c, is a function of f_c' in normal weight concrete, his recommendation for transfer length reduced to an expression without the modulus as a factor. That expression is not reported here.

$$L_t = \frac{1250 f_{si} d_b}{E_c}$$ **Equation 2.12**

Buckner also reviewed the available data on development length. He suggested that many researchers have proposed constant bond stress in relation to flexural bond length, but that linear bond stress more accurately modeled behavior. To incorporate this into his equation for development length, Buckner uses the variable λ and gives two equations for its determination. One is for general applications and the other for cases when strand stress at ultimate moment is approximated using Equation 18-3 of ACI 318 [2]. The equation he formulates is given as Eqn. 2.13, where β_1 and ω_p are the same factors defined in ACI 318.

$$L_d = L_t + \lambda(f_{ps} - f_{se})d_b$$ **Equation 2.13**

$$\lambda = \left(0.6 + 40\varepsilon_{ps}\right) \quad or \quad \left(0.72 + 0.102\frac{\beta_1}{\omega_p}\right)$$

where $(1.0 \leq \lambda \leq 2.0)$

2.3.4.7 Current ACI 318 and AASHTO Guidelines [2,1]

The ACI and AASHTO guidelines for transfer and development length use similar equations. The transfer length is first mentioned in ACI 318 in Chapter

25

11: Shear and Torsion. Here it states that the transfer length can be assumed to be 50 strand diameters. This is later discussed more fully in Chapter 12 of the ACI Code where the development length is defined as the combination of the transfer and flexural bond lengths. The portion attributed to transfer is given as Eqn. 2.14. The previous statement that the transfer length is equal to 50 diameters is based on this equation with f_{se} equal to 150 ksi (1,034 MPa).

$$L_t = \frac{f_{se}}{3} d_b \qquad \textbf{Equation 2.14}$$

The equation that ACI 318 uses to describe the development length is given in this excerpt from the code:

12.9.1 – Three- or seven-wire pretensioning strand shall be bonded beyond the critical section for a development length, in inches, not less than

$$\left(f_{ps} - \frac{2}{3} f_{se} \right) d_b \qquad \textbf{Equation 2.15}$$

where d_b is strand diameter in inches, and f_{ps} and f_{se} are expressed in kips/in2. The expression in parenthesis is used as a constant without units.

In the commentary this equation is expanded to show the contribution of transfer and flexural bond length, which is Eqn. 2.16:

$$L_d = \frac{f_{se}}{3} d_b + \left(f_{ps} - f_{se} \right) d_b \qquad \textbf{Equation 2.16}$$

The new AASHTO LRFD Design Specifications [1] gives Eqn. 2.15 for determination of the development length. Due to the higher levels of prestressing being used in construction, the transfer length has been increased in the new provisions. The AASHTO code indicates the "transfer length may be taken as 60 strand diameter."

Chapter 3: Beam and Component Specifications

3.1 INTRODUCTION

This chapter discusses design, specifications, and manufacture of the beams and components to be produced for the entire research study. Since the project was a feasibility study of the use of pretensioned HPLC concrete bridge beams, the number of test beams commissioned by TxDOT was small. A total of eight beams with various combinations of concrete strength and type of concrete used in the beams and decks were fabricated for this research project. This chapter includes manufacture and design of all eight beams.

3.1.1 Nomenclature

To give the reader a coherent understanding of the beam identifiers in this thesis a nomenclature was developed to describe each beam. This system is shown in Figure 3.1.
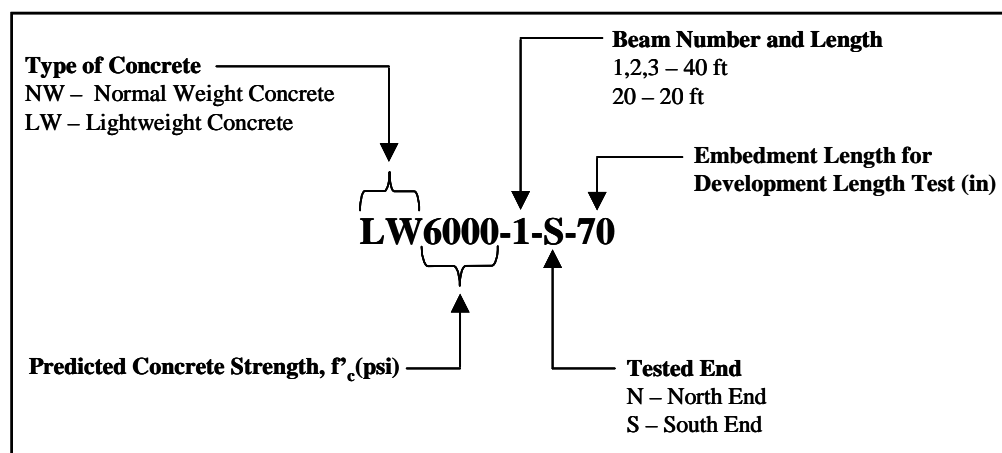
Figure 3.1: Beam Nomenclature

The full beam designation is not used at all times in the thesis because sometimes the reference in the text will be to a set of beams. For example, LW8000 refers to the four lightweight 8,000-psi (55.2-MPa) beams of various lengths and LW6000-20 refers to one beam, 20-ft (6.1-m) in length but includes both ends of the beam. For transfer length tests, the reference NW6000-1-N refers to one beam and one end of the beam. For the development length tests, the reference LW6000-1-N-80 refers to one beam, one end, and the embedment length to be tested.

3.1.2 Number of Beams

A total of eight pretensioned AASHTO Type I beams were produced at Heldenfels Prestressing Plant in San Marcos, Texas. In addition to the six 40-ft (12.2-m) long full size beams originally commissioned for the project, two 20-ft (6.1-m) beams were also produced. The purpose of the reduced length 20-ft (6.1-m) beams was to introduce the prestressing plant to lightweight concrete, identify any problems in the mix designs, and ensure that all the facilities were in order at the plant to produce the actual test beams. This was a valuable undertaking because several potential production problems were corrected and the subsequent fabrication of the six test beams occurred without any major problems.

The six 40-ft (12.2-m) test beams were produced on two different days, in groups of three, due to the time constraints of instrumenting and measuring the beams after the forms were removed. One normal weight concrete beam and two lightweight concrete beams with a predicted 28-day compressive strength of 6,000 psi (41.4 MPa) were cast one day and then the pretensioning force in the

strands was released the next day. The other three lightweight concrete beams with a predicted 28-day compressive strength of 8,000 psi (55.2 MPa) were then produced in a similar way two days later.

3.1.3 Variables

The only property that was varied among the beams was the concrete mix design. This was done so that the measurements performed on each beam could be directly compared to the other beams and the type of concrete would be the only basis for difference among the results. A normal weight 6,000-psi (41.4 MPa) concrete mix obtained from Capital Aggregates was used for one beam (NW6000), which would be used as the control mix in the experiments. A lightweight 6,000-psi (41.4 MPa) concrete mix developed as part of this research project was used on two beams (LW6000). Finally, a lightweight 8,000-psi (55.2 MPa) concrete mix developed as part of this research project was used on the last three beams (LW8000). These variables can be seen in Table 3.1, with further explanation of the deck properties given in the following sections.

Table 3.1: Test Beam Concrete Properties

Beam ID	Length	Beam Concrete	Deck Concrete	Lightweight Deck Panels
LW6000-20	20-ft	LW 6000-psi	None	N/A
LW8000-20	20-ft	LW 8000-psi	None	N/A
NW6000-1	40-ft	NW 6000-psi	NW 5000-psi	No
LW6000-1	40-ft	LW 6000-psi	NW 5000-psi	No
LW6000-2	40-ft	LW 6000-psi	NW 5000-psi	Yes
LW8000-1	40-ft	LW 8000-psi	NW 5000-psi	No
LW8000-2	40-ft	LW 8000-psi	NW 5000-psi	Yes
LW8000-3	40-ft	LW 8000-psi	LW 5000-psi	No

Notes:
1 ft = 0.305 m
1 psi = 6.895 kPa
LW = Lightweight
NW = Normal Weight

3.2 DEVELOPMENT OF 20-FT DESIGNS

Several variables were tested by including production of the two 20-ft (6.1-m) beams in the test program. The beams were a shorter length than the other six beams that would be tested because they were not part of the original study. Their main purpose was to be a check of the production plants ability to produce the lightweight concrete. One beam would be cast with the LW6000 mix design while the other beam used the LW8000 mix design. These were the same mixes that were later used for the 40-ft (12.2-m) beams. To gain valuable information from the production of these beams, they were designed to test the lightweight concrete under the most congested and highest level of prestressing conditions that might be applied in an actual AASHTO Type I bridge girder. This was determined by the TxDOT Bridge Design Division after running several computer models. The most heavily congested portion of the beam was at the ends, which is

shown in Figure 3.2. The typical dimensions of an AASHTO Type I beam and the strand pattern for these beams is shown in Figure 3.3. The strand number is given below each strand in the figure.

Figure 3.2: Congestion of Reinforcement at End of Beam
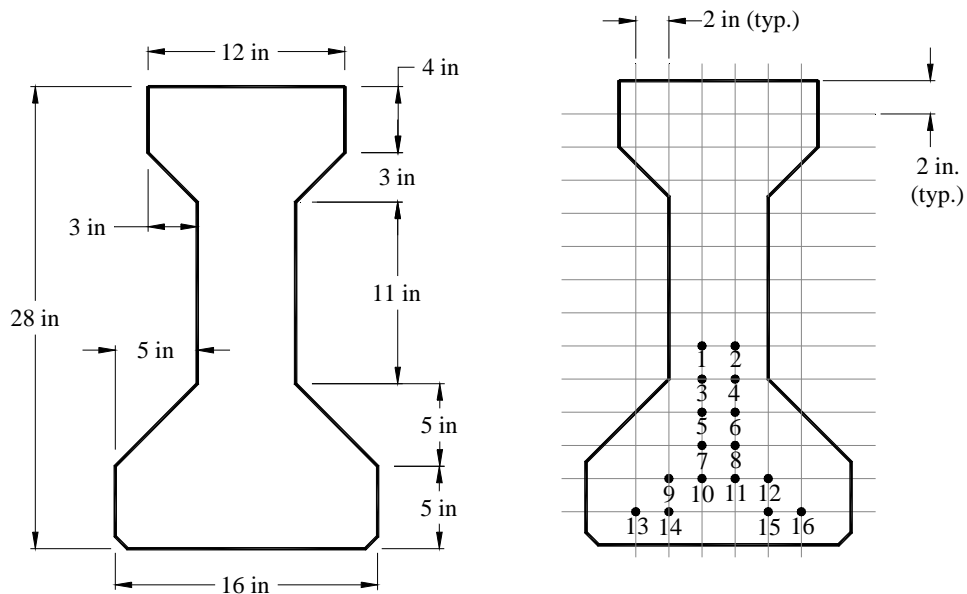
Figure 3.3: AASHTO Type I Cross Section and Strand Pattern for 20-ft Beams

These beams were also to be used as a teaching aid for the research personnel in applying the measurement devices since many of the people working on this phase of the project had had no prior experience with the equipment. The data obtained would also give some initial data to help assess the adequacy of the amount of instrumentation required. Also, with the combination of expected lower tensile strength of the lightweight concrete and the maximum number of strands in the beam, these beams would show if end splitting cracking or cracking at the top of the member would occur. Neither of these effects was predicted by calculations and did not occur in the actual beams

3.3 DEVELOPMENT OF 40-FT DESIGNS

The use of a 40-ft (12.2-m) length for the test beams was determined by their effectiveness in past studies [7]. This would allow two tests to be performed on one beam without damage from one test unduly influencing the next test. By using one beam for two tests it would be possible to control the independent variables of the tests while knowing that the dependent variables, based on material properties, were the same. This was especially advantageous during development length testing where two different embedment lengths could be tested to help determine the development length.

The 40-ft (12.2-m) beams used 12 strands placed in the pattern illustrated by Figure 3.4, with strand number labeled below each strand. This pattern is typical of a pattern that might be used in construction. Two strands were placed in the top flange to ensure that tension did not occur in this area, which might result

in unwanted cracking. The bottom 10 strands were placed on the bottom two rows
to give the largest possible moment arm depth.
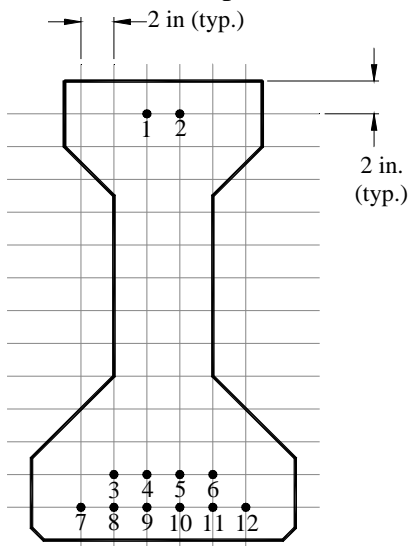
Figure 3.4: 40-ft Beam, 12 Strand Pattern

The passive reinforcement used in the beams was determined by
successful patterns used in similar tests and by nominal TxDOT requirements.
The amount of shear reinforcement used was more than would traditionally be
used in a beam of this size. This was due to the fact that the selected shear span
for the tests would be between 60 – 80 in (1,524 – 2,032 mm). Therefore higher
than normal shears would be produced in the beam. Design of shear
reinforcement was based on precluding shear failure in the beam at the ultimate
load. A shear failure of the beam would not give any valuable data concerning the
development length of the strands. From shear calculations, it was determined that
double #4 stirrups were required in the end 10-ft (3.05-m) of the beam to safely
prevent this type of failure. Details of the reinforcement can be seen in Figure 3.5
and 3.6.
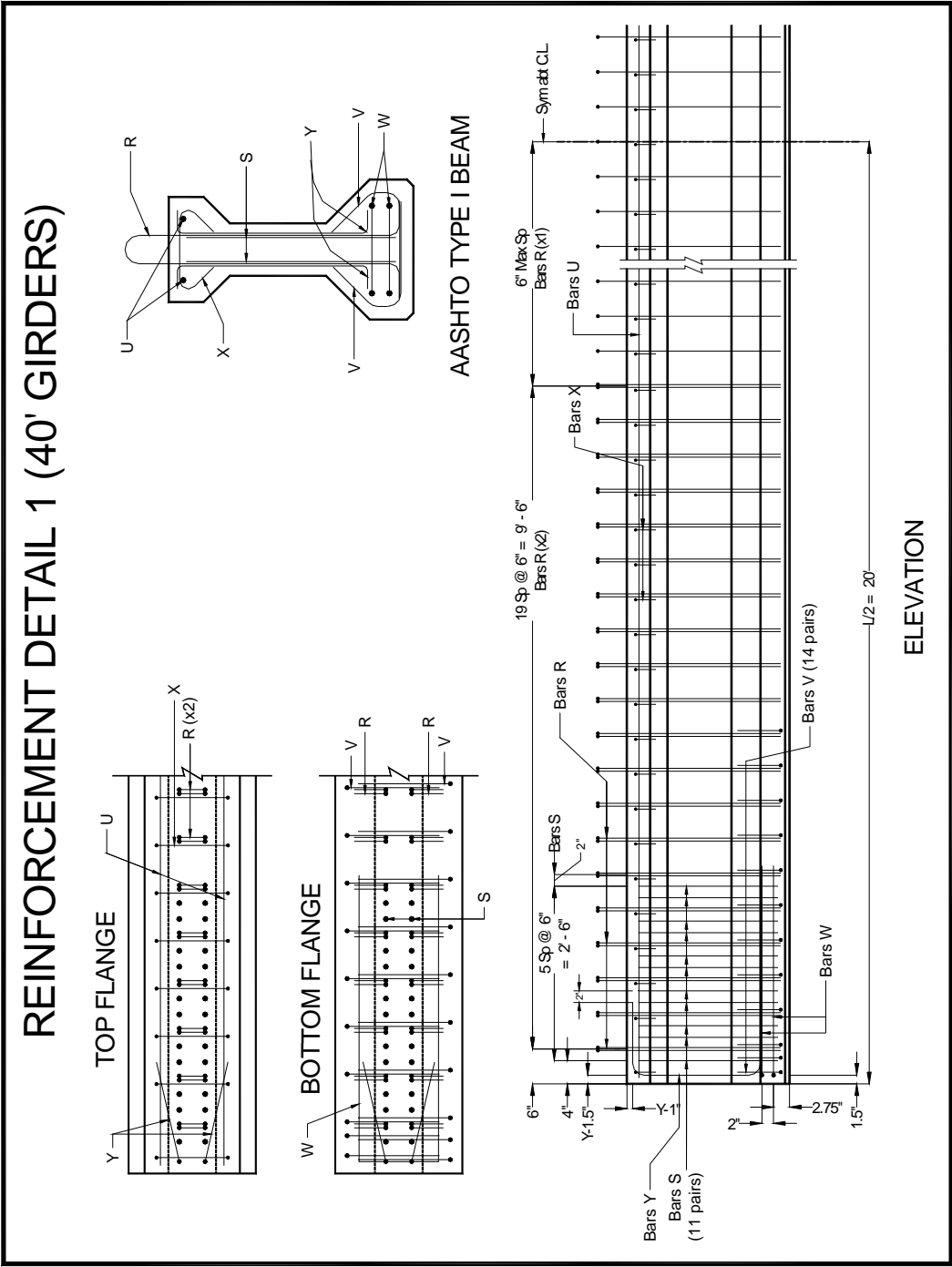
Figure 3.5: 40-ft Test Beam Reinforcement Details

34
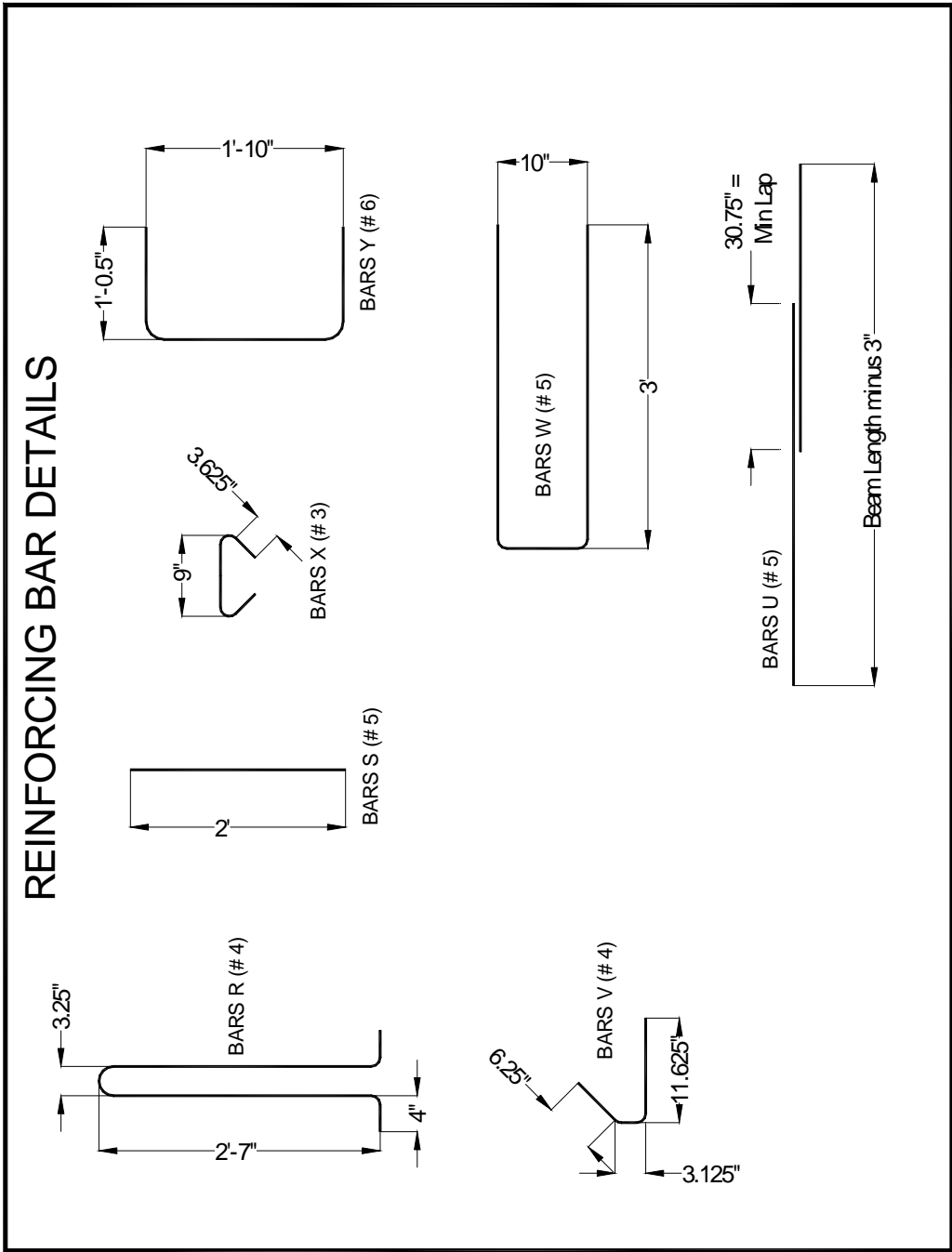
Figure 3.6: Reinforcing Bar Details

35

To perform development length testing on beams that accurately modeled a real bridge girder, a reinforced concrete deck was added at the Ferguson Structural Engineering Laboratory (FSEL). The type of concrete and deck details varied between beams as shown in Table 3.1. However, other details such as the depth and width of the slab and the amount of reinforcement were kept constant. The normal weight and lightweight decks that were cast using reinforcement details similar to those used in Texas bridges. The amount of reinforcement was determined by AASHTO code provisions [1]. The reinforcement details of the deck can be seen in Figure 3.7. When the lightweight deck panels were used, a different reinforcement detail had to be used, which is explained in the next section.
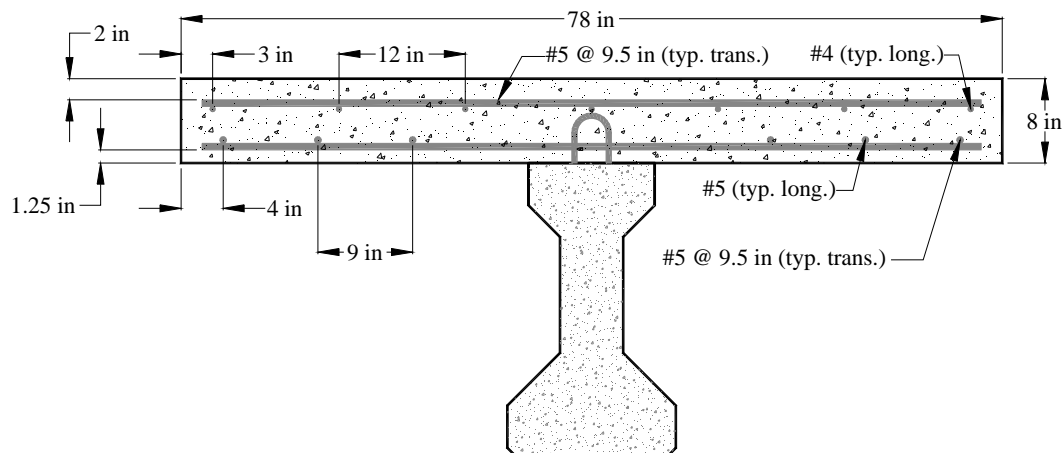
Figure 3.7: Normal and Lightweight Concrete Deck Details

3.4 LIGHTWEIGHT DECK PANELS DESIGN

Stay in place normal weight concrete deck panels are frequently used in construction to simplify the amount of formwork needed in the field. Typically, the panels are pretensioned with 3/8-in (9.52-mm) strand at 190 ksi (1,310 MPa). These panels are manufactured at a plant and therefore the quality is higher than would be produced in the field. These panels are then shipped to the bridge site for installation. The panels span the gap between beams and therefore minimal formwork is required for the casting of the deck. The panels create a stable and safe working surface for the top layer of steel to be placed.

The initial proposal for this study did not include any type of deck panel. It was decided that lightweight panels be included in this study after a meeting with TxDOT. The purpose of using lightweight deck panels was that the weight of the concrete in most bridges is typically the most significant load to which a bridge is subjected. By using lightweight panels, the dead load on the bridge could be reduced. This would allow larger span lengths or wider spacing of the girders. This was an idea that TxDOT was interested in exploring. The panels were manufactured at Austin Prestress and the concrete provided by Rainbow Materials, who had had extensive experience with lightweight concrete. A picture of the actual casting is shown in Figure 3.8.

Figure 3.8: Lightweight Concrete Panel Casting

In the field, a panel would span the distance between two beams. Since this study only involved single beams with composite decks of a fixed width, a system had to be devised which would simulate field conditions. The interior edge of the panel was supported on the beam and did not require any modification from standard practices. Here the panel was supported on the edge of the beam by a 1-in (25.4-mm) wide by ½-in (12.7-mm) high layer of fiberboard. This detail is used to give more area to which the cast-in-place concrete can bond to the beam and create better composite action. This detail is also used because cracking problems have occurred in panels where the panel has rested directly on the beam [10]. Three inches of the ends of the strands in the transverse direction of the panel were left exposed. This would create dowel action on the free end of the panels to

help support the load when the formwork was removed. These details are illustrated in Figure 3.9.
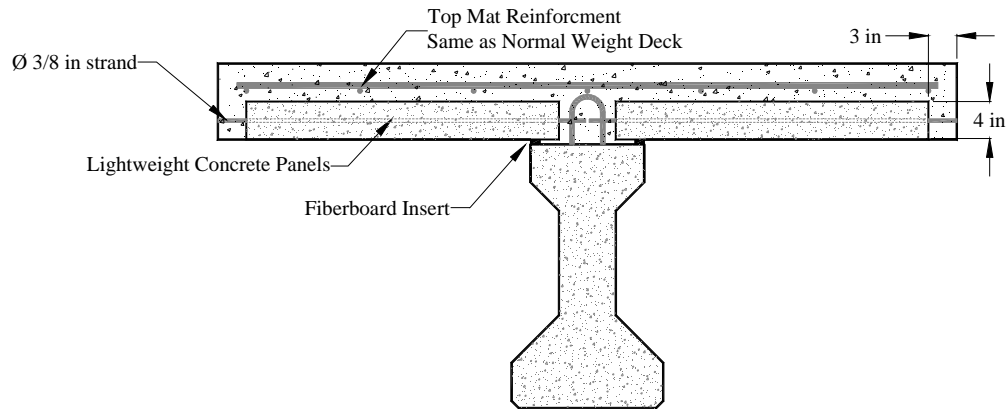
Figure 3.9: Lightweight Deck Panel Details

The actual cross-section of the beam is shown in Figure 3.10. This shows the effectiveness of the fibrous material in creating a space for concrete to fill, adding to the shear capacity and bond between the beam and deck. After the cast-in-place deck concrete had cured, peepholes were drilled into the fiberboard every 4-ft (9.8-m) to ensure that concrete had penetrated this area. No areas were found that had not been filled with concrete.

39

Figure 3.10: Beam and Deck Cross-Section with Panels

Two different size panels had to be manufactured to fit the 40-ft (12.2-m) deck length. The layout of the panels is shown in Figure 3.11. The panels labeled "A" had extra reinforcement exposed on their ends so that steel would extend to the end of the beam.
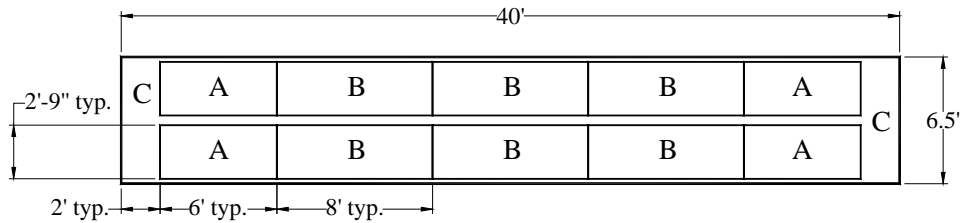
A - 4' x 6' Lightweight Concrete Panel
B - 4' x 8' Lightweight Concrete Panel
C- Cast-In-Place Normal Weight Concrete

Figure 3.11: Top View of Deck with Lightweight Panel Layout

3.5 MATERIAL PROPERTIES

3.5.1 Concrete

The concrete mix designs were developed at FSEL and are reported on in detail in a report by Heffington [22]. Three different concrete mixes were used in the production of the prestressed beams. The designed final compressive strength of the NW6000, LW6000, and LW8000 were 6,000 psi (41.4-MPa), 6,000 psi (41.4-MPa), and 8,000 psi (55.2-MPa), respectively. All the mixes were required to have a 3,500-psi (24.1-MPa) release strength at one day. The release strength presented one problem for the mix design of the 6,000-psi (41.4-MPa) lightweight concrete. No mix that was developed for this research study had a one-day release strength of 3,500-psi (24.1-MPa) and a 28-day compressive strength of 6,000-psi (41.4-MPa). When mix designs were selected for the two lightweight concrete mixes, all mix data obtained by this study was analyzed. Two mixes that had 3,500-psi (24.1-MPa) one-day release strengths and a difference of 1,000-psi (6.90-MPa) in their 28-day strength were selected. The final strengths of the lightweight concretes did not vary as much as was expected at the time of the development length tests. The mix designs for the normal weight and both lightweight mixes are given in Table 3.2. A summary of the relevant compressive strength properties, along with the unit weights, for all three concrete mixes used in this study are given in Table 3.3.

Table 3.2: Mix Designs

Material	NW6000	LW6000	LW8000
Water	250	222	247
Cement (Type III)	517	504	671
Fly Ash	0	168	316
3/4 in Hard Rock Coarse Aggregate	1869	0	0
3/4 in Lightweight Coarse Aggregate	0	1264	1123
Sand	1355	1149	1029
Retarder	12	12	12
Superplasticizer	20.4	34	54

Notes:
1) Quantities in lbs and oz
2) Quantities per yd^3

Table 3.3: Concrete Properties

Beam ID	Compressive Strength (f'$_c$), psi / (MPa)		Unit Weight
	1-day	Long Term	lb/ft^3 / (kN/m^3)
NW6000	3,490 (24.1)	5,500 (37.9)	149 (23.4)
LW6000	4,900 (33.8)	8,130 (56.1)	118 (18.5)
NW8000	5,560 (38.3)	7,850 (54.1)	122 (19.2)

3.5.3 Prestressing Steel

The prestressed steel reinforcement used in the test beams for this study was supplied by American Spring Wire Corporation. It was specified as ½-in

(12.7-mm), low-relaxation, ASTM A416, Grade 270 ksi (1,860 MPa). Mill certificates indicate an ultimate stress of 270 ksi (1,860 MPa) and a elastic modulus of 28,000 ksi (193,000 MPa).

3.5.2 Reinforcing Steel

Mild steel reinforcement used in the test beams for this study was supplied by Border Steel. It was specified as Grade 60. Mill certificates indicate a yield stress of 66 ksi (455 MPa) and an ultimate stress of 100 ksi (6.90 MPa)

3.6 FORMING, PLACEMENT, AND CURING OF CONCRETE

The forming used at Heldenfel's Prestressing Plant for the beams was all metal forms along the sides of the beam. Both metal and wood forms were used as end forms, depending on what was available at the plant. The metal end forms tended to leave a better finish to the concrete, but were more difficult to remove due to their stiffness. The transport and placing of the concrete was performed by a sidewinder truck. Two lifts of concrete were placed for each beam because this allowed better consolidation of the concrete as it was placed. Hand-held vibrators were used to consolidate and remove air bubbles from the concrete. No external vibration was applied to the side forms. The finishing of the top of the beam was done by trowels. The surface was left rough so that a better bond could be established between the beam and deck when the deck was cast. After finishing, heavy mat blankets soaked in water were placed on top of the beams to minimize water loss. The beams were allowed to cure for one day until the cylinder compressive strength was near 3,500 psi (24.1 MPa).

The decks of the beams were all cast at FSEL. The forms used were all wood. Placement of the concrete was accomplished by overhead bucket. Bull floats were used to finish the top surface of the concrete. Creating a very smooth finish was not necessary, so trowels were not used after bull floating. The finish of the concrete was adequate to allow a small area to be ground down and strain gauges placed. Plastic sheeting covered the entire unprotected surface of the concrete. Water was applied to the top of the deck while it cured to prevent water loss. The decks were allowed to cure for four days before the forms were removed.

Chapter 4: Transfer Length Testing

4.1 INTRODUCTION

The forms were removed from the concrete girders the day after casting. Instrumentation was placed on the beams to determine the transfer length after release of the pretensioning on the same day. Two different types of instrumentation were placed on the beams to obtain data on the transfer length. One method, DEMEC Strain Measurement, involved measurement of the strain in the concrete along the beam face. The other method, strand draw-in, measured the distance that the strand moved into the face of the concrete at the end of the beam. This chapter details the different types of instrumentation and measurement as well as the results and discussion of the transfer length testing.

4.2 INSTRUMENTATION AND MEASUREMENT FOR DETERMINING TRANSFER LENGTH

This section describes instrumentation and measurement techniques used on the beams for transfer length testing. The two methods described are DEMEC strain measurement and strand draw-in.

4.2.1 DEMEC Strain Measurements

The transfer length was previously defined as the length over which the effective prestressing force is transferred completely from the strand to the concrete. Theoretically, for a beam with straight tendons, the force in the concrete beyond the point at which this occurs is the location where the effective prestress force becomes constant and therefore the prestressing moment exerted on the

beam is also constant. This moment develops a linear strain distribution in the cross-section of the beam that remains constant along the length of the beam at any distance beyond the transfer length. This strain in the concrete can be measured and the data used to determine the transfer length.

The system used to measure the strain in the concrete for this project was the DEtachable MEChanical (DEMEC) Strain Measurement System. The DEMEC System involves gluing small metallic discs, ¼-in (6.4-mm) in diameter, to the face of the concrete spaced at the gauge length of the DEMEC gauge. Initially, the distance between the discs is measured before the strands are released to give an initial reading. This is the zero stress state of the concrete. The strands are then released and another measurement is taken of the distance between the discs. The difference between this reading and the previous one is the strain in the concrete and is measured directly by the DEMEC gauge. The accuracy of this device is ±25 microstrain [38]. This system is shown being used at the pretensioning plant in Figure 4.1.
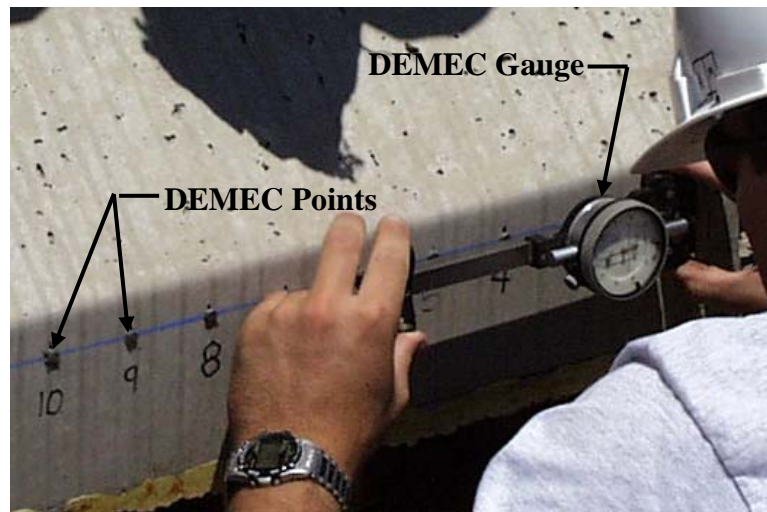
Figure 4.1: DEMEC Points and Measurement of Concrete Strains

It was determined from past use of this system that a spacing of 1.97 in (50 mm) would provide enough data to give a smooth strain profile [7,26]. The spacing and layout of the DEMEC points is shown in Figure 4.2. The distance that the DEMEC points extended along the beam was determined from calculations of the theoretical transfer length. For the pair of 20-ft (6.1 m) beams, the DEMEC points were placed to a distance of 60 in (1,525 mm) from the end of the beam, or 30 DEMEC points. After reviewing the data and determining that a longer constant strain plateau was desired for the subsequent beams, the distance was increased to 79.7 in (2,025 mm), or 40 DEMEC points. The gauge length of the DEMEC gauge used was 7.87 in (200 mm) and therefore 36 readings could be obtained from each set of DEMEC points. Each beam was instrumented with points on both sides of the beam. Therefore, each beam had two lines of points on its north and south end, corresponding to its east and west face, equaling a total of four lines of DEMEC points per beam. DEMEC points were placed on both sides

of the beam so that variation of the strain in that area could be averaged using the readings from both sides of the beam.
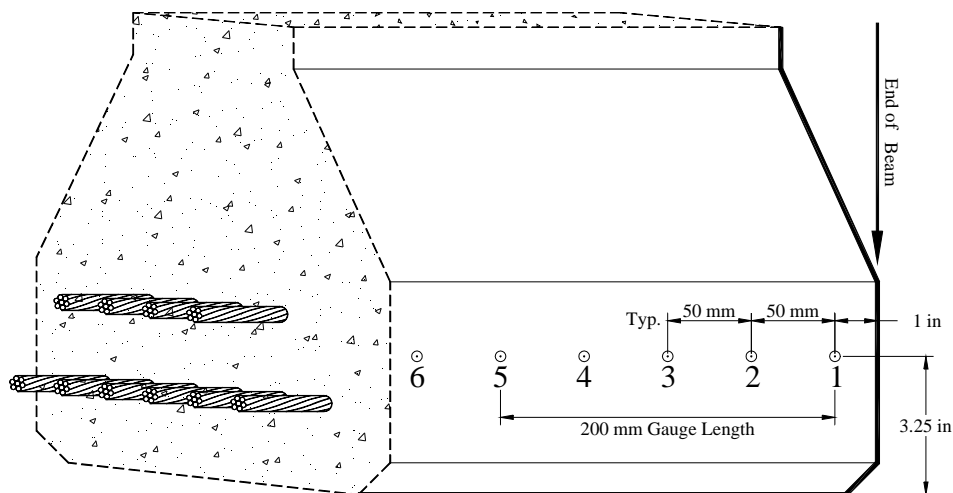
Figure 4.2: Spacing and Layout of DEMEC Points

4.2.2 Draw-In Measurements

A method to determine the effectiveness of the bond between the concrete of the beam and the prestressing strand is to measure the draw-in of the strand after the prestress is released. The draw-in is a measurement of how far the strand at the face of the concrete is pulled into the beam after the prestress is released. Other terminology for this phenomenon besides draw-in is "suck-in" or "free end slip" [7]. The draw-in measurement can also be correlated with the transfer length of the strand since they both involve the bonding of the concrete to the strand [6,20].

Draw-in measurements were performed at the plant, one day after the beams were cast. A 4-ft (1.21-m) space had to be allotted between the ends of the

beams because instrumentation had to be placed on the strands before release. This allowed removal of the end forms and enough working space to place the instrumentation and measure the draw-in values.

To measure the draw-in, aluminum U-channel measuring 1in x 1in x 1in (25.4 mm) and cut to a ½-in (12.7-mm) length was attached to each of the strands with a metal hose clamp. This method had been used successfully in past studies [7,26]. Plastic zip ties were used on some of the 20-ft (6.1-m) specimens to test which system worked better. Use of the metal hose clamps, while being more time consuming to install, was found to be a more effective method and therefore these were used on all 40-ft (12.2-m) specimens. A typical setup of one of these devices attached to a strand is shown in Figure 4.3. The surface of the concrete that would act as a datum for measurement was rough. Therefore, a glass slide was glued to the concrete at this location to provide a smooth surface at this point.
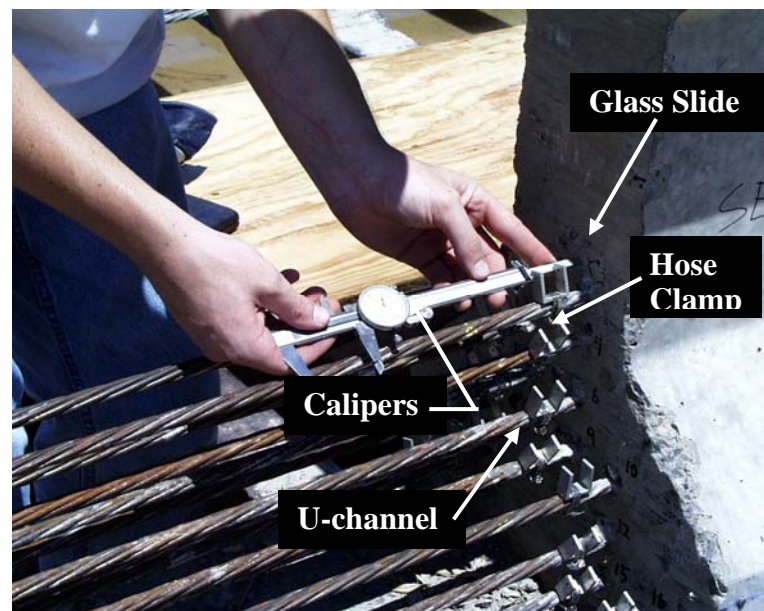
Figure 4.3: Instrumentation and Measurement of Strand Draw-In

49

To measure the draw-in, two measurements of the distance between the end of the channel and the face of the concrete had to be taken. The first measurement was performed before the pretensioning was released. After release another measurement was taken. All measurements were performed with analog calipers as shown in Figure 4.3. The point of contact of the end of the calipers and glass slide was marked with permanent marker along with the orientation of the calipers. This ensured that when the measurement was performed the second time, error would not be introduced by measuring a different point or orientation on the face of the beam.

The intended method of release of the pretensioning in the stands was by hydraulic jacking followed by gradual release of the pressure. This is the method typically used at the pretensioning plant. It would also facilitate measurement of draw-in because the strands would have little tendency to unwind and cause movement of the channel that was not associated with strand draw-in. The other method of release sometimes used is flame cutting of the strands. This instantaneously releases the prestress and there is a tendency for the twisted strand to unwind and ruin any opportunity for measurement. Unfortunately, due to communication problems at the plant, the top strands of beam LW6000-2 and LW6000–3 were flame cut and there was some unwinding of strand as shown in Figure 4.4. This did not seem to affect the readings of those strands because some of the prestress had been released and the hose clamps stopped the unwinding from extending into the area between the face of the concrete and the hose clamp.

Figure 4.4: Flame Cut Strands and Unwinding of Ends

4.3 DATA REDUCTION

The data from both the DEMEC strain and the strand draw-in measurements had to be reduced so that it could be used to determine the transfer lengths of the beams. This section describes these operations and the significance of the reductions.

4.3.1 DEMEC Strain Profile Smoothing

The value obtained from the measurement of two DEMEC points 7.87 in (200 mm) apart is applied to the middle of these two points. The 36 values (40 DEMEC Points) obtained from measuring one strip of points could be used to give a profile of the strain along the concrete, but this would not fully utilize the spacing of the DEMEC points. Some points overlapped the area in between the measurement of two points. The mid-point of these points falls in the area of the

measurement of the original two points. These points include information about the strain in this area and therefore were also used in determining the strain in this area. This technique is called smoothing the data [38] and is illustrated in Figure 4.5. The procedure takes three consecutive values and applies their average to the middle of these points. The general equation for this technique is given in Equation 4.1 [38].

$$\varepsilon_{i,smoothed} = \frac{\varepsilon_{i-1} + \varepsilon_i + \varepsilon_{i+1}}{3}$$ **Equation 4.1**
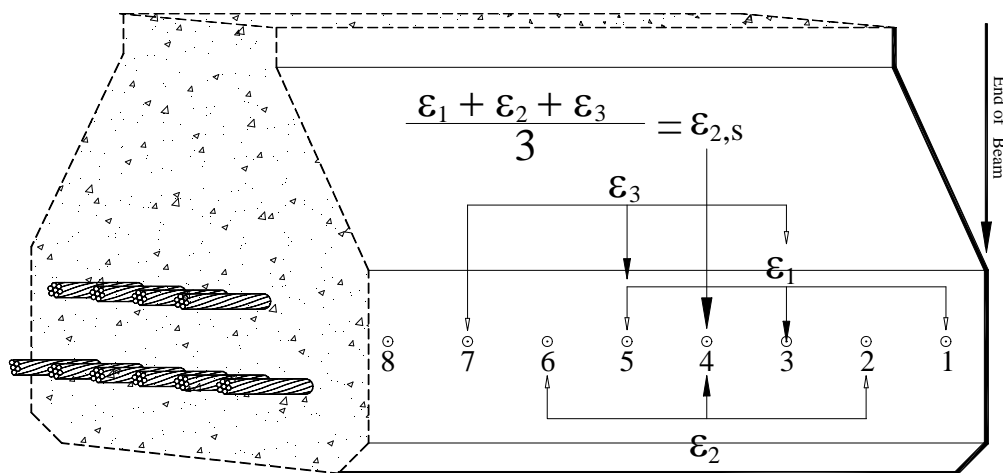
Figure 4.5: DEMEC Strain Profile Smoothing

The data obtained from the measurement of DEMEC points tends to have quite a bit of scatter associated with it. This is due to irregularity in the elastic modulus of the concrete at one-day combined with the precision of the DEMEC system. The smoothing technique will lessen this scatter and reduce the effect of data points that have values higher or lower than the average. By smoothing the data it is easier to define the plateau at which the constant strain in the beam is established.

52

The other operation necessary to reduce the data is to average the strain profiles for both sides of the beam. This will remove irregularities in the DEMEC data that only occurred on one side of the beam and accounts for differential heating of the beam due to sun exposure. The combination of both techniques allowed a much more precise establishment of the constant strain plateau. A plot of the smoothed and averaged data from one end of a beam is compared to the raw data in Figure 4.6.
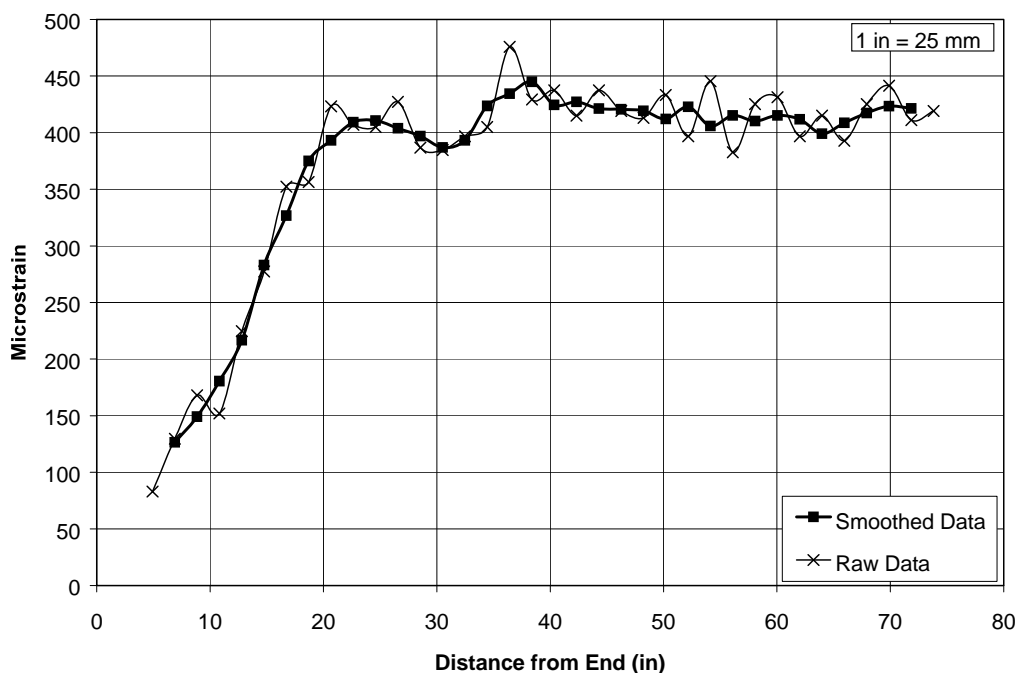
Figure 4.6: Strain Data Smoothing

4.3.2 Effect of Elastic Shortening on Draw-In Data

The difference in the values recorded from the measurement of the distance between the concrete and the end of the U-channel under prestressed and

released conditions is not the actual draw-in of the strand. Since the strand is initially under a high stress, elastic elongation of the strand occurs. Therefore, this elongation must be subtracted from the total displacement measured to arrive at the actual draw-in of the strand. Figure 4.7 shows the measured value before release, L_o, the measured value after release, L_r, the difference between these values, Δ_t, which is a combination of elastic shortening, Δ_e, and the actual draw-in, Δ_d. Using these values and the strain in the steel under the prestressed conditions, ε_{si}, it is possible to formulate Equation 4.2 that describes the actual draw-in of the strand after release.

$$\Delta d = \frac{\Delta t - \varepsilon_{si} \cdot L_r}{1 + \varepsilon_{si}}$$
<div align="right">**Equation 4.2**</div>
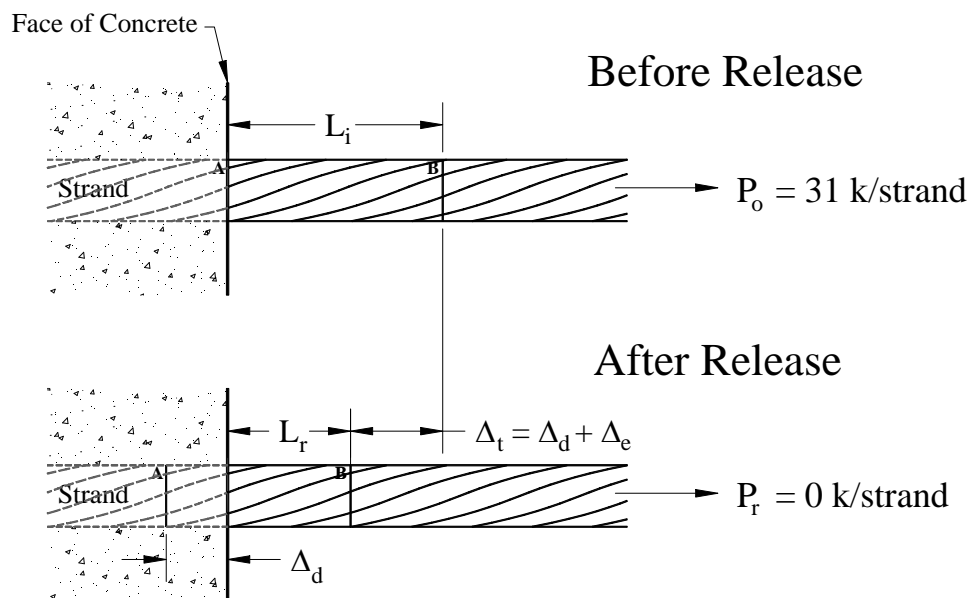
Figure 4.7: Draw-In Illustration

4.4 METHODS TO DETERMINE TRANSFER LENGTH

Many methods exist for determining the transfer length based on different types of measurements. Two methods for analyzing the data of the DEMEC strain measurements are used in this thesis. Another method is used to determine the transfer length from the strand draw-in values.

4.4.1 95% Average Maximum Strain

The first method used to determine transfer length was the 95% Average Maximum Strain (95% AMS) method [38]. The first step involves determining the point at which the strain is constant or the 100% strain plateau. This is a subjective determination based on viewing the stain profile. Once the starting point is defined, the average maximum strain (AMS) can be determined by averaging the data after this point.

The next step is to take 95% of the AMS and plot this line against the strain profile. The intersection of these two lines defines the transfer length, L_t. A typical profile with this method applied to it is illustrated in Figure 4.8. The individual strain profiles with the transfer length determined by the 95% AMS Method are all given in Appendix C.
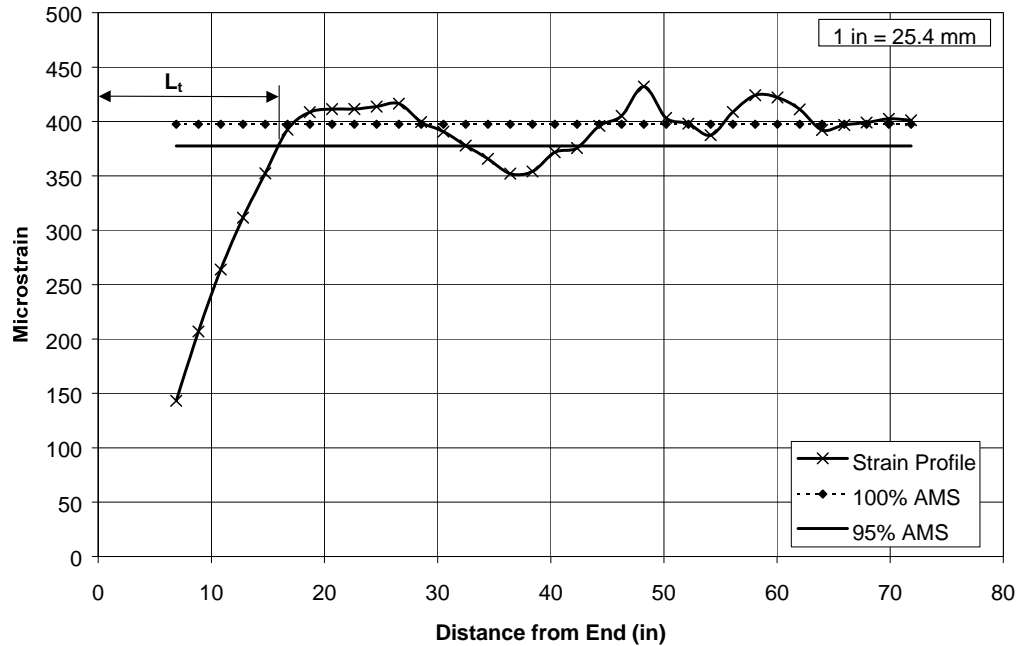
Figure 4.8: 95% Transfer Length Method

4.4.2 Slope-Intercept

The other method used with the DEMEC strain data is called the Slope-Intercept Method [33]. It is based on the assumption that the strain profile is typically bilinear. It is similar to the 95% AMS Method in that the AMS must be determined. However, another subjective judgment must be made for this method. It involves determining the slope of the increasing strain portion of the profile. Both the AMS line and the sloped line are then plotted on the strain profile and the intersection of these two lines defines the transfer length, L_t. This method is illustrated in Figure 4.9.

This method can give very similar results to the 95% AMS Method when the data is bilinear. It was used to verify the results of the 95% AMS Method for

56

the some of the beams. It could not be used on all the data because some of the profiles were extremely erratic, which was more common in the lightweight concrete beams. Use of this method for such profiles led to huge disparities between the value of transfer length from this method and the 95% AMS method. Also, some of the lightweight concrete beam data did not have a bilinear relationship and in those cases correlation between the methods was poor.
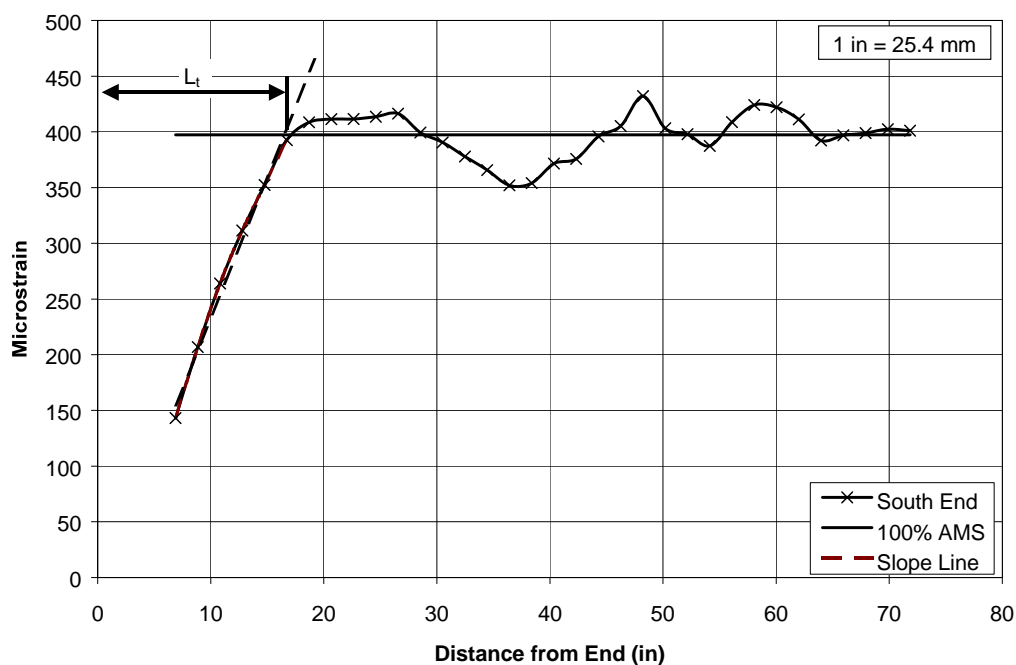
Figure 4.9: Slope-Intercept Method

4.4.3 Strand Draw-In

The values obtained from measurement of the draw-in can also be used to determine transfer length. The equation used to compute the transfer length from the amount of draw-in is given in Equation 4.3 [20]. In this equation L_t is the transfer length, Δ_d is the measured draw-in, ε_{si} is the initial strain in the steel due

57

to prestress, and α is a factor that adjusts for the type of strain curve. A value of $\alpha=2$ is used for a bilinear strain profile while $\alpha=3$ is used for a parabolic strain profile.

$$L_t = \frac{\alpha \cdot \Delta_d}{\varepsilon_{si}}$$

Equation 4.3

As discussed in Chapter 2, Russell and Burns [39] use a value of $\alpha=2$ in their formulation of the transfer length. The notation is different from Equation 4.3, but the equation is essentially the same. The value of $\alpha=2$ will be used for comparison in this discussion because it is a baseline to which all the values can be compared. The corresponding equation for transfer length is given in Equation 4.4.

$$L_t = \frac{2E_{ps}}{f_{si}}\Delta_d$$

Equation 4.4

4.5 TEST RESULTS

This section gives the results of the DEMEC strain and strand draw-in measurements for determining transfer length.

4.5.1 DEMEC Strain Measurement Results

The smoothing and averaging of the raw strain profile data was helpful in removing some of the irregularity in the different profiles. Despite this, it was still difficult to determine exactly where the strain plateau began on some of the strain profiles. A best estimate of the beginning of the plateau was found and the transfer lengths determined by the 95% AMS method with the results given in Table 4.1. As mentioned in Section 4.4.2, the slope-intercept method was used to

verify the 95% AMS method results on some of the strain profiles, but these results are not given here

Table 4.1: 95% AMS Transfer Length Results

Beam ID	Transfer Length, in	Transfer Length, mm
NW6000-1-N	20.9	530
NW6000-1-S	15.7	400
LW6000-20-N	37.2	945
LW6000-20-S	37.6	955
LW6000-1-N	37.8	960
LW6000-1-S	18.3	465
LW6000-2-N	33.9	860
LW6000-2-S	20.7	525
LW8000-20-N	37.2	945
LW8000-20-S	37.0	940
LW8000-1-N	36.6	930
LW8000-1-S	24.8	630
LW8000-2-N	35.4	900
LW8000-2-S	40.7	1035
LW8000-3-N	33.9	860
LW8000-3-S	36.6	930
Ave. NW6000	18.3	465
Ave. LW6000	30.9	785
Ave. LW8000	35.3	896

Due to the amount of scatter in the data, it was decided that all the data from the strain profiles of similar beams should be averaged. This gave a much clearer picture of what was occurring in the beams. These averaged strain profiles (ASP) are displayed as the heavy lines in Figure 4.10. The ASP from the normal weight beam data produced a profile that was expected, which was a bi-linear relationship in the strain profile. The lightweight beams did not produce ASP's that were typical. The LW6000 and LW8000 beams had ASP's that were very similar. These profiles are unique among transfer length tests in that they have a

59

preliminary plateau before the strain becomes constant. This could also be interpreted as a tri-linear curve. If this were a random occurrence, the profiles of different beam sets should not correlate so closely

The ending plateau strain of both lightweight concrete ASP curves is know to be the strain that should be developed in the beam because the difference in the strains of the normal weight and lightweight concrete beams is proportional to their different moduli of elasticity. The calculated ratio of the average lightweight concrete strain to the average normal weight concrete strain was 1.95. The calculated ratio of the average lightweight concrete elastic modulus to the average normal weight concrete modulus was 1.86. This correlation is evidence that the ASP's were accurate in predicting the strain plateau and therefore a reasonable approximation of the strain profile. Also, displayed on Figure 4.10 is a $\pm 10\%$ band to the ASP's. Most of the data fits within this band and therefore it seems that the averaging of data is meaningful.
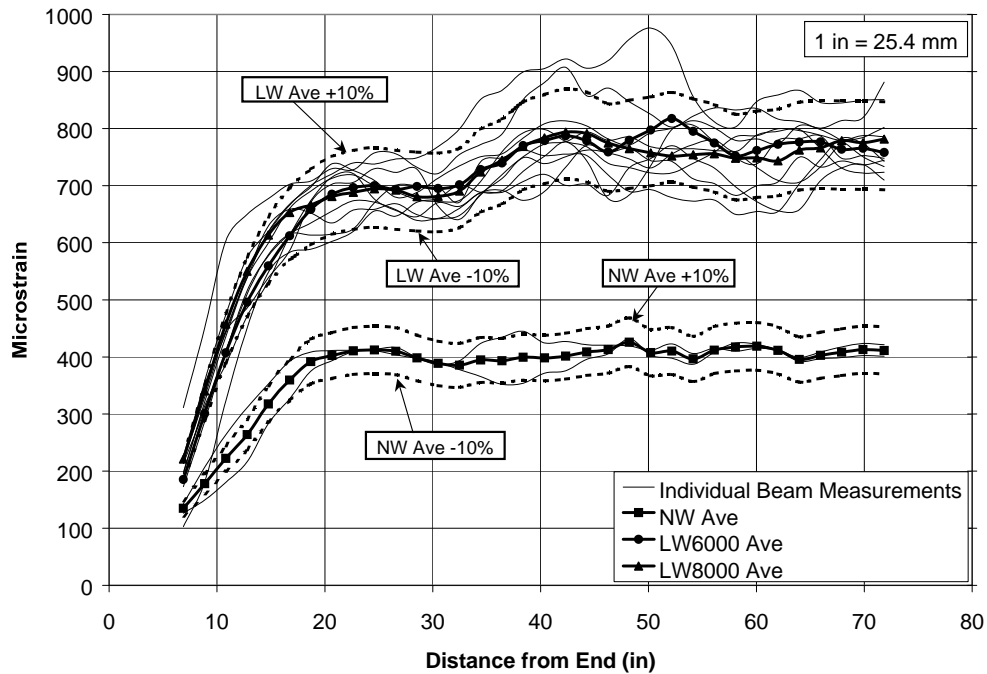
Figure 4.10: Average Strain Profiles

Using the averaged strain profiles, the 95% AMS method was again applied to the data. The results are given in Table 4.2. The better agreement between the two lightweight mixes is consistent with what is expected since both concrete mixes had similar moduli of elasticity. Also, the two concretes did not vary in strength as much as expected.

61

Table 4.2: Averaged Profile Transfer Lengths

Beam ID	Average Strain Profile Transfer Length, in / (mm)
NW6000	18.2 (463)
LW6000	35.8 (910)
LW8000	34.4 (875)

4.5.2 Draw-In Results

The exact draw-in values were determined from Equation 4.2 and these values are given in Table 4.3. This table compares the draw-in associated with all the strands, only the bottom strands, and only the top strands along with the maximums and minimums within all these groups (the strand on which these occurred is identified). This was done to see if there was any significance in the amount of draw-in due to the number of strands in an area, which did not seem to be a factor.

Table 4.3: Comparison of Draw-In Values

Beam ID	Strand Data					Notes
	Average All	**Max All**	**Min All**	**Average Top**	**Average Bottom**	
NW6000-1-N	0.047	0.056 (3)	0.039 (8)	0.047	0.047	
NW6000-1-S	0.054	0.063 (9)	0.041 (1)	0.052	0.054	7,12 bad
LW6000-20-N	0.066	0.100 (9)	0.033 (11)	x	x	zip ties
LW6000-20-S	0.053	0.077 (12)	0.031 (15)	x	x	
LW6000-1-N	0.046	0.066 (7)	0.035 (8)	0.045	0.047	
LW6000-1-S	0.049	0.074 (12)	0.028 (7)	0.047	0.050	
LW6000-2-N	0.047	0.059 (3)	0.032 (2)	0.037	0.049	
LW6000-2-S	0.050	0.062 (1,6)	0.042 (5,7)	0.053	0.050	9-12 bad
LW8000-20-N	0.036	0.064 (10)	0.020 (15)	x	x	zip ties
LW8000-20-S	0.038	0.054 (3)	0.021 (16)	x	x	
LW8000-1-N	0.045	0.057 (1)	0.040 (12)	0.050	0.044	
LW8000-1-S	0.042	0.067 (8)	0.015 (12)	0.041	0.042	
LW8000-2-N	0.039	0.051 (9)	0.034 (4,7)	0.050	0.042	2 bad
LW8000-2-S	0.042	0.054 (9)	0028 (5)	0.045	0.042	
LW8000-3-N	0.044	0.060 (8)	0.027 (2)	0.036	0.046	
LW8000-3-S	0.044	0.061 (2)	0.030 (4)	0.059	0.040	3,7-8 bad
LW6000	**0.052**			**0.045**	**0.049**	
LW6000*	**0.049**					
LW8000	**0.041**			**0.047**	**0.042**	
LW8000*	**0.042**					
NW6000	**0.050**			**0.049**	**0.051**	

Notes:
All units in inches (1 in = 25.4 mm)
* - Indicates that data from zip ties is not used in average
( ) - Indicates strand number

Despite the significant variance in the maximum and minimum values, it is interesting to note that there was not much variance in the amount of draw-in among all the 6,000-psi (41.4 MPa) mixes. Including the normal weight concrete but not including the zip-tie measurements, the average values ranged between 0.046 in (1.17 mm) and 0.053 in (1.35 mm). The range of values for the 8,000-psi (55.2 MPa) mixes was between 0.038 in (0.97 mm) and 0.045 in (1.14 mm). It is also interesting to note that both the lightweight and normal weight 6,000-psi (41.4 MPa) concrete mixes had average values of 0.049 in (1.24 mm) and 0.050 in (1.27 mm). These beams were released on the same day, which might be a factor

because all the measurements were done at the same time. The 8,000-psi (55.2 MPa) mixes were cast several days later and the average for these beams was 0.042 in (1.07 mm). Whether this was a function of the strand used in the beams or a correlation between the strengths of the beams is unknown.

The results from applying Equation 4.3 to the draw-in values are given in Table 4.4. The minimum and maximum values that are generally associated with α for normal weight concrete are given. This range will typically encompass the value obtained from the DEMEC measurement results [7,26]. The last column of the table is the α that was obtained from Equation 4.3 when the transfer length from the DEMEC measurement results is substituted into the equation. Values obtained from measurements using the zip-tie method are also included for comparison but these values are not included in the averages to keep the test method consistent. It should be noted that the values for α using the DEMEC data gives values between 2 and 3 for the normal weight concrete. However, most of the values for α in the lightweight beams exceed 3. This indicates that this method may not be valid for lightweight concrete. The shape of the average strain profiles in Figure 4.10 is another indicator that this method may not be accurate. The profiles do not have a bi-linear or parabolic shape, which the equations are based on.

Table 4.4: Transfer Length Values from Draw-In Testing Using Eqn. 4.3

Beam	Average Draw-In	L_t (α=2)	L_t (α=3)	α using Demec
NW6000-1-N	0.0466	14.6	21.8	2.87
NW6000-1-S	0.0535	16.7	25.1	1.88
LW6000-20-N*	0.0660	20.6	30.9	3.61
LW6000-20-S	0.0526	16.4	24.7	4.58
LW6000-1-N	0.0463	14.5	21.7	5.23
LW6000-1-S	0.0493	15.4	23.1	2.38
LW6000-2-N	0.0469	14.7	22.0	4.62
LW6000-2-S	0.0504	15.7	23.6	2.63
LW8000-20-N*	0.0362	11.3	17.0	6.58
LW8000-20-S	0.0378	11.8	17.7	6.27
LW8000-1-N	0.0450	14.1	21.1	5.21
LW8000-1-S	0.0415	13.0	19.5	3.83
LW8000-2-N	0.0387	12.1	18.1	5.86
LW8000-2-S	0.0422	13.2	19.8	6.18
LW8000-3-N	0.0442	13.8	20.7	4.90
LW8000-3-S	0.0443	13.8	20.8	5.29
NW6000	**0.0501**	**15.6**	**23.5**	**2.38**
LW6000	**0.0491**	**15.3**	**23.0**	**3.88**
LW8000	**0.0420**	**13.1**	**19.7**	**5.36**

Notes:

All units in inches (1 in = 25.4 mm)

* - Indicates that zip ties were used

Average values do not include values from * data

4.6 DISCUSSION OF TEST RESULTS

This section will discuss the results of the transfer length testing. Comparisons of the results will be made to concrete properties as well as the equations that attempt to describe transfer length.

4.6.1 Comparison of Methods

The average values found for the transfer length from all the methods are given below in Table 4.5. This gives a concise example of the variability that is inherent in determining transfer length. The variability in the lightweight concrete data is much greater than that of the normal weight concrete. This is due to the fact that most of the methods to determine transfer length were developed for normal weight concrete.

Table 4.5: Comparison of Transfer Length Methods

Beam ID	Individual Strain Profiles, in / (mm)	Average Strain Profiles, in / (mm)	Draw-In (α=2) in / (mm)	Draw-In (α=3) in / (mm)
NW6000	18.3 (465)	18.2 (463)	15.6 (397)	23.5 (596)
LW6000	22.1 (562)	35.8 (910)	15.4 (390)	23.0 (585)
LW8000	29.7 (755)	34.4 (875)	13.1 (333)	19.6 (499)

The table indicates that the draw-in results assume a completely different pattern than the DEMEC data. Namely, the LW8000 beams have the smallest transfer lengths. This is directly opposite of the data from the strain profiles which are a more direct measure of the transfer length. The average values from the individual strain profiles seem to indicate that the transfer length increases with the strength of the concrete. However, this is misleading because conventional equations usually equate a higher concrete strength with smaller transfer lengths. This is directly opposite the trend shown by the strand draw-in data. The averaged strain profile values give data that seems reasonable because their transfer lengths

can be clearly identified on the graph of each ASP without misinterpretation. The fact that the transfer lengths for the lightweight concrete mixes are similar for this method is reasonable because the strengths of these mixes did not vary by much and they both had similar moduli of elasticity.

As mentioned in Chapter 3, only six full size beams were cast along with two preliminary 20-ft (6.1-m) beams. This gave a total of 2, 6, and 8 sets of data for the NW6000, LW6000, and LW8000 beams for determining transfer length, respectively. Therefore, the following discussion must be viewed as preliminary due to the small sample size. Also, it should be noted that two different materials are being compared and that the basis models for determining transfer length were developed for normal weight concrete and not lightweight concrete.

4.6.2 Comparison to Concrete Properties

This section compares the transfer length and the concrete properties. The properties to be compared are the strength of the concrete and the modulus of elasticity.

Some of the equations used to define transfer length empirically use the strength of the concrete as a term in the equation [46,33]. Therefore, whether a trend existed between the concrete compressive strength and transfer length was examined. A comparison of the concrete strength and ASP transfer length values are given Table 4.6. Figure 4.11 displays these values along with the individual strain profile values. The graph seems to indicate that as the concrete strength increases, so does the transfer length. It is difficult to conclude that this is the actual trend of the data since any number of different sloping lines could be drawn

67

through the lightweight concrete data points. Viewing the normal weight and lightweight concrete beams separately, the lightweight data has a similar transfer length despite the different strengths of the concrete. No clear correlation is apparent from the data. Previous researchers have found trends using concrete compressive strength [46,33]. This is possible when the same type of material is used between tests. Applying the trend of previous research to the data in this study, as the concrete compressive strength increases, the transfer length should decrease. As stated previously, this is not the case for the data presented.

Table 4.6: Comparison of Transfer Length and f'$_{ci}$

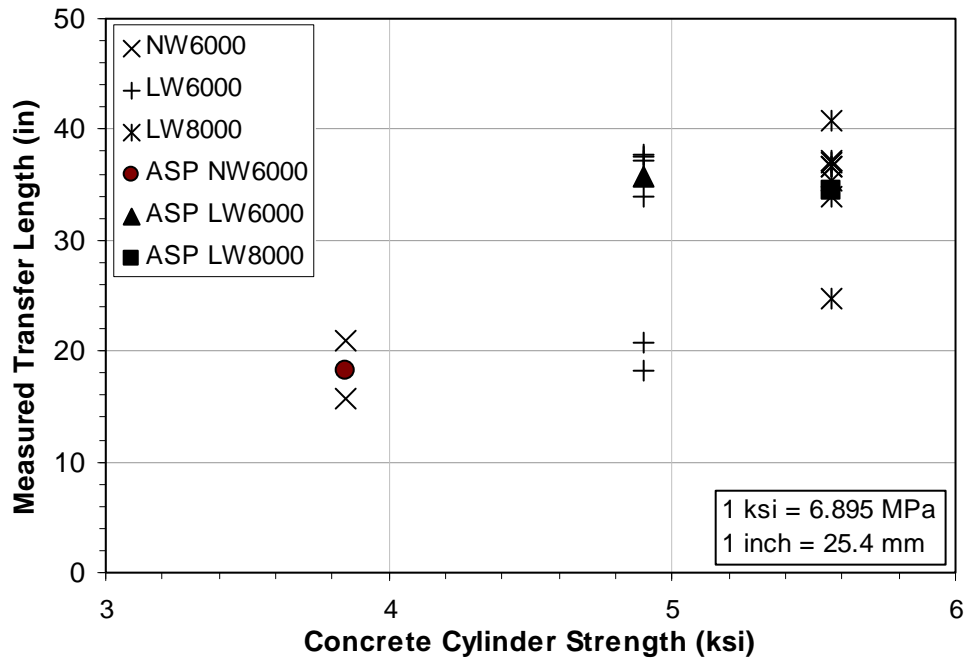| Beam ID	f'$_{ci}$ psi / (MPa)	Ave. Strain Profile Transfer Length, in / (mm)
NW6000	3,849 (26.54)	18.2 (463)
LW6000	4,902 (33.80)	35.8 (910)
LW8000	5,563 (38.36)	34.4 (875)

Figure 4.11: Comparison to Concrete Strength

Some equations that describe transfer length use the square root of f'_c as a variable. The ACI 318 Code gives an equation that relates the modulus of elasticity of normal weight concrete to the square root of f'_c [33]. The conclusion that can be drawn from this is that the modulus of elasticity may affect transfer length. It is logical assumption that the modulus of elasticity should affect the transfer length because it is a measure of the stiffness of the concrete and therefore affects the strains in the concrete, which determines the transfer length. To examine if a correlation between these properties existed in the data for this study a plot of the modulus of elasticity versus the transfer lengths was created. This plot is shown in Figure 4.12.
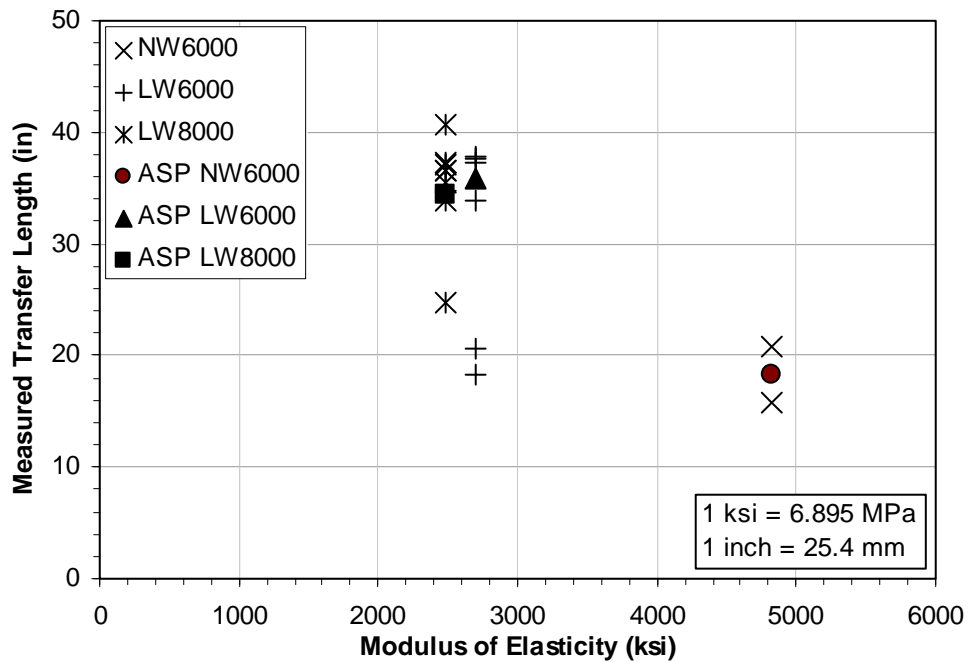
Figure 4.12: Modulus of Elasticity vs. Transfer Length

The trend from the plot indicates that as the modulus of elasticity increases, the transfer length decreases. This is consistent with an equation developed by Buckner for determining transfer length, which uses the modulus in the denominator [13]. This model will be examined further in Section 4.6.3.

Table 4.7 gives a correlation between the transfer length and initial modulus of elasticity, f'$_{ci}$. Included in this table is the transfer length divided by the inverse of the modulus. If the modulus of the concrete was a factor that influenced the transfer length, then these values should similar. The result is that these values are similar, which supports the theory that modulus plays an important role in determining transfer length.

Table 4.7: Comparison of Transfer Length and Modulus of Elasticity

Beam ID	E_{ci} ksi / (MPa)	Ave. Strain Profile Transfer Length, in / (mm)	$\dfrac{L_t}{\left(1/E_{ci}\right)} \times 10^{-3}$
NW6000	4,829 (33,296)	18.2 (463)	88.0
LW6000	2,693 (18,568)	35.8 (910)	96.5
LW8000	2,489 (17,162)	34.4 (875)	85.7

4.6.3 Comparison to Transfer Length Equations

There are many equations that attempt to describe transfer length. Most of these equations are based on studies of normal weight concrete and therefore may not apply to lightweight concrete directly. This section will compare the transfer lengths with some of the popular expressions for transfer length. More importantly, it will compare the transfer length to the ACI Building Code [22] and AASHTO Code [21] equations, which are used for design.

Each comparison uses a graph that plots the predicted transfer length versus the measured transfer length. The dashed line on each graph represents complete agreement between the predicted and measured values. For the model that a graph represents to be conservative, 95% of the data should fall below the dashed line.

Table 4.8 gives the values for the calculated transfer lengths for the different beams. These expressions were chosen because of the difference between the expressions. Some depend on the diameter of the strand alone and others depend on the concrete strength or the modulus of elasticity. From the

previous discussion of transfer length in comparison to concrete properties, it is predicted that equations using the modulus of elasticity as a variable will give better correlation with the results.

Table 4.8: Transfer Length Equations and Predicted Values for Beams

Author	Transfer Length Equation	L_t NW6000	L_t LW6000	L_t LW8000
ACI 318 [2]	$L_t = \dfrac{f_{se}}{3} d_b$	32.1 (815)	30.7 (781)	30.5 (774)
	$L_t \approx 50 \cdot d_b$	25.0 (635)	25.0 (635)	25.0 (635)
AASHTO Shear Provisions [1]	$L_t = 60 \cdot d_b$	30.0 (762)	30.0 (762)	30.0 (762)
Russell & Burns [39]	$L_t = \dfrac{f_{se}}{2} d_b$	48.2 (1223)	46.1 (1171)	45.7 (1161)
Zia & Mostafa [46]	$L_t = 1.5 \dfrac{f_{si}}{f'_{ci}} d_b - 4.6$	35.0 (888)	26.5 (672)	22.8 (578)
Buckner (FHWA) [13]	$L_t = \dfrac{1250 f_{si} d_b}{E_c}$	26.3 (667)	47.1 (1197)	51.0 (1295)

In some studies of normal weight concrete it was found that the ACI 318 Code equation was a conservative estimate of the transfer length [7]. This is also the case for the normal weight concrete beams measured in this study, as shown in Figure 4.13. This figure compares the ACI 318 Code equation using f_{se} as a variable in the equation for transfer length (Eqn. 2.14). The value for f_{se} was calculated based on the recommendations of ACI 318 [45]. All the normal weight data falls below the line that signifies complete agreement between equation and measurement. This equation is not conservative for most of the lightweight

concrete data, except for three points. This equation was formulated to be a conservative estimate of the transfer length. Therefore, it is reasonable to conclude that the ACI 318 Code equation does not model the transfer length for lightweight concrete based on the limited data sample from this study.
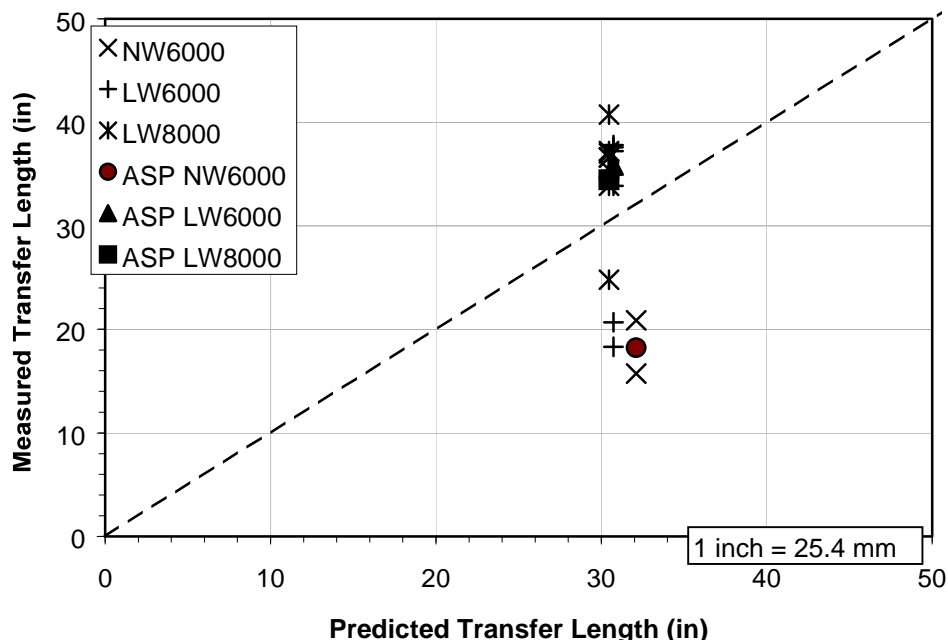

Figure 4.13: Comparison to ACI 318 Code

The ACI 318 Code gives an approximation to the transfer length equation as $50d_b$ [2]. This approximation is based on an effective stress in the strands of 150 ksi (1,034 MPa). This stress is usually reached at some time after 28 days. The beams in this study were measured the day of release and therefore had an effective stress above 180 ksi (1,241 MPa) for all beams. It is clear from Figure 4.14 that this model only fits the normal weight concrete beam. Therefore, it is conservative in the case of normal weight concrete because the effective stress in the strand is much higher than the model assumes. It also indicates that the model

73

is less conservative than the ACI 318 equation for transfer length in this study because the effective stress used in the approximation is lower than the actual stress, leading to smaller transfer lengths.

The data for the lightweight concrete beams is nearly 10 in (254 mm) on average above the predicted value for transfer length. Only two data points from all the lightweight data falls below the line that indicates agreement between model and measured data. Since this model is dependent on f_{se} equal to 150 ksi (1,034 MPa) and was developed for normal weight concrete it cannot be used to accurately determine transfer length in lightweight concrete beams.
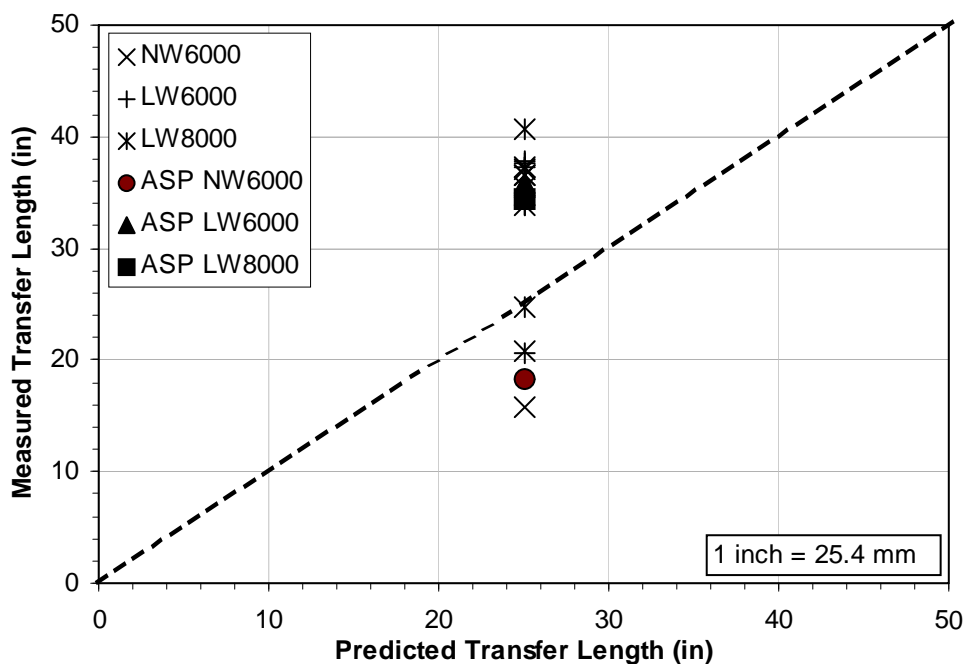

Figure 4.14: Comparison to ACI 318 Approximation

The new AASHTO Shear Specifications are more conservative than the ACI 318 Specifications and consider the transfer length to be $60d_b$ [1].This is done to update the code to the current practices of prestressing where higher

74

initial prestresses are used and low relaxation strands are common. Despite this, the model still underestimates the transfer length of the lightweight and a similar argument can be given as the one stated above for the ACI 318 approximation. The data for the normal weight concrete is again conservative, as would be expected due the increased multiplier on the strand diameter. The comparison of this AASHTO model to the data is shown in Figure 4.15.
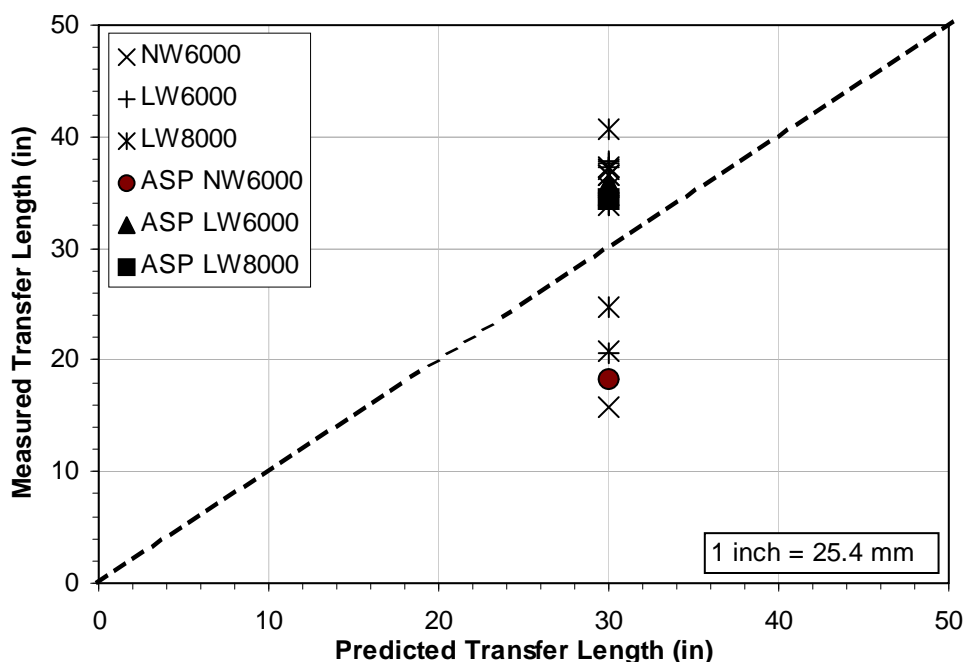

Figure 4.15: Comparison to AASHTO Shear Provisions

Russell and Burns developed a model that included much of the existing data on transfer length at that time, not just the data from one study. The result was an equation very similar to ACI 318, but with a different stress in the denominator [39]. Figure 4.16 shows that Russell and Burns's model covers all the data including the lightweight values and is conservative. It includes all the values from the lightweight beams with a factor of safety, but overestimates the

transfer length in the normal weight beams by over 100%. Despite the fact that this model accurately bounds all the data in this study, it is important to note that the model does not accurately model the trend in the data.
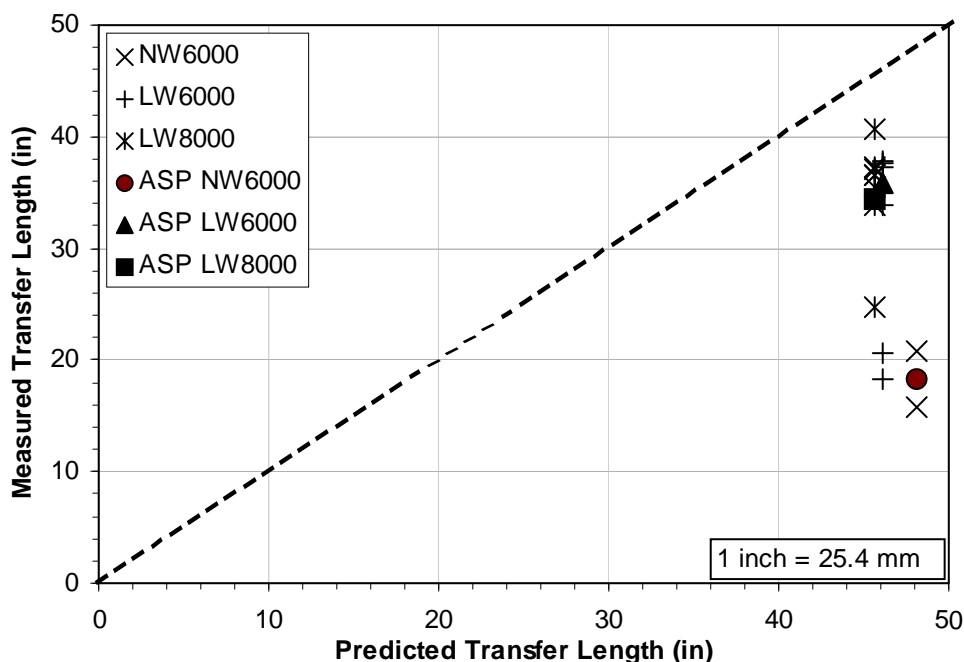

Figure 4.16: Comparison to Russell & Burns

The previous four models used f_{se} and d_b as variables in the equations to describe the transfer length. The only model that made a conservative estimate for the transfer length was the Russell and Burns model. All the models unanimously failed to predict the correct trend of the data. Therefore, using only the strand diameter to predict transfer length for normal weight and lightweight concrete is not possible. The two equations that used f_{se} as a variable predicted a trend that was opposite that of the data. This indicates that these variables alone cannot describe the behavior of normal weight and lightweight concrete transfer lengths together.

76

The next two models use a combination of the two variables described above, f_{se} and d_b. Also included in these models are properties of the concrete. The Zia and Mostafa model uses concrete compressive strength as a variable and the Buckner model uses the modulus of elasticity of the concrete as a variable. As shown earlier, the concrete compressive strength does not seem to affect the transfer length in a way that is expected from past research [33,43]. Specifically, as concrete strength increases, the transfer length should decrease.

In the Zia and Mostafa model the concrete compressive strength is in the denominator (Eqn. 2.10). Therefore, since the compressive strengths of the lightweight concretes in this study were larger than the normal weight concrete, the model would predict smaller transfer lengths for the lightweight concrete beams. However, as discussed earlier, the trend between compressive strength for normal weight and lightweight concrete was not typical. Therefore, despite the increased strength of the lightweight concrete over the normal weight concrete, it is not expected that this model would fit the lightweight data well. This is exactly what the data shows, as shown in Figure 4.17. Again, as was seen in the comparison with only the concrete strength, the trend of the data is opposite to the predicted line.
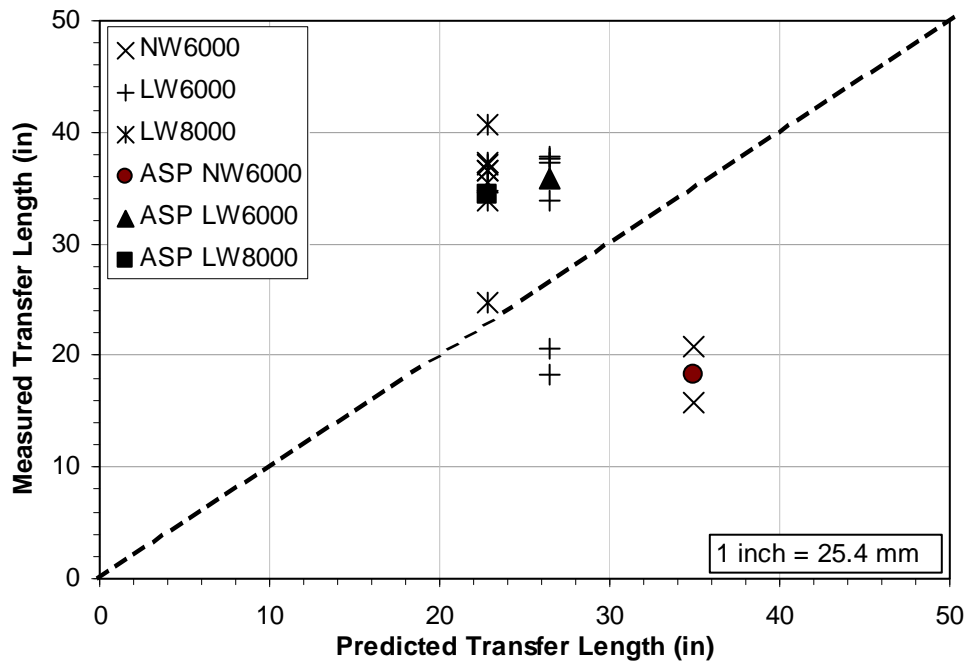
Figure 4.17: Comparison to Zia & Mostafa

The reason for the opposite trend in the data when the compressive strengths are compared to the transfer lengths is due to the difference in elastic modulus between the normal weight and lightweight concretes. A model that accounts for this difference was developed by Buckner [13]. It uses the modulus of elasticity as a variable in the denominator of the transfer length (Eqn 2.13) and therefore fits the relationship discussed between the transfer length and elastic modulus discussed earlier. Figure 4.18 shows that the model is conservative for all the data and follows the trend of the data. Also, since the modulus of the lightweight concrete tends to level out despite increases in compressive strength [22], one would expect to see the lightweight data gather in the same area. The

78

data seems to follow this trend, but more testing needs to be performed before a definitive trend can be established.

The figure also shows a similar amount of conservatism between data sets that was not seen in the Russell and Burns model. Changing the constant in this equation could lead to an accurate representation of the transfer length. This is shown in the figure by the bold line that best fits the averaged strain profile data. The results of this comparison leads to the conclusion that an accurate model that incorporates lightweight as well as normal weight concrete can be developed for transfer length. The key to the accuracy of this model is the use of the modulus of elasticity in the equation that describes behavior, with the results shown in Figure 4.18.

The plot shows Measured Transfer Length (in) on the y-axis (0 to 50) versus Predicted Transfer Length (in) on the x-axis (0 to 60). Legend: ✕ NW6000, + LW6000, ✳ LW8000, ● ASP NW6000, ▲ ASP LW6000, ■ ASP LW8000.

$$L_t = \frac{900\, f_{si} d_b}{E_c}$$
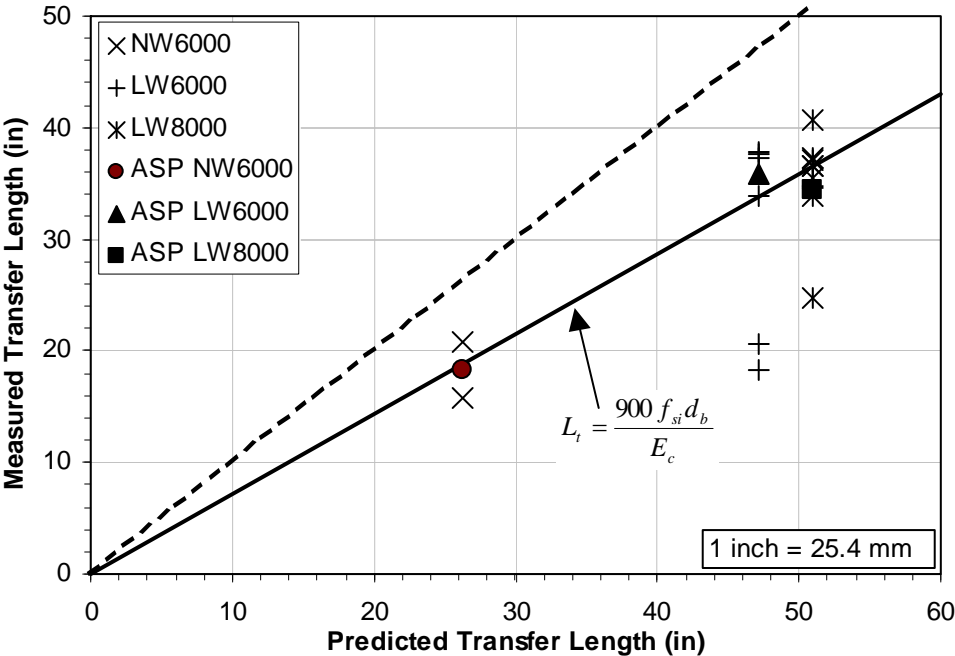
1 inch = 25.4 mm

Figure 4.18: Comparison to Buckner

The last comparison made is between the draw-in data and the measured transfer lengths. The dashed line in Figure 4.19 represents Equation 4.4 [39]. This graph shows that this model tends to underestimate the transfer length for all the data. This may be because the draw-in is more affected by the concrete strength than the elastic modulus. This is definitely the trend exhibited by the data. The concrete strengths of the NW6000 and LW6000 mixes were similar at the time of draw-in testing and the average of the measured values was very close. The strength of the LW8000 concrete mix was higher and the average of the draw-in values was less than those of the other mixes.
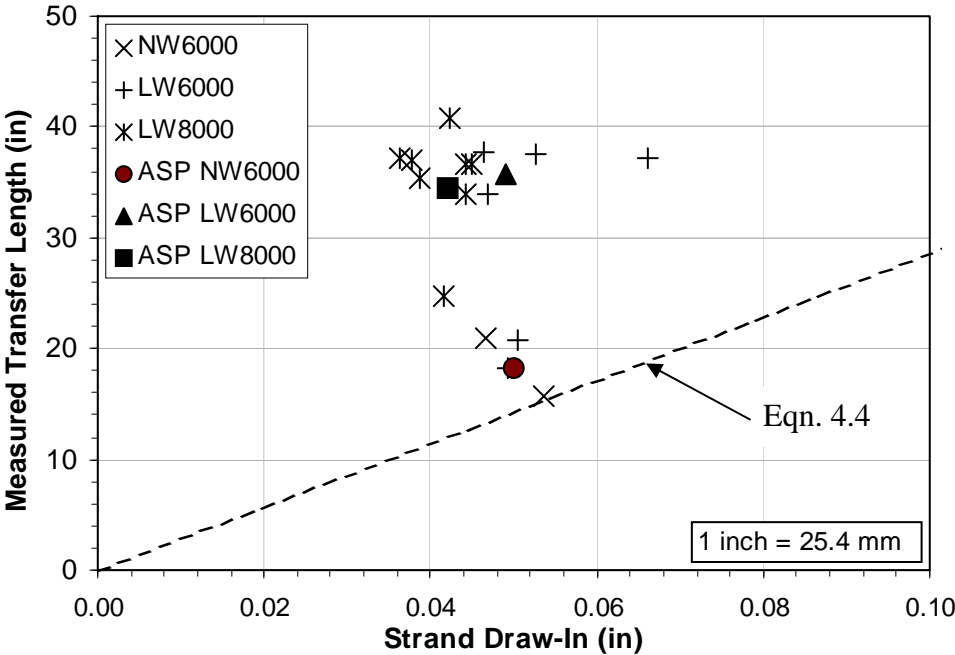

Figure 4.19: Compareison of Strand Draw-In to Transfer Length

Chapter 5: Development Length Testing

5.1 INTRODUCTION

The final phase of testing for this stage of the research project was full-scale testing of the AASHTO Type I precast pretensioned prestessed beams with composite decks. The main focus of the tests performed on the 40-ft (12.2-m) long specimens was evaluation of the development lengths. In addition to investigating the development lengths, the tests would also determine the moment resisting capacity of the composite beams. Although the tests could not directly determine the development length for each test, they could be used to determine whether the development length was less than or greater than the tested embedment length. This information would be used to determine whether the ACI 318 and AASHTO code and design specifications along with other proposed development length equations accurately modeled the behavior of the beams.

The development length is an important quantity to determine because if the bond between the concrete and strand is not sufficient to develop the ultimate moment capacity of the composite beam, then the full strength of the beam based on design equations cannot be achieved. It was important to observe whether the code provisions and development length equations, generally based on tests of normal weight concrete girders, were conservative for lightweight concrete.

The beams were constructed 40-ft (12.2-m) long so that it was possible to conduct two development length tests per beam at a span length of 24 ft (7.3 m). The maximum embedment length that was tested was 80 in (2,032 mm). Prior

testing of similar normal weight AASHTO Type I concrete beams at the FSEL indicated that damage from one test would not extend into the other end of the same beam when it was repositioned for the next test [7]. Due to the small number of specimens, this was advantageous because it allowed twice as many development length tests as beams.

5.2 TEST SETUP

This section describes the layout and apparatus used for loading and supporting the concrete beams. Much of the test setup used for the beam testing had been proven to be effective by tests of a similar nature that had been performed at FSEL in the past [7,26].

5.2.1 Load Setup

The width of the deck slab was selected based on the fact that the FSEL had a loading frame with a 7-ft (2.1-m) clear distance between its support legs. With a 6.5-ft (2.0-m) width of the deck slab, this would leave 3 in (76.2 mm) between each side of the edge of the deck and the legs of the loading frame. Attached to the load frame was a steel I-beam on which the load actuator could move such that the load could be placed anywhere between the support legs. Each leg of the loading frame was tied down to the floor by four threaded rods The loading frame and components are shown in Figure 5.1.
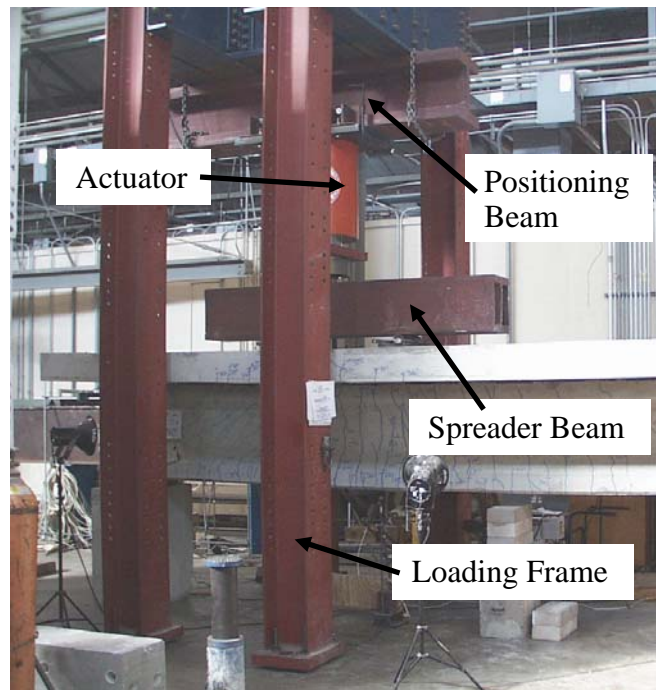
Figure 5.1: Load Frame and Components

5.2.2 Beam Setup

A steel spreader beam was used to transfer the load from the actuator to the concrete beam. This distributed the load from the single point of contact of the actuator to two points on the concrete beam. Two 2.5-in (63.5-mm) diameter steel rollers were used to transfer the load from the steel spreader beam to the concrete beam. These rollers were free to move on steel loading pads which assured that horizontal shear was not transferred to the prestressed composite concrete test beam. Steel bumpers were welded to the sides of the loading pads to ensure that the rollers could not roll off the pads. Finally, the steel pads were secured in the desired position with hydrostone between the pad and the top of the deck, which would produce a uniform stress distribution over the entire loading pad area. The

distance between the centerlines of the loading pads was 3 ft (0.91 m). This arrangement is shown in Figure 5.2.
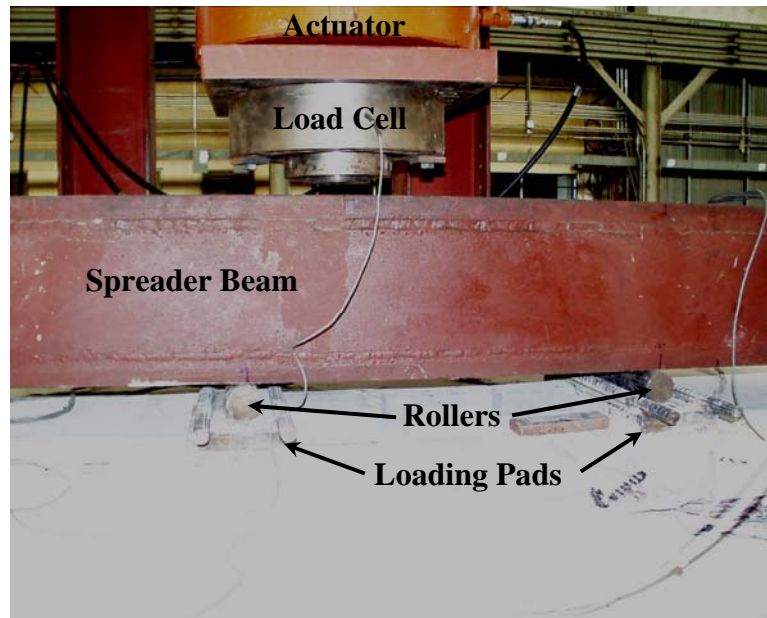

Figure 5.2: Spreader Beam and Load Pads

To bring the test specimen up to the height of the actuator, two reinforced concrete blocks 3-ft (0.91-m) high were used as supports. To distribute the load applied at the supports steel reinforced elastometric bearing pads were placed between each support block and the prestressed beam. This arrangement is shown in Figure 5.3.
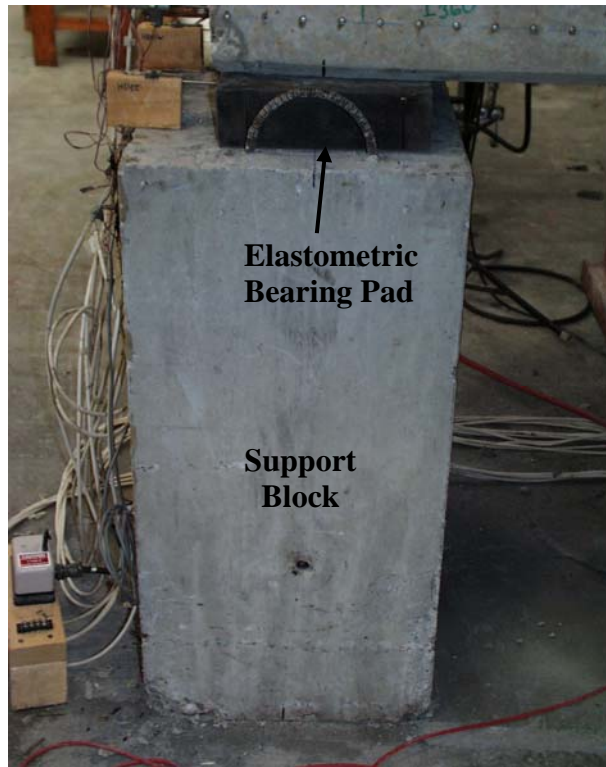
Figure 5.3: Support Set-Up

5.2.3 Test Geometry

As indicated previously, the span length to be tested was 24 ft (7.32 m), as shown in Figure 5.4. This arrangement ensured that damage from cracking from one test did not overlap the next test area. With a span length of 24 ft (7.32 m), approximately 16-ft (4.88-m) of the beam was cantilevered off the middle support.

The distance from the end of the beam to the first loading point on the beam was the embedment length, L_e. To develop a constant moment region between this point and the next loading point on the beam, the actuator load had to be placed a certain distance, a, from the first load point on the beam. This was

based on the static moment from the applied load and dead weight of the beam. Due to the distributed load from the self-weight of the beam, a perfectly constant moment region could not be developed. However, since the magnitude of the applied moment was much greater than the moment due to dead load, a nearly constant moment region was developed. The geometry of this test setup is shown in Figure 5.4.
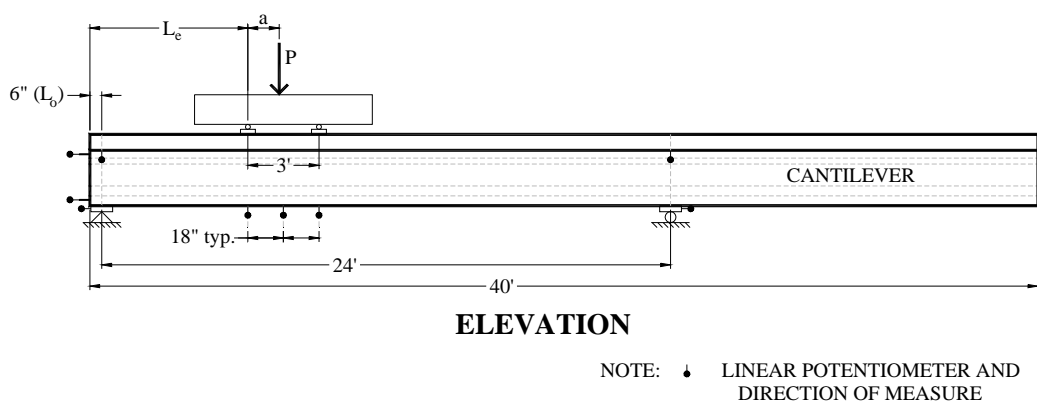

Figure 5.4: Geometry of Test Set-Up

Since only the normal weight (NW6000-1) and the two lightweight beams (LW6000-1 & -2) were to be tested in this portion of the research project, the embedment length that was chosen for each test had to be chosen with care so that valuable data was obtained from each test. The normal weight beam would be the control in the experiment. Therefore, the two embedment lengths used for these tests should bracket all the other embedment lengths tested on the lightweight concrete beams. The ACI 318 and AASHTO design equation (Eqn. 2.15) predicted a development length of 82 in (2,083 mm) for the normal weight concrete beam. It was decided that 80 in (2,032 mm) should be used as the first embedment length because previous research indicated that it was unlikely that

the beam would actually have bond failure at the code development length [7. A 60-in (1,524–mm) embedment length test was the other test performed on the normal weight beam because this was the smallest distance that should produce a flexural failure, rather than a shear failure. Also, if the tests were successful at 60-in (1,524–mm), there would be no doubt that the development lengths for all the beams was less than that given in the ACI and AASHTO codes.

The ACI 318 and AASHTO equation (Eqn. 2.15) for development length was used to calculate the development length of the lightweight concrete beams. Based on these calculations, the development length of these lightweight concrete beams was 86.3 in (2,192 mm). The testing of the normal weight beam was completed before testing of the lightweight beams and no bond failure had occurred at a 60 in (1,524 mm) embedment length. Therefore, based on these tests, the lightweight concrete beams were not expected to experience bond failure at an 80 in (2,032 mm) embedment length. If bond failure had occurred at 80 in (2,032 mm), then the next test would have used a longer embedment length.

Table 5.1 lists the embedment lengths that were used for the tests of the beams reported in this thesis along with the load point distance, a, as shown in Figure 5.4. Tests with similar embedment length are referred to as companion beams. There were two companion beams for each embedment length tested. The tests between these companion beams varied the type of concrete in the prestressed beam or the type of deck system. The embedment length is also the length of the shear span with the highest value of shear in the beam.

Table 5.1: Development Length Tests

Beam ID	Embedment Length, in / (mm)	a in / (mm)	Lightweight Deck Panels
NW6000-1-N-80	80 (2,032)	10.8 (274)	No
NW6000-1-S-70	60 (1,524)	9.18 (233)	No
LW6000-1-N-80	80 (2,032)	9.6 (244)	No
LW6000-1-S-70	70 (1,778)	9.12 (232)	No
LW6000-2-N-70	70 (1,778)	9.12 (232)	Yes
LW6000-2-S-60	60 (1,524)	7.68 (195)	Yes

5.3 INSTRUMENTATION

The beams were instrumented to record measurements of load, deflection, strain, and strand slip during the tests. The different types of measurements and instrumentation are described in the sections that follow.

5.3.1 Load

The load applied to the spreader beam by the actuator was measured in several ways. A load cell was attached to the actuator and the strain measurements were recorded by the data acquisition system. To check that the load cell was reading the true load applied to the beam, several back-up systems were used. An analog pressure gauge was attached to the hydraulic line and this pressure was read each time the loading was stopped. The load could be determined by multiplying the pressure by the known area of the loading ram. This method was

only accurate to a hydraulic pressure of ±25 psi, which was accurate enough to serve as a rough check of the digital measurements from load cell data. During one of the test, a digital pressure gauge was also attached to one of the lines to measure the pressure at the same interval as the strain in the load cell was being measured. These values were compared after the test to check that the load cell was measuring accurately during the test. All the checks performed on the load cell measurements indicated that it performed within the nominal parameters specified for the load cell. The actuator and attached load cell was previously shown in Figure 5.2.

5.3.2 Beam Displacement

To measure the deflection of the beam due to the applied load, three linear potentiometers were used in the constant moment region. One potentiometer was placed under the near load point, one midway between the loads, and one under the far load point. The distance between each consecutive potentiometer was 18 in (457 mm). The displacement capacity of all these potentiometers was 6 in (152 mm). The setup of these devices is shown in Figure 5.6 and their locations were previously indicated in Figure 5.4.
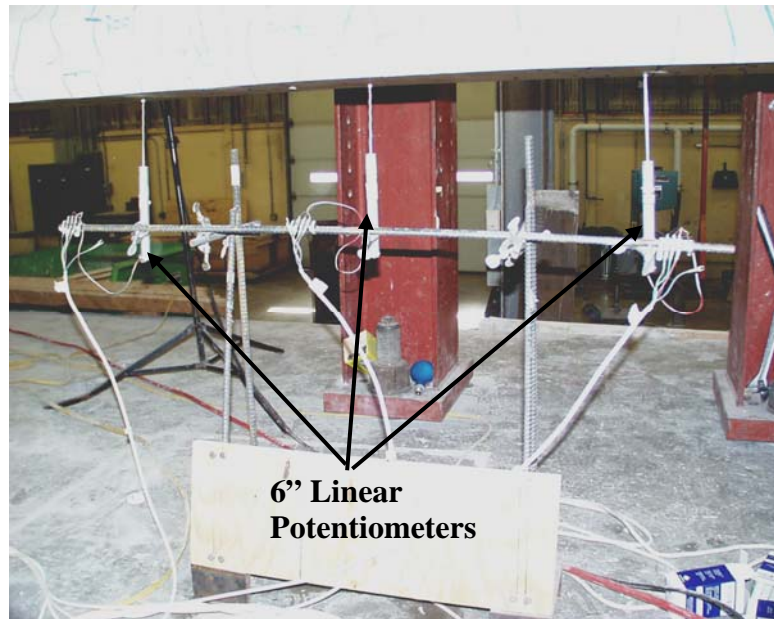
Figure 5.6: Beam Displacement Potentiometers

A manual backup of this system was also employed. Two holes were drilled into the face of the prestressed concrete beam at the mid point of each of the supports at the centroid of the precast pretensioned concrete beam to support two screws. Piano wire was tied to each of these screws and tensioned. A 1/100-in division ruler and a mirror were glued to the beam at the mid point between the load points such that the piano wire crossed the ruler as shown in Figure 5.7. The actual displacement of the beam, without support displacement, could then be read at each load point during the test. The mirror was used to line up the piano wire with its reflection so that no error was introduced by readings that were not consistently level.
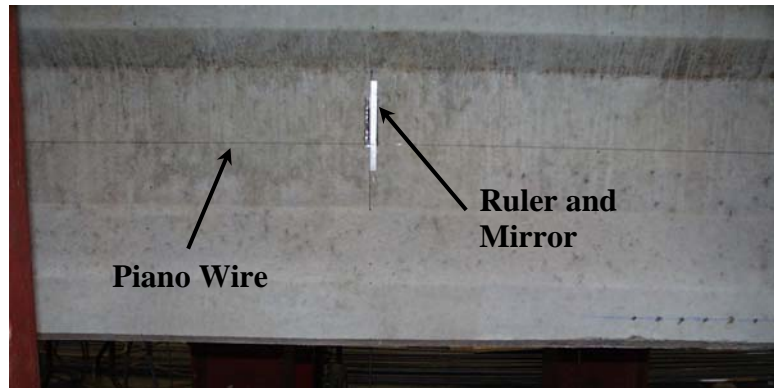
Figure 5.7: Manual Deflection Instrumentation

5.3.3 Support Displacement

Linear potentiometers were also used to measure vertical and horizontal deflections of the bearing pads due to the applied load. Two potentiometers, with 2-in (50.8–mm) displacement capacities, were used to measure the horizontal displacement of the support pad to determine if equal amount of displacement were occurring in the support pad. This system was used for each support pad, as shown in Figure 5.8.

Figure 5.8: Horizontal Displacement Measurement of Bearing Pad

Two string potentiometers, with 5-inch (127 mm) displacement capacities, were used to measure the vertical displacement of the beam at the deck level. Two string pots were used at each end to determine if any twisting of the beam occurred during the tests, as shown in Figure 5.9.
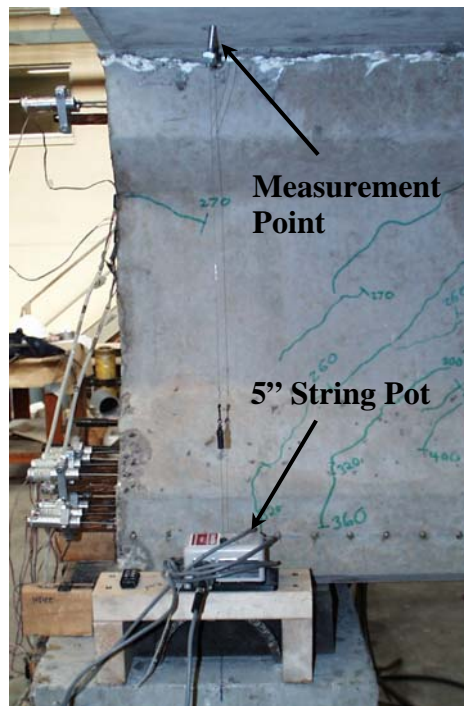

Figure 5.9: Vertical Displacement Measurement of Bearing Pad

5.3.4 Strand Slip

An important measurement that was recorded during the test was the amount of strand slip that occurred at the exposed ends of the prestressing strand. This was accomplished with the use of linear potentiometers attached to each of the strands. All the potentiometers had a 2-in (50.8-mm) displacement capacity. A specially designed clamp was attached to the strand and a potentiometer secured

to this device, as shown in Figure 5.10. The potentiometer measured the distance between the face of the concrete and the front end of the potentiometer. A glass slide was placed between the concrete and the end of the potentiometer. This gave a smooth surface for the end of the potentiometer to bear against on the end face of the beam. Every strand was instrumented to measure strand slip.
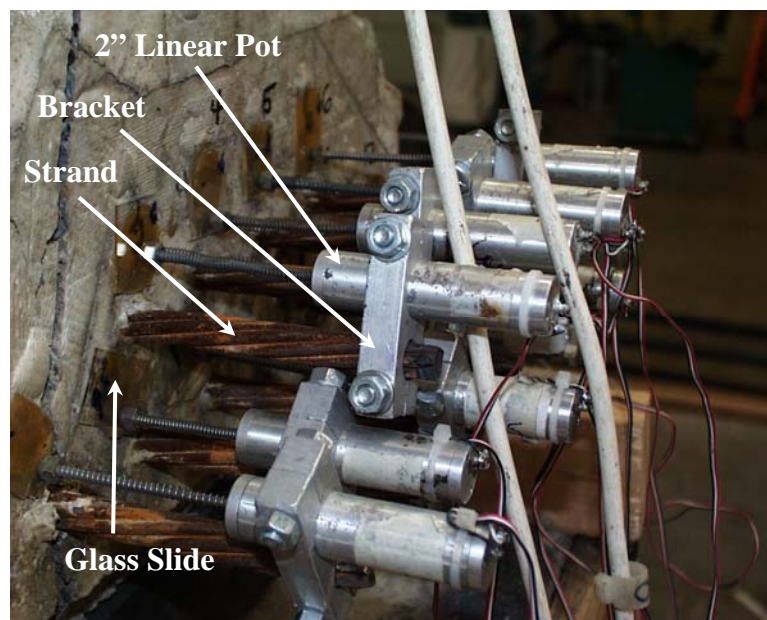

Figure 5.10: Strand Slip Setup

5.3.5 Concrete Strain

Concrete strain gauges were placed on the deck to measure the strains during the tests. This strain data was useful in determining the point at which the concrete was about to crush during the tests. Strain gauges were placed in a pattern as illustrated in Figure 5.11 with the actual gauges shown in Figure 5.12. This instrumentation allowed the strains between the load points to be measured by the six gauges placed near the centerline of the beam. The uniformity of the

strain in this region would indicate whether a constant moment region had been established. Also, the two gauges on the outside edge of the slab were used to check the strain uniformity across the width of the slab.
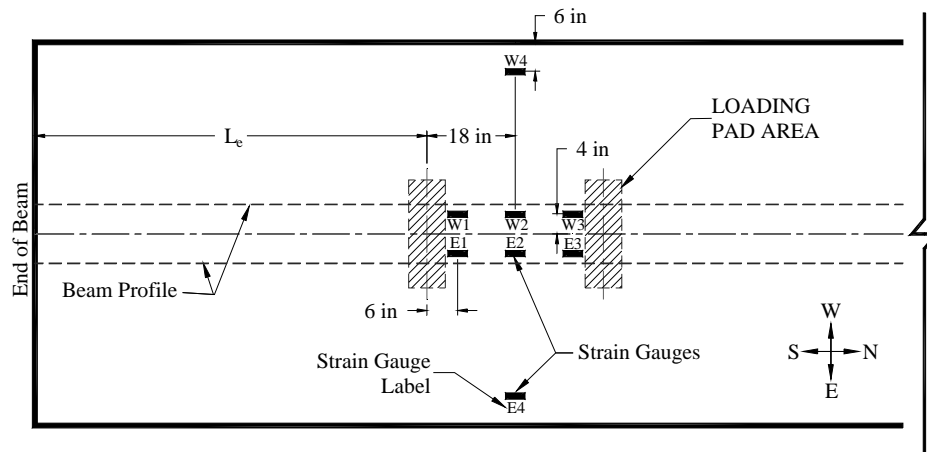

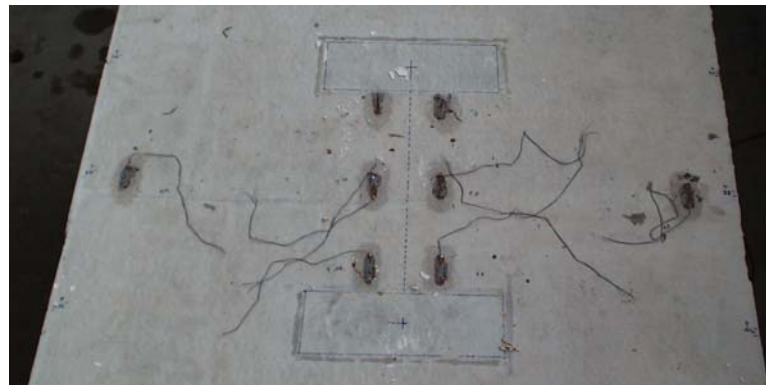**Figure 5.11: Strain Gauge Placement**

Figure 5.12: Actual Strain Gauge Placement

5.3.6 Data Acquisition

All data was recorded on a computer running an Excel measurement program called Measure. When loading, data was taken every two seconds for all channels. When loading was stopped and cracks were being marked, data was

94

acquired every 10 seconds for all channels. A picture of the data acquisition computer and equipment is shown in Figure 5.13.

Figure 5.13: Data Acquisition System

5.4 TEST PROCEDURE

Before loading of the beam proceeded, all instrumentation was checked to ensure that it was working within the nominal parameters specified for each instrument. Linear potentiometers were checked by inserting gauge blocks of a precise length and recording the output for displacement. The beam was loaded to less than 50 kips (223 kN) to check that all strain gauges and the load cell were functioning correctly.

After this pretest check had been performed, the beam was loaded in 30 kip (134 kN) increments. When loading was stopped at each load increment, data was recorded for the values of the manual deflection, pressure gauge, computer

load, and computer deflection for the test record in case of power failure. This was also when the cracks were marked on the beam.

When the cracking load was reached, the next load step was to reduce the load to zero followed by reloading to the prior load level. The data from the unload/reload was used to show that the original stiffness could still be relied upon after initial cracking. Loading after cracking increased by 30 kips (134 kN) per load step. When significant yielding of the beam had occurred and another 30 kips (134 kN) could not be gained in load, loading continued until a certain deflection was reached. Plots of the load-deflection curves for all the test performed are given in Appendix D. Loading was stopped when one of the following events occurred: a) the flexural cracks had opened to a point which indicated that the pretensioning steel was near its ultimate strength, b) cracking or crushing was observed in the deck concrete, or c) a point was reached beyond which it did not seem safe to proceed.

5.5 DATA REDUCTION

Most of the data obtained from the tests could be used directly for analysis purposes. Some data was manipulated to give more concise values that were indicative of general behavior. Averages were taken of the strain in the slab. The horizontal deflections of the bearing pads were averaged to determine the actual distance of the span length being tested. The only data that was intentionally corrected was for the vertical deflection of the support bearings. The average vertical deflections from the bearing pads at each load level were extrapolated to the point where the potentiometer was located along the beam. Then this data was

96

subtracted from the data recorded from the potentiometer to give the true deflection of the beam.

When this process was performed on the data it was found that the modified deflection data did not agree with the manual data recorded from the stressed wire deflection system. This was due to the fact that the beam was rotating around a point on the bearing pad different than the pad centerline where the potentiometer was located. Much of the downward deflection of the bearing pad was occurring inside the location of the potentiometer. Some of the vertical deflection values from these readings indicated that the beam was displacing upward at the point of measurement because of the tendency of the beam to rotate about the inside corner of the bearing pad. Therefore, after comparing the raw vertical deflection data from the middle potentiometer under the beam, the values modified by the deflection of the bearing pad, and the manual measurements it was found that the manual measurements, were nearly identical to the raw data of the center potentiometer. The center potentiometer data was therefore used for the deflection results and the following discussion.

5.6 DEVELOPMENT LENGTH TEST RESULTS

This section deals with both the observed and numerical results obtained from development length testing of the beams. Observed results include all the subjective observations that were made during the tests, which include the type of failure, the type of cracking pattern, and other miscellaneous observations. The numerical data deals with the data obtained from the data acquisition system.

These results include the load, deflections, concrete strains, and strand slip from various measurement devices presented in the next five subsections.

5.6.1 Critical Values

This section gives the results of the test data obtained from the load and beam deflections. A summary of these values is given in Table 5.2. The value for the load at initial flexural cracking of the beam is given as P_{cr}. The ultimate load reached during each test is designated as P_u. The ratio of the ultimate load and the cracking load is also given. The ultimate moment, M_u, is based on the calculation described in Section 5.2.3 corrected to include the decrease in span length during testing due to curvature of the beam. This curvature caused the load to be concentrated on a smaller portion of the bearing pad towards the inner edge of the pad, reducing the actual span length. The deflection was determined from the center potentiometer and is labeled Δ_u.

Table 5.2: Loads, Deflections and Ultimate Moment

Beam ID	L_e in (mm)	P_{cr} kips (kN)	P_u kips (kN)	P_u / P_{cr}	Δ_u in (mm)	M_u k-in (kN-m)
NW6000-1-N-80	80 (2,032)	203 (903)	328 (1,459)	1.62	1.79 (45.4)	16,500 (113,768)
NW6000-1-S-60	60 (1,524)	234 (1,041)	425 (1,890)	1.82	3.00 (76.2)	16,800 (115,836)
LW6000-1-N-80	80 (2,032)	182 (810)	329 (1,463)	1.81	2.95 (75.0)	16,500 (113,768)
LW6000-1-S-70	70 (1,778)	200 (890)	375 (1,668)	1.88	3.53 (89.6)	17,000 (117,215)
LW6000-2-N-70	70 (1,778)	204 (907)	360 (1,601)	1.76	2.91 (73.8)	16,300 (112,389)
LW6000-2-S-60	60 (1,524)	233 (1,036)	409 (1,819)	1.76	2.53 (64.2)	16,200 (111,699)

The data in Table 5.2 indicates several trends. The first trend, shown in Figure 5.14., is that tests with similar embedment lengths had similar cracking and ultimate loads. The largest difference in cracking load between similar tests occurred between NW6000-1-N-80 and LW6000-1-N-80, where the cracking load differed by 10%. The other pairs with similar embedment lengths had very similar cracking loads regardless of the type of concrete used in the prestressed beam or whether lightweight panels were used. This was not expected due to the lower tensile strength of the lightweight concrete compared to the normal weight concrete [22].

The ultimate loads for beam pairs with similar embedment lengths were also similar, as shown in Figure 5.14. The maximum deviation of a pair of beam tests at the same embedment length was 4%, which occurred in two sets of companion beams, the 60-in (1,524-mm) and 70-in (1,778-mm) embedment length tests. The ratio between the ultimate load and the cracking load is also shown above each column in Figure 5.14.
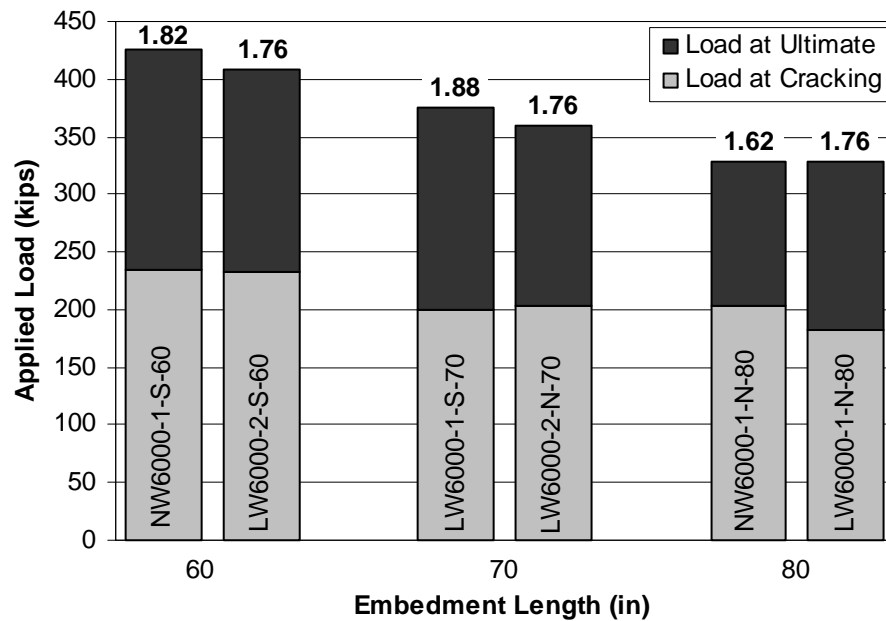
Figure 5.14: Comparison of Cracking and Ultimate Load

The ultimate loads were predicted to be similar for tests with similar embedment lengths because the load at failure depends on the ultimate moment that can be developed in the beam. A direct comparison of this for all the beam tests can be seen by the ultimate moments developed in the beams, as given in Table 5.2 and shown in Figure 5.15. The ultimate moment that can be developed in the beam at failure is dependent on the area and stress of the concrete in compression and the tensile force in the steel. At failure of the beams in this study, the neutral axis depth was less than 3 in (76.2 mm), and all the composite beams had at least a 4-in (102-mm) layer of normal weight concrete, with similar properties in all the tests, at the top of the deck and the same amount of steel in all the beams and decks. Therefore, it is logical to conclude the ultimate moment that the beams could withstand would be similar because the material properties at the

critical section were the same. Calculations based on ACI 318 validate this theory [2]. The largest deviation from the average ultimate moment occurred in test LW6000-1-S-70, which had a difference of less than 3%.
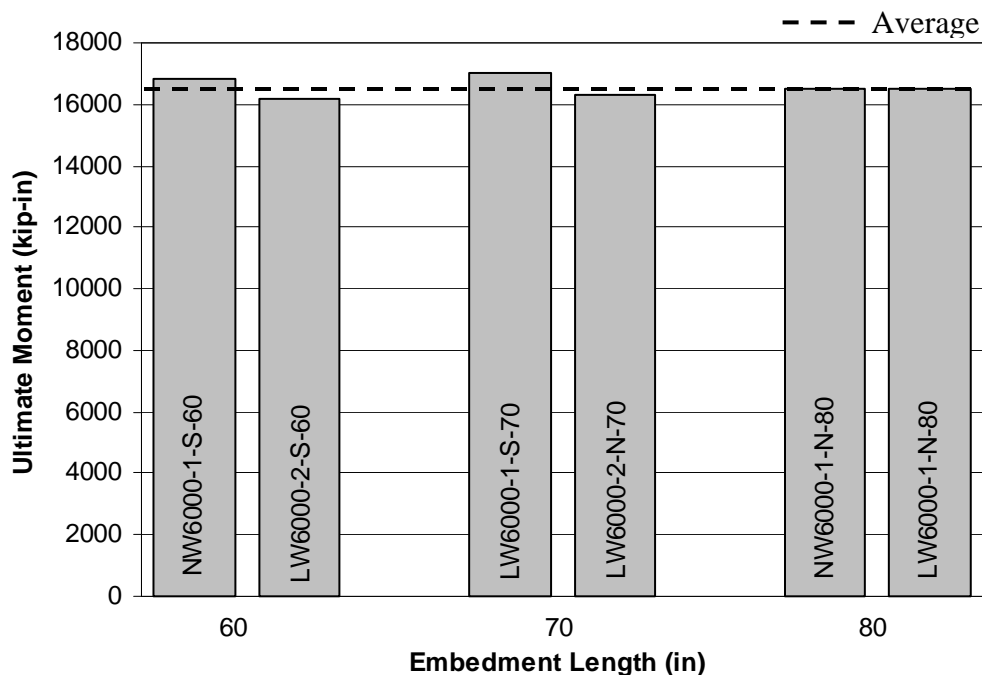
Figure 5.15: Comparison of Ultimate Moments

The ultimate deflection for all the tests are shown in Figure 5.16. The last five tests had a similar amount of deflection associated with the ultimate load. This is reasonable because as mentioned previously, the material properties acting near failure are the same. Therefore, the beams should behave similarly at failure, which they do. The NW6000-1-N-80 could have probably withstood more deflection, but since this was the first test a more conservative approach was taken in testing.
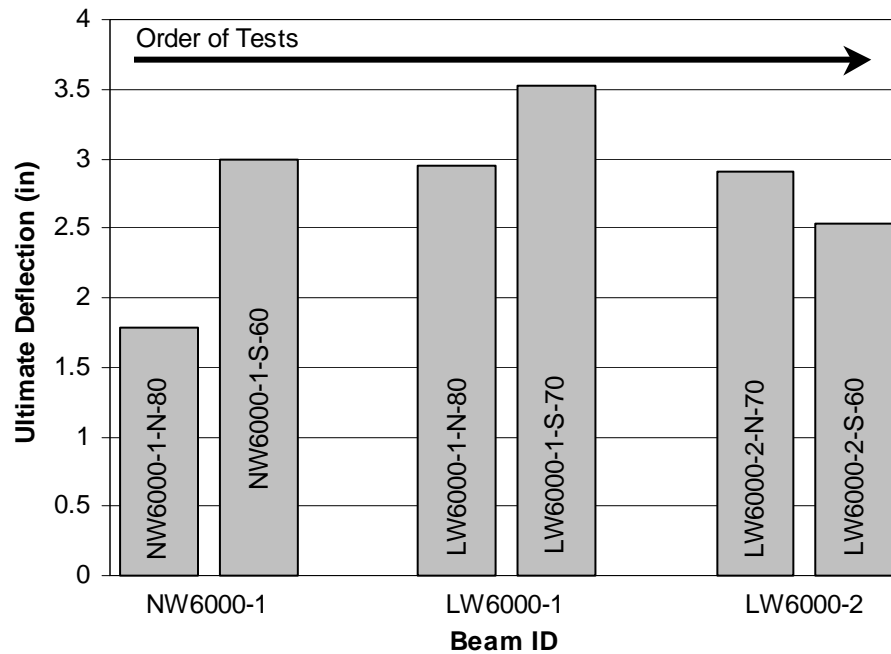
Figure 5.16: Comparison of Ultimate Deflections

5.6.2 Initial Stiffness

The elastic modulus of a material relates the amount of deflection in a material to the applied force. As the elastic modulus decreases, the deflection produced by a constant force increases. For the different concretes used in this study, the elastic modulus of the lightweight concrete was approximately one-half that of the normal weight concrete [22]. Therefore, it is logical to assume that the amount of lightweight concrete present in the cross-section of the composite beams should affect the initial stiffness measured before flexural cracking occurs. The trend should indicate that lightweight beams with similar embedment lengths as normal weight beams should have a lower initial stiffness. The lightweight beams using lightweight panels should also have a lower stiffness than their

102

companion beam with normal weight decks. This is the trend that the data shows as given in Table 5.3 and shown in Figure 5.17. The beams are compared by embedment length because this factor affects the initial stiffness of the test. In Figure 5.17 the area of the cross-section that is composed of lightweight concrete is designated by a black fill.

Table 5.3: Initial Stiffness Comparison

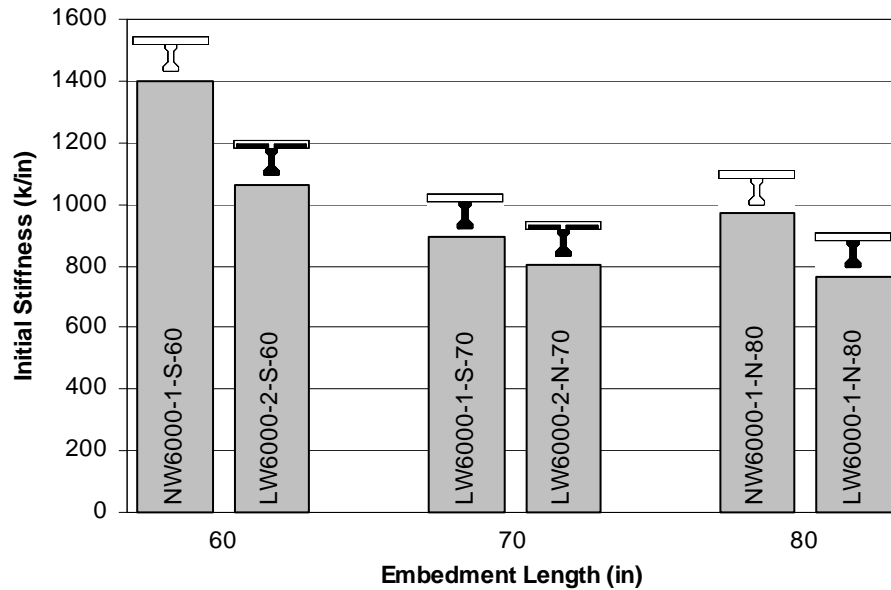| Beam ID	L_e in (mm)	Initial Stiffness k/in (kN/mm)
NW6000-1-N-80	80 (2,032)	968 (170)
LW6000-1-N-80	80 (2,032)	765 (134)
LW6000-1-S-70	70 (1,778)	897 (157)
LW6000-2-N-70	70 (1,778)	803 (141)
NW6000-1-S-60	60 (1,524)	1,397 (245)
LW6000-2-S-60	60 (1,524)	1,065 (186)

Figure 5.17: Comparison of Initial Stiffness

5.6.3 Strand Elongation

This section summarizes the approximate amount of strand elongation that occurred at the bottom layer of prestressing strands. This was calculated, using a linear strain distribution, based on the known depth of the concrete cracking deck and the maximum strain in the deck. Plots of the strain-load relationship for each test are given in Appendix E. A linear extrapolation of these values was used to determine the amount of strain caused in the steel by the loading. Then the amount of strain due to the initial prestress was added to obtain the final total strain in the steel. This data, given in Table 5.4 and shown in Figure 5.18, shows that the strands in the beams had reached a level of strain that corresponded with development of the nominal ultimate strength of the strand. The crack width at the strand level is also given in Table 5.4 as a comparison to show the size of the

104

cracks that had opened up at the bottom flange in the constant moment region during the testing.

Table 5.4: Strand Elongation and Crack Widths

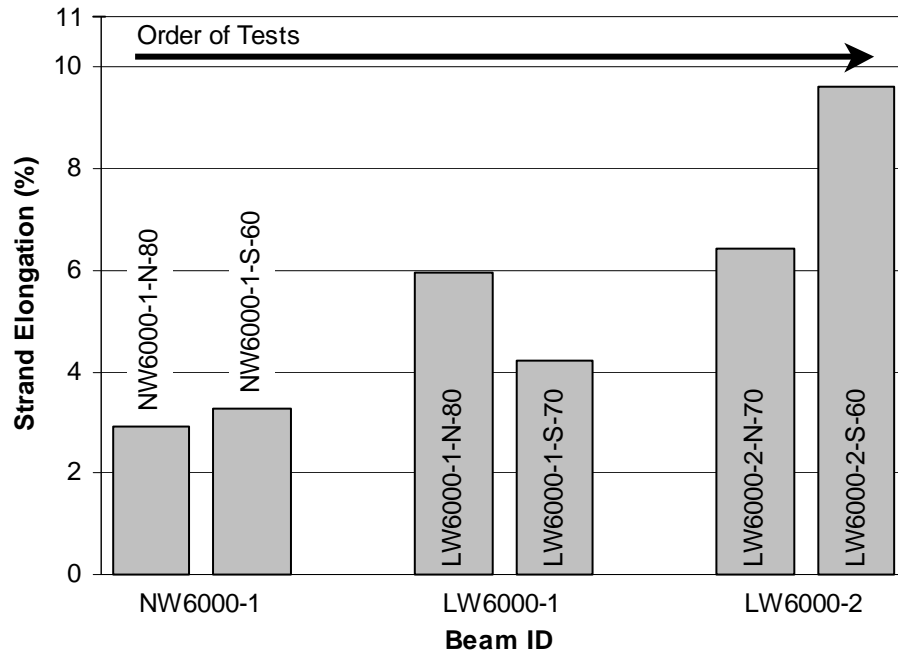| Beam ID	L$_e$ in (mm)	Depth of Cracking at Ultimate, in / (mm)	Concrete Strain at Top, microstrain	Strand Elongation (%)	Max. Crack Width, in (mm)
NW6000	80 (2,032)	2.67 (67.8)	2,033	2.9	0.079 (2.00)
NW6000	60 (1,524)	3.03 (77.0)	2,688	3.3	0.157 (3.99)
LW6000-1	80 (2,032)	2.52 (64.0)	4,349	6.0	0.197 (5.00)
LW6000-1	70 (1,778)	2.78 (70.6)	3,266	4.2	0.300 (7.62)
LW6000-2	70 (1,778)	1.89 (48.0)	3,462	6.4	0.118 (3.00)
LW6000-2	60 (1,524)	1.44 (36.6)	4,015	9.6	0.118 (3.00)

Figure 5.18: Comparison of Strand Elongation

The smallest amount of elongation occurred in NW6000-1-N-80, which had 2.9% strand elongation. Yielding of prestressing strand is typically considered at 1%, therefore this amount corresponds to approximately three times the yield strain. This also indicates that the maximum load could not be increases dramatically above this point because the steel had reached a level where the stress was not increasing significantly with increased strain. The elongation of 9.6% in LW6000-2-60 may not be the actual elongation of the strand because this could exceed the breaking strain of the strand and as indicated by the mill certificates. None of the strands ruptured during the tests. This high value may be attributable to the type of failure that occurred in this beam, which contained lightweight concrete panels. The cracking on the outside edge of the slab, where

106

the depth was measured, may not have corresponded to the actual depth of cracking at the area immediately above the beam web.

5.6.4 Strand Slip

The data recorded from the instrumentation on the prestressing strands should indicate whether the strand had developed its full strength or whether a bond failure had occurred. Bond failure would be indicated by strand slip. If the test results indicated that strand slip was occurring below a certain embedment length then it could be conclusively said that the development length was larger than this distance.

The data given in Table 5.5 and shown in Figure 5.19 indicates that strand slip only occurred during the testing of LW6000-1-N-80. All of the other measurements for the other tests indicated a slip of less than 0.01 in. This amount of displacement is attributed to variability of the data acquisition system and not actual movement of the strands.

Table 5.5: Strand Slip

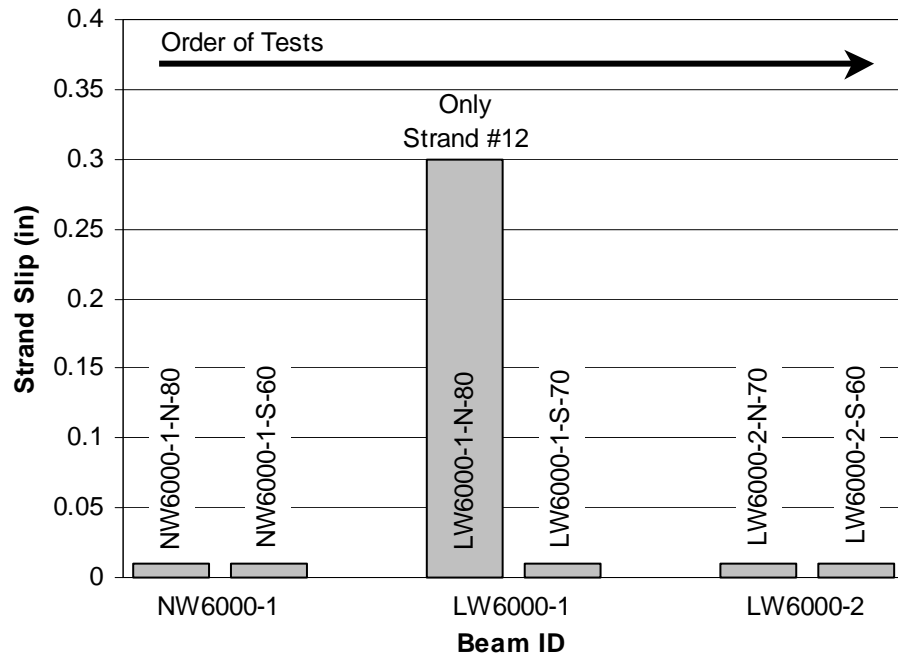| Beam ID	L_e in (mm)	Slip in (mm)	Strand #	Load kips (kN-m)
NW6000-1-N-80	80 (2,032)	< 0.01 < (0.25)		
NW6000-1-S-60	60 (1,524)	< 0.01 < (0.25)		
LW6000-1-N-80	80 (2,032)	0.3 (7.62)	12	328 (2,262)
LW6000-1-S-70	70 (1,778)	< 0.01 < (0.25)		
LW6000-2-S-70	70 (1,778)	< 0.01 < (0.25)		
LW6000-2-S-60	60 (1,524)	< 0.01 < (0.25)		

Figure 5.19: Comparison of Strand Slip

The fact that strand number 12 slipped during test LW6000-1-N80 indicates that the bond for this individual strand alone was not sufficient. The data from the test indicates that the other strands did not slip and therefore had sufficient bond to develop their full strength. The slip of strand 12 is probably due to the manufacturing process. Strand 12 lies on the outside edge of the strand layout (refer to Figure 3.4) and therefore it is very possible that this strand could have been oiled in the forming process. This would reduce the affect of adhesion in creating bond stress and reduce the amount of friction required to slip the strand. The fact that testing of the same beam at an embedment length of 70 in (1,780 mm) produced no strand slip also gives credence to this theory. If strand slip had also occurred during the test with an embedment length of 70 in (1,778

mm) then the strand slip in the test LW6000-1-N-80 could not be attributed to random deviance.

5.6.5 Type of Failure

This section deals with subjective observations of the beams during the testing. The type of failure that the beams were designed for was flexure. Extra stirrups were placed in the beams to ensure that the short shear spans of the tests had ample shear strength such that flexural failure of the specimen would occur. Only a flexural failure would indicate whether the bond between the strand and concrete was sufficient to develop the full strength of the strand.

During the tests the beams were continually examined for shear and flexural cracking. Flexural cracking was characterized by cracks that formed at the bottom flange of the beam and extended upward from this point. Shear cracking was characterized by cracks that began in the web of the beam and extended diagonally in both directions as load was increased. On the shorter shear span beams, shear cracking occurred before flexural cracking. But even for these beams the widths of the shear cracks did not increase to the extent of the flexural cracks as loading increased up to failure. This is due to the amount of vertical web reinforcement placed in this area (refer to Figure 3.5), which prevented the cracks from dramatically increasing in width after they formed.

From observation of the beams during the tests it was determined that all beams experienced flexural failure. Along with this failure, some other local failures occurred during the tests. Crushing or surface cracking of the deck concrete occurred in some of the test specimens. This cracking usually occurred

near one of the loading points on the deck because the stress is most concentrated at this point due to the steel loading pad. When cracking appeared in the deck, the test was stopped and the load at this time was considered the ultimate load. Also, since the moment developed between the loading points can not be perfectly constant, one of the load points will have the largest moment in the beam section directly underneath it. This type of failure is displayed in Figure 5.20.
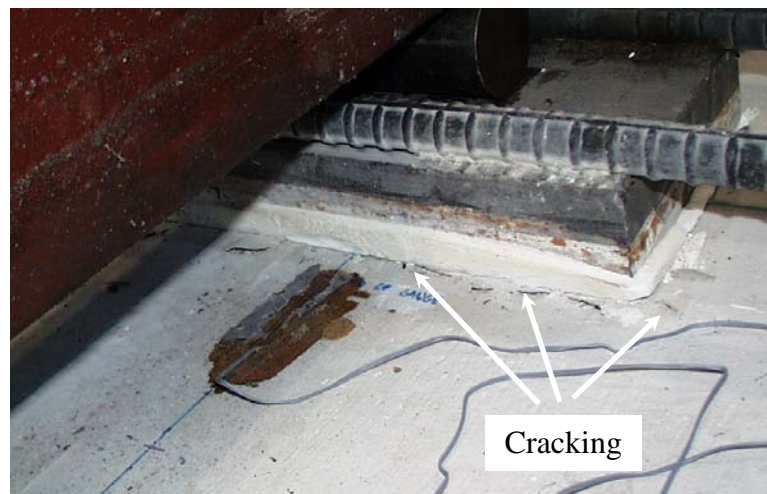

Cracking

Figure 5.20: Cracking of Deck Concrete

The testing of the LW6000-2 beam with lightweight panels introduced a unique type of failure. This failure was designated as spalling of the support concrete at the end of the beam in the bottom of the beam flange. The failure did not extend into the web of the beam for either test of LW6000-2. This failure is shown in Figure 5.21. Both tests of this beam had similar spalling of the support concrete. It could not be precisely determined why this spalling was occurring only in these test beams but a theory was developed as explained later. The only differences between this beam and NW6000-1 and LW6000-1 is that the depth of

the composite section was increased by ½ in (12.7 mm) due to the fiberboard inserts and the lightweight panels were used in construction.
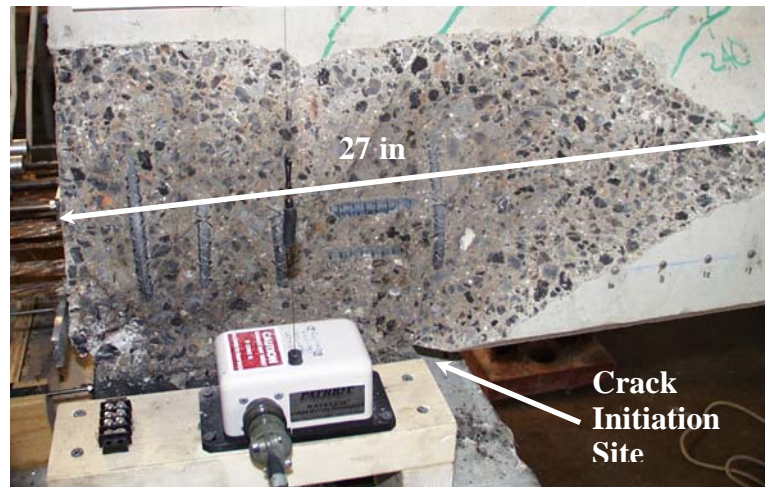

Figure 5.21: Spalling at Support

To show that the load that the spalling failure occurred at does not affect service loading conditions in design, the ratio of the spalling load, P_{spall}, to the cracking load is shown in Figure 5.22. This figure shows that the spalling occurred well above the cracking load and very near the ultimate load of the test. On average, the spalling occurred 173% above the cracking load and at 98% of the ultimate load. Also, since this spalling occurred near the ultimate load, it does not affect the performance of the beam at any time before this, which is evident by the data previously presented.
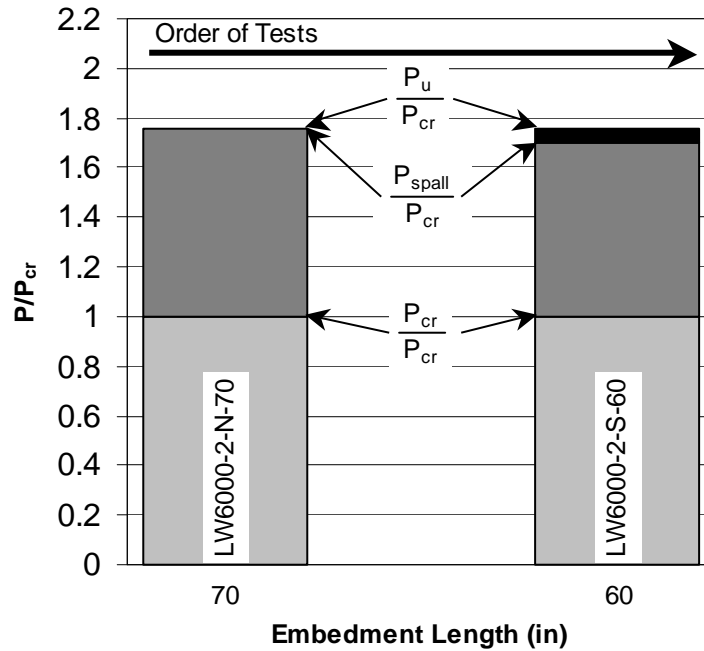
Figure 5.22: Spalling as Ratio of Cracking Load for LW6000-2

Due to the lower tensile strength of the lightweight concrete, it was theorized that the distributed load applied by the bearing pad put the flange of the beam into deep beam bending. Also, due to the curvature of the beam, the beam had to bear on less area as the load increased and therefore more stress was concentrated in a smaller area of the beam flange. The failure looked very similar to a split cylinder test. Once the stress exceeded the rupture stress, a crack was initiated and as the stress redistributed, it exceeded the cracking strength of the concrete and the crack unzipped along the length of the concrete in the flange of the support. If this theory were true, then it would be expected that the spalling might also occur on the other lightweight beams. Neither of the two tests

112

involving the LW6000-1 beam with a normal weight concrete deck had this type of failure.

The spalling occurred completely on the outside of the reinforcing cage. When this failure occurred on the LW6000-2-N-70 test, part of strand 12 was exposed. Since the ultimate load had already been reached, this failure did not affect the ultimate load capacity of this test. For the LW6000-2-S-60, the spalling occurred before the ultimate load was reached and the ultimate load only increased 3% after this failure occurred. The spalling in this case probably did not affect the ultimate load because the ratio of ultimate load to cracking load was very similar to the other 60-in (1,524-mm) embedment length test performed on NW6000-1-S-60 as previously shown in Figure 5.14. Therefore, it seems that the spalling of the support concrete did not affect the performance of the beams. Also, no slip occurred in the strands closest to this failure and therefore the support spalling did not affect the development length.

The lightweight panels also introduced another type of failure that was not seen in the decks without panels. This failure mechanism was a V-shaped crack that initiated from the point at which two panels butted against each other. Since there was no continuous steel between the panels, the joint between panels acted like a hinge. When the beam deflected, this hinging action of the panels caused cracks to spread out laterally from this point. It caused a type of pinching of the concrete above the joint due to the weakness of the joint between the panels. In the LW6000-2-N-70 test, final crushing of the deck occurred in this region, which was associated with the ultimate load applied to the beam. The location of this

113

failure was 88-in (2,235-mm) from the end of the beam, near the panel joint between Panel A and B, which was located at 96 in (2,438 mm) (refer to Figure 3.11). The crushing occurred approximately midway between the loading points, which was unlike the other cracking/crushing of the other tests which occurred near one of the load points. This failure is shown in Figure 5.23.
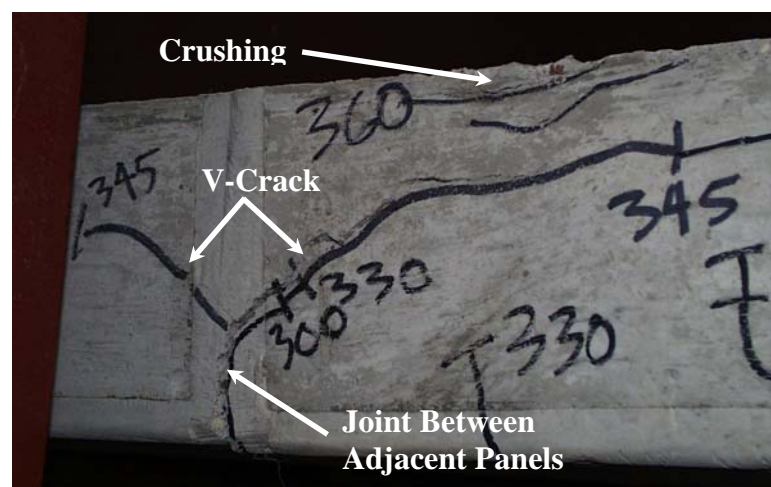

Figure 5.23: V-Cracking at Edge of Two Panels for LW6000-2-N-70

The type of failure for each beam is summarized in Table 5.6. Strand slip was not described in this section, but was explained in detail in the previous section.

Table 5.6: Types of Failure

Beam ID	Type of Failure
NW6000-1-N-80	Flexural Failure
NW6000-1S-60	Flexural Failure, Deck Crack Initiation
LW6000-1-N-80	Flexural Failure, Deck Crack Initiation
LW6000-1-S-70	Flexural Failure, Strand Slip, Deck Crack
LW6000-2-N-70	Flexural Failure, Complete Deck Crack, V-Crack, Spalling at Support in Beam Flange
LW6000-2-S-60	Flexural Failure, Deck Cracking Initiation, V-Crack, Spalling at Support in Beam Flange

5.6.6 Cracking Pattern

The observations reported in this section are related to the type of cracking pattern that occurred in each beam. This section does not include the failure types of cracking as described previously but only the general pattern of cracking for the beams. Since all the beams failed in flexure, they all had cracking patterns that were very similar. Due to this, the cracking pattern for each beam is not described in detail, but only general patterns are explained that apply to all beams.

There were three general zones along the span that exhibited different types of cracking. These zones also corresponded with the position of the applied load. The first zone is located between the end of the beam and the first load point. This zone exhibited both flexural and shear cracking, as shown in Figure 5.24. The dominant type of cracking was shear cracking. Almost all of the shear

cracks are inclined at a 45-degree angle. The cracks indicated as "Shear Cracks" in Figure 5.24 formed in the web before extending in both directions with increased load. The flexural cracks are also indicated and formed in the flange and then extended upwards toward the deck as load was increased. These flexural cracks are not vertical but have some inclination.
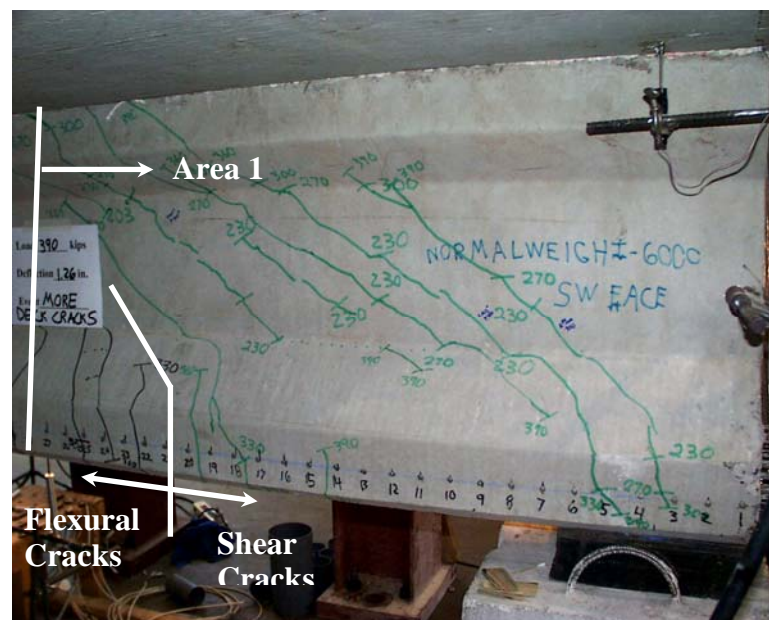

Figure 5.24: Zone 1 - Cracking Pattern

The second zone was the constant moment region of the span. Due to reduced shear in this region, all the cracks were flexural and these cracks were vertical. Some cracks did tend to have some inclination near the outer areas of the constant moment region. This pattern is shown in Figure 5.25.

Figure 5.25: Zone 2 – Cracking Pattern

The final zone that exhibited typical cracking for the beams was the section of span between the constant moment region and the middle support, designated as Zone 3. Similar to Zone 1, both flexural and shear cracks occurred in this area. The flexural cracking was more extensive than in Zone 1. A difference in the shear cracking also occurred. The shear cracks did not appear gradually as they did in Zone 1, rather there would be a thumping sound during the test and a shear crack would appear closer to the middle support than the previous one. This pattern can be seen in Figure 5.26, along with the other zones indicated previously.
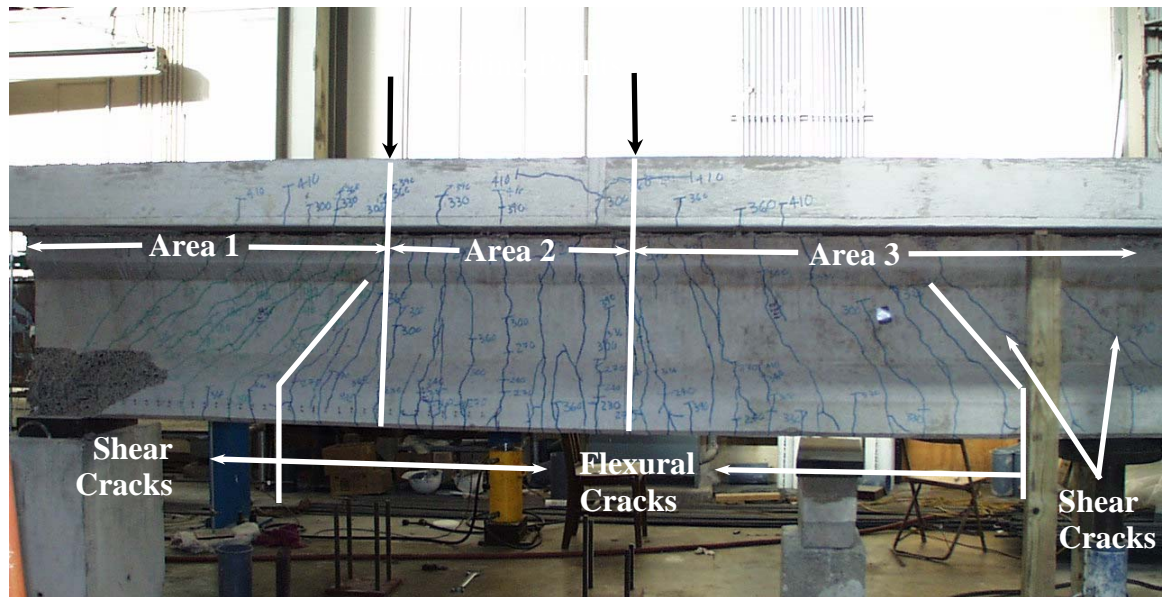
Figure 5.26: Typical Cracking Pattern

5.7 DISCUSSION

This section uses the data obtained from the test results to make comparisons with the values obtained from calculations based on material properties.

5.7.1 Comparison to Predicted Moments

The ultimate moments that could be developed in the beams were calculated by two methods. Both methods used a strain compatibility approach. Whitney Stress Block and Stress Block Factors were the two methods used [15]. The predicted failure load using of these two methods of calculation for each test were very similar as is shown in Table 5.7. Also listed in this table is the ultimate moment developed during the test. Since Whitney Stress Block is used in the ACI

318 Code for design purposes, the ratio of the ultimate moment to the Whitney Stress Block ultimate moment for each test is also given in the table.

Table 5.7: Calculated Moment Comparison

Beam ID	Whitney Stress Block, k-in (kN-mm)	Stress Block Factors, k-in (kN-mm)	Ultimate Moment, k-in (kN-mm)	Ultimate / Whitney
NW6000-1-N-80	14,850 (2,620)	14,870 (2,623)	16,500 (2,911)	1.11
NW6000-1-S-60	14,890 (2,627)	14,900 (2,628)	16,800 (2,964)	1.13
LW6000-1-N-80	14,830 (2,616)	14,850 (2,620)	16,500 (2,911)	1.11
LW6000-1-S-70	14,830 (2,616)	14,850 (2,620)	17,000 (2,999)	1.15
LW6000-2-N-70	14,860 (2,621)	14,870 (2,623)	16,300 (2,875)	1.10
LW6000-2-S-60	14,860 (2,621)	14,870 (2,623)	16,200 (2,858)	1.09
Averages	**14,850 (2,620)**	**14,870 (2,620)**	**16,470 (2,900)**	**1.11**

Standard Deviation | **0.02**

The reason for the 11% average difference between the actual and predicted values is due to the conservative nature of Whitney's design theory. This is the method used in ACI 318 and therefore has some conservativeness associated the design method. The tight cluster of data indicated by the 2% standard deviation indicates that the design equation has a similar amount of conservativeness in predicting the ultimate moment for both the normal weight and lightweight concrete beams.

119

5.7.2 Behavioral Comparison

This section gives a comparison of the load-deflection plots of the test beams. This is displayed in Figure 5.27, where all the plots are given on one graph so that direct comparisons can be made. Plots of the individual load-deflection plots for each test are given in Appendix D. The largest difference between companion beams was between NW6000-1-N-80 and LW6000-1-N-80. The magnitude of the displacement to which the normal weight beam was displaced was not as large as the lightweight beam. The NW6000-1-N-80 test was the first test conducted for this research project and therefore more conservatism was used during this test than was used during the other tests. A similar test on another project had failed catastrophically prior to this test and therefore this test was run rather conservatively.

Except for stiffness, the plots for companion beams with the same embedment length follow the same path regardless of the type of concrete used in the pretensioned beam. There is excellent agreement between the 60-in and 70-in (1,524-mm & 1,778-mm) companion beams. Most interesting is the behavior of the two beams tested with a 60 in (1,524 mm) embedment length. One used normal weight concrete for beam and deck and the other used lightweight concrete for the beam and panels. This indicates that despite the lower stiffness of the lightweight concrete beams, the behavior of the lightweight concrete beams after cracking is very similar to the normal weight concrete beam.
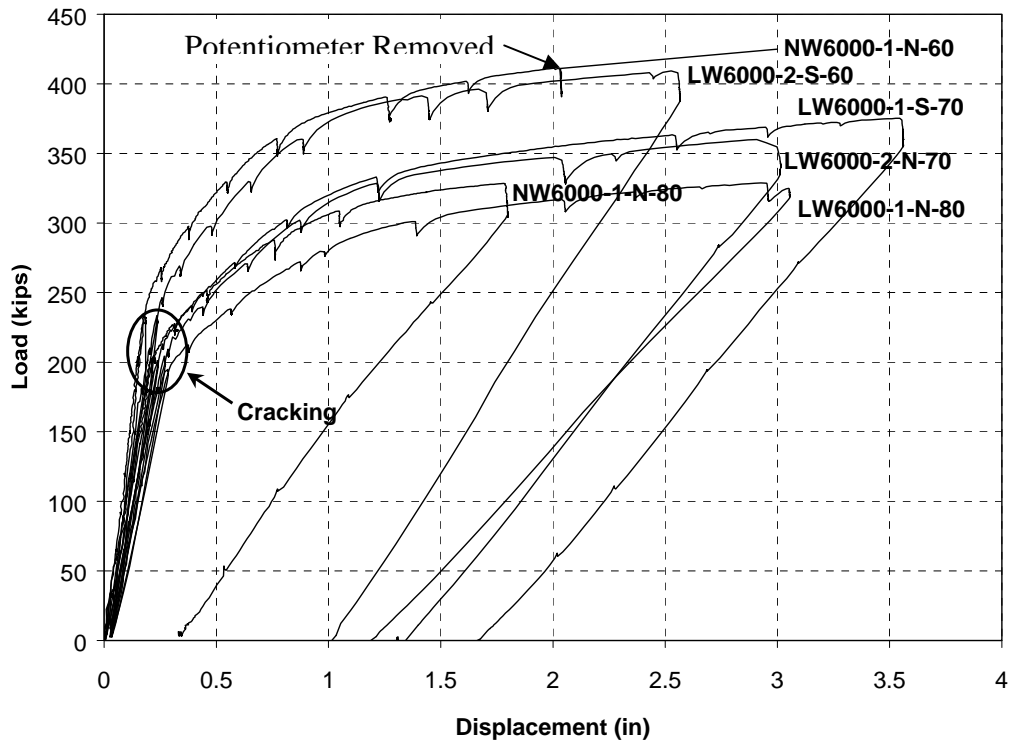
Figure 5.27: Load-Displacement Plots for all Tests

5.7.3 Calculated Development Lengths

Many equations have been formulated to describe the development length of prestressing strand in normal weight concrete. The ACI and AASHTO codes do not differentiate between normal weight and lightweight concrete. The equation for development length uses the effective stress in the strand as a means of determining the development length. Other equations use the concrete properties directly in the equations for development length. The various equations studied and the calculated values for the development length of the beams for this study are presented in Table 5.8.

121

Table 5.8: Calculated Development Lengths

Author	Development Length Equation	L_d NW6000 in / (mm)	L_d LW6000 in / (mm)	L_d LW8000 in / (mm)
ACI 318 / AASHTO [22,21]	$L_d = \left(f_{ps} - \dfrac{2}{3} f_{se} \right)$	82 (2,091)	86 (2,193)	86 (2,193)
Zia & Mostafa [8]	$L_d = L_t + 1.25(f_{pu} - f_{se})d_b$	88 (2,246)	92 (2,328)	92 (2,344)
Buckner (FHWA) [2]	$L_d = L_t + \lambda(f_{ps} - f_{se})d_b$	78 (1,984)	104 (2,630)	102 (2,601)
Mitchell [12]	$L_d = L_t + (f_{ps} - f_{se})d_b\sqrt{\dfrac{4.5}{f'_c}}$	69 (1,753)	67 (1,694)	68 (1,724)
Actual L_d	Determined from testing	< 60 < (1,524)	< 60 < (1,524)	< 60 < (1,524)

This table indicates that the actual development lengths of the beams in this study, regardless of type of concrete used in the beams, is less than the predicted development length. This is true for all the models studied. It should also be noted that these models were developed for normal weight concrete. It is difficult to give an exact development length for any of the beams tested in this study due to the small number of tests and the fact that extensive bond failure did not occur in any of the tests. Only one strand had any slip during the tests (LW6000-1-N-80). A test on the same beam with a shorter embedment length was performed and no strands slipped which indicated that the slip was a random occurrence. Therefore, based on the results of the six tests performed, the development length for the NW6000 and LW6000 beams is less than 60 in (1,524 mm).

Chapter 6: Summary and Conclusions

6.1 SUMMARY

The overall objective for research Project 0-1852: Prestressed Structural Lightweight Concrete Beams is to determine the feasibility of using high performance lightweight concrete beams in Texas bridges. The scope of this thesis in accomplishing this task was the manufacture of six test beams, transfer length testing of all six beams, and development length testing of three of the these beams. The beams had an AASHTO Type I cross-section and were cast with both normal weight and lightweight concrete.

The beams were manufactured at Heldenfel's Prestressing Plant in San Marcos, Texas. The precast pretensioned prestressed concrete beams were prestressed with 12 – ½-in (12.7-mm) diameter, Grade 270-ksi (1,861 MPa), low-relaxation steel strands. They were released from their forms at one day at which time instrumentation was placed on the beams and measurements taken to determine the transfer lengths following transfer of the prestress force to the concrete. The beams were then brought to the Ferguson Structural Engineering Laboratory of the University of Texas at Austin where composite concrete decks, varying the type of concrete and deck panels, were cast on the beams. Development length testing was performed at each end of the beam, thereby obtaining two sets of data from each beam. Setup of the test was carefully designed to ensure that damage occurring in the test area at one end of the beam did not intrude into the other test area at the other end of the beam [7].

123

6.1.1 Use of Lightweight Concrete

Two HPLC mixes were developed in this research project to be used in the manufacture of the beams in this study. The parameters specified for the mixes included a minimum one-day compressive strength of 3,500 psi (24.1 MPa) for both mixes and a final compressive strength of 6,000 and 8,000 psi (41.4 – 55.2 MPa). In addition, the unit weight was required to be between 118 – 122 lb/ft^3 (1,864 – 1,928 kg/m^3). The actual test properties of the concrete are given below in Table 6.1.

Table 6.1: Concrete Properties

Beam ID	Compressive Strength (f'$_c$), psi / (MPa)		Unit Weight lb/ft^3 / (kg/m^3)
	Transfer Length Tests (1-day)	Development Length Tests	
NW6000	3,490 (24.1)	5,500 (37.9)	149 (2,387)
LW6000	4,900 (33.8)	8,130 (56.1)	118 (1,890)
NW8000	5,560 (38.3)	7,850 (54.1)	122 (1,954)

The manufacturing of the concrete beams using lightweight concrete occurred as a normal operation without special treatment by the workers casting the beams. No significant problems were encountered that might not occur with normal weight concrete.

The scope of this thesis does not extend into detailed discussion of the fresh properties of lightweight concrete. For more information regarding the HPLC mixes and properties, see a thesis prepared by Heffington [22].

124

6.1.2 Transfer Length Testing

Transfer length is defined as the distance required to transfer the fully effective prestressing force from the strand to the concrete in a pretensioned prestressed concrete beam. The determination of this quantity was accomplished by two different methods: measurement of the concrete strains and strand draw-in.

The concrete strain measurements were performed using a DEMEC Strain Measurement System. The strain was measured every 50 mm using a 200-mm gauge length. The data was reduced to give a strain profile for each end of the beams. The transfer length was then determined for each profile using the 95% Average Maximum Strain Method [38]. Due to variability in the data of the individual strain profiles, the data from similar beams were averaged to obtain average strain profiles for which the transfer length was determined.

Unlike the strain measurements, the draw-in testing data could not be used directly to give the transfer length. The transfer length was determined by applying the draw-in data with Equation 4.3, assuming $\alpha=2$.

A summary of the average transfer lengths results from the individual strain profiles, average strain profiles and draw-in values are given in Table 6.2.

Table 6.2: Summary of Transfer Length Results

Beam I.D.	Transfer Length (L_t), in / (mm)		
	Individual Strain Profiles	Average Strain Profiles	Strand Draw-In
NW6000	18.3 (465)	18.2 (463)	15.6 (396)
LW6000	30.9 (785)	35.8 (910)	15.3 (389)
LW8000	35.3 (897)	34.4 (875)	13.1 (333)

6.1.3 Development Length Testing

The development length was approximated by testing a beam at a certain embedment length and determining the type of failure that occurred. If the failure was flexural in nature and no bond failure occurred then the development length for that beam was consisted to be less than the tested embedment length. Another test would be performed at a smaller embedment length and the results examined to determine the type of failure. By performing this procedure on the test beams, the exact development length could not be determined but it could be determined whether the development was less than a certain embedment length.

To determine the type of failure that occurred, the beams were instrumented to record applied load, horizontal and vertical deflections, concrete strains and strand slip. The most definitive example of bond failure was strand slip, though this only occurred in one beam. Due to the limited number of tests that have been performed in this study, it is difficult to give a definitive answer about the exact development length. However, it is possible to give an estimate of the development length. Since no bond failure occurred at an embedment length

of 60 in (1524 mm), the development length is less than this for both the normal weight and lightweight concrete beams in this study. The data obtained from development length testing is shown in Table 6.3.

The test program also determined the ultimate moment that could be developed in the critical cross section at failure for each test and compared this value was to the predicted ultimate moment (Whitney's Theory). All tests indicated that the measured value was greater than the actual value found in the tests. An average of 10% difference, on the conservative side, between these values was found for the six tests performed, which is expected due to the conservative nature of the design equations to determine the ultimate moment based on Whitney's theory. Values for actual/predicted ultimate moment ratios for each test are also given in Table 6.3.

Table 6.3: Summary of Development Length Testing

Beam ID	Embedment Length, in / (mm)	Maximum Strand Slip, in / (mm)	Predicted Development Length, in / (mm)	Ultimate Moment, k-in / (kN-mm)	Actual / Predicted Ultimate Moment
NW6000-1-N-80	80 (2,032)	< 0.01 < (0.25)	< 60 < (1,524)	16,500 (2,911)	1.11
NW6000-1-S-60	60 (1,524)	< 0.01 < (0.25)	< 60 < (1,524)	16,800 (2,964)	1.13
LW6000-1-N-80	80 (2,032)	0.3 (7.62)	< 60 < (1,524)	16,500 (2,911)	1.11
LW6000-1-S-70	70 (1,778)	< 0.01 < (0.25)	< 60 < (1,524)	17,000 (2,999)	1.15
LW6000-2-N-70	70 (1,778)	< 0.01 < (0.25)	< 60 < (1,524)	16,300 (2,875)	1.10
LW6000-2-S-60	60 (1,524)	< 0.01 < (0.25)	< 60 < (1,524)	16,200 (2,858)	1.09

Standard Deviation **0.02**

6.2 CONCLUSIONS

Though the research project has not completed all of the testing and this thesis only deals with a subset of the objectives involved, preliminary conclusions can be made based on the results of the tests reported in this thesis.

6.2.1 Use of Lightweight Concrete

The following conclusions can be drawn from the use of high performance lightweight concrete in manufacturing:

1) The use of lightweight concrete did not affect the manufacture of the AASHTO Type I beams.

2) No cracking problems occurred at release in the lightweight beams, even under the most heavily prestressed conditions that might occur in design.

3) The use of lightweight concrete in precast pretensioned deck panels did not affect the manufacturing process or their successive use in deck construction.

6.2.1 Transfer Length Testing

The following conclusions can be drawn about the transfer length of normal weight and lightweight concrete based on the tests performed in this research study:

1) The ACI and AASHTO codes are a conservative estimate of the transfer length of normal weight concrete, but underestimate the transfer length of lightweight concrete.

2) The transfer length at transfer of the prestressing force for ½-in (12.7-mm) strands in the normal weight concrete beams in this study was 18.3 in (465 mm).

3) The transfer length at transfer of the prestressing force for ½-in (12.7 mm) strands in the lightweight concrete beams in this study was 35.1 in (892 mm).

4) Most of the models developed to predict transfer length were developed for normal weight concrete and do not accurately model the behavior of lightweight concrete.

5) The modulus of elasticity is a consistent factor in determining the transfer length for both normal weight and lightweight concrete.

6) Buckner's model for determining transfer length, though developed for normal weight concrete, is a conservative and accurate estimate for both normal weight and lightweight concrete.

6.2.2 Development Length Testing

Based on the limited tests performed, the following conclusions are drawn about the development length test results:

1) The ACI and AASHTO codes are a conservative estimate of the development length for the normal and lightweight beams tested in this study.

2) The development length models identified in this study, all of which were developed for normal weight concrete, appear to be a

conservative estimate for both the normal and lightweight concrete beams in this study.

3) The development length for ½-in (12.7-mm) strand in the normal weight concrete beam in this study was less than 60 in (1524 mm).

4) The development length for ½-in (12.7 mm) strand in the lightweight concrete beams in this study was less than 60 in (1524 mm).

5) The ultimate moments developed in the beams at failure were similar and did not seem to be a function of the type or compressive strength of concrete used in the beam or deck panels.

6) Use of lightweight deck panels did not affect the development length for ½-in strands in the beams.

7) Spalling of the support concrete occurred in two of the six tests performed in this study. Both beams in question used lightweight concrete deck panels. The failure occurred on average at 73% above the cracking load and at 98% of the ultimate load. Therefore, it is not a concern for service loading. Whether this spalling is coincident or a behavioral aspect of the lightweight concrete deck panels requires further testing.

6.3 CONTINUING RESEARCH

During the writing of this thesis the remaining three lightweight beams were in the process of development length testing. When this testing is completed, a complete report of the results of the entire research project will be reported by

Thatcher. His report will draw conclusions based on the complete set of results and give recommendations for the use of lightweight concrete in Texas bridges.

Appendix A: Notation

a   Distance from first load point to location of actuator

b   Coefficient indicating diameter of prestressing strand

d_b Nominal diameter of prestressing strand

E_c Modulus of elasticity of concrete

E_{ci} Modulus of elasticity of concrete at transfer

f'_c Concrete compressive strength

f'_{ci} Concrete compressive strength at transfer

f_{pi} Initial stress in strands, before relaxation losses

f_{ps} Stress in prestressing strands at nominal strength

f_{pu} Ultimate tensile strength of prestressing strands

f_r Modulus of rupture of concrete

f_s Stress in prestressing strands

f_{se} Effective stress in prestressing strands after losses

f_{si} Stresss in prestressing strands immediately before transfer

L_d Development length of prestressing strands

L_e Embedment length of prestressing strands

L_{fb} Flexural bond length of prestressing strand

Li   Distance from face of concrete to measurement point on strand before transfer

L_o Distance to centerline of support bearing pad from end of beam

L_r	Distance from face of concrete to measurement point on strand after transfer
L_t	Transfer length of prestressing strand
M_u	Ultimate moment strength
P_{cr}	Applied load at first flexural crack
P_u	Applied load at ultimate moment strength
α	Coefficient indicating shape of bond stress distribution in transfer zone
β_1	Factor defining average size of rectangular stress block
ε_{ps}	Strain in prestressing strand at nominal strength
ε_s	Strain in prestressing strands
ε_{si}	Strain in prestressing strand immediately before transfer
Δ_d	Change in length of prestressing strand associated with strand draw-in
Δ_e	Change in length of prestressing strand associated with elastic shortening
Δ_t	Total measured draw-in of prestressing strand
λ	Coefficient indicating bond stress distribution
ρ	Ratio of tension reinforcement
ρ_b	Reinforcement ratio producing balanced strain conditions
ρ_p	Ratio of prestressed reinforcement
ω_p	$\rho_p f_{ps}/f'_c$

Appendix B: English to SI Unit Conversion

English	Multiply by	= SI
1 psi	6,8948	Pa
1 ksi	6.8948	MPa
1 in	25.4	mm
1 lb	4.448	N
1 kip	4.448	kN
1 oz	28.349	g
1 kip-in	0.112997	kN-m

Appendix C: Concrete Strain Profiles
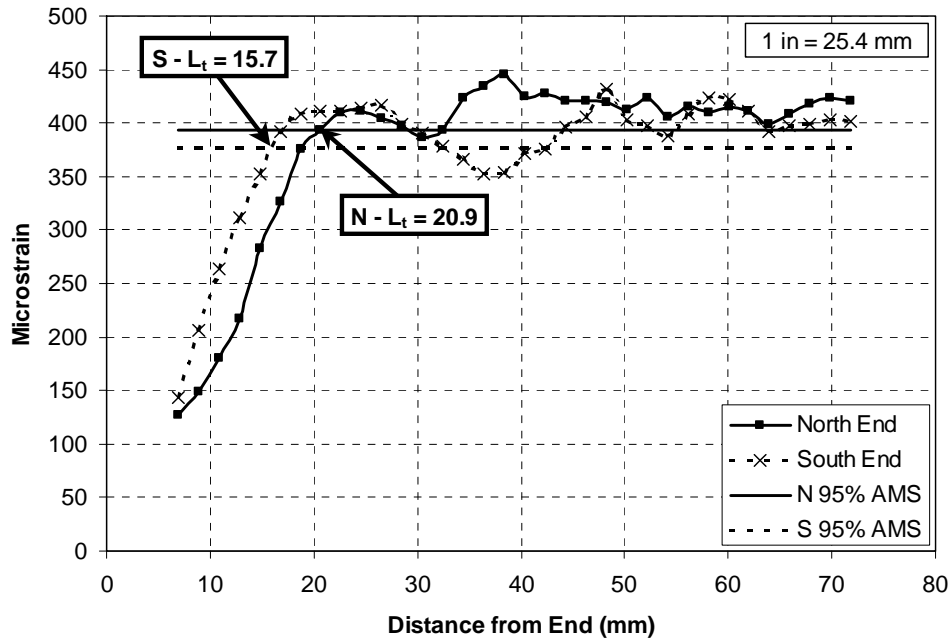
Figure C.1: Strain Profiles for NW6000-1
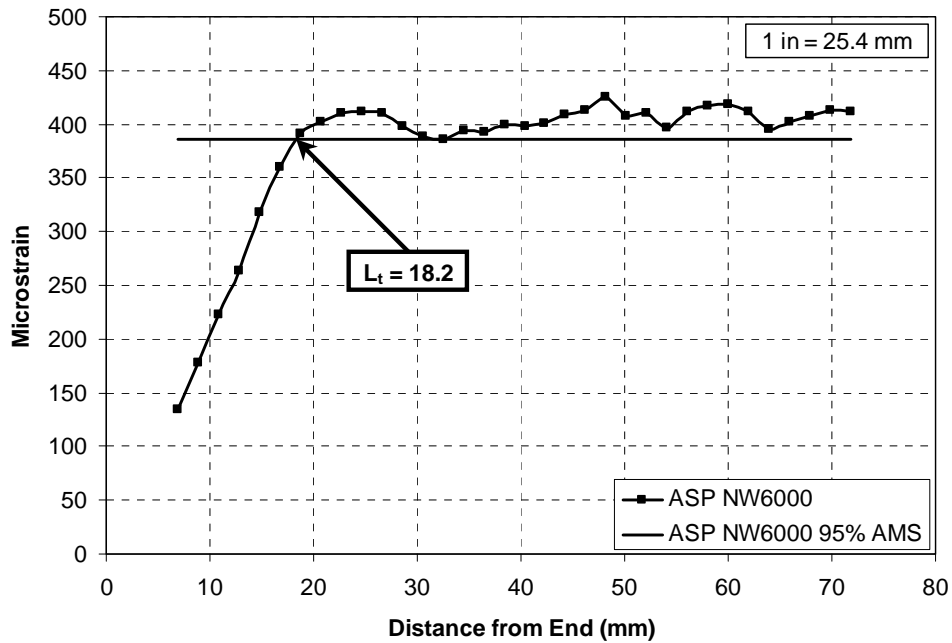
Figure C.2: Average Strain Profile for NW6000
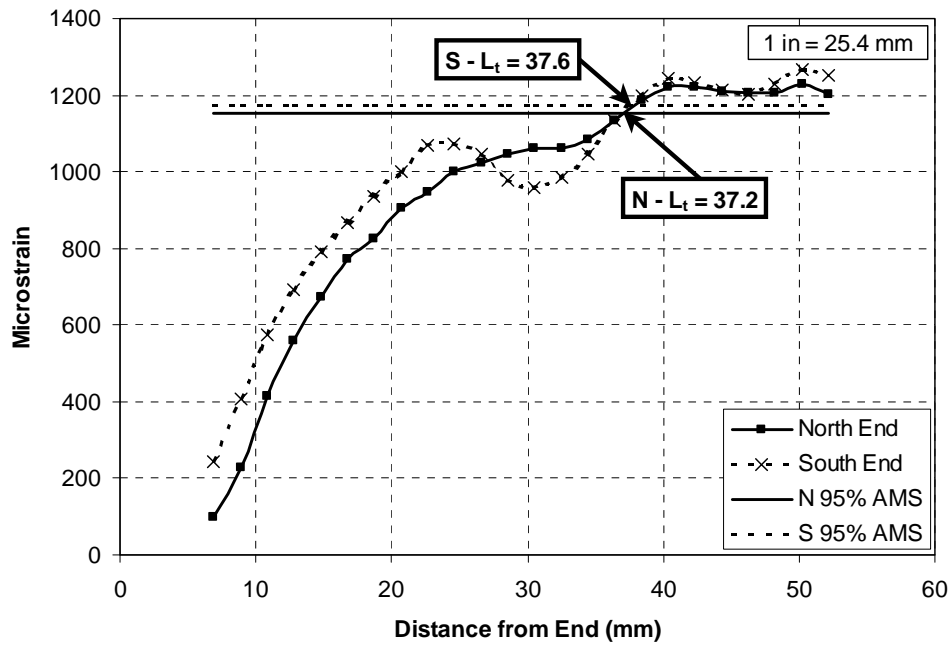
Figure C.3: Strain Profiles for LW6000-20
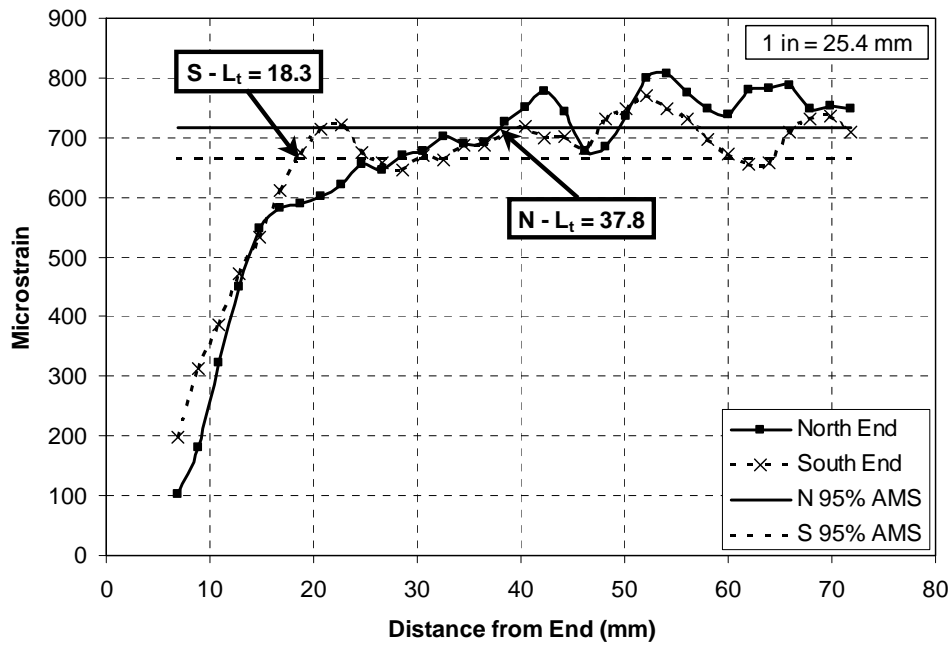
Figure C.4: Strain Profiles for LW6000-1

137
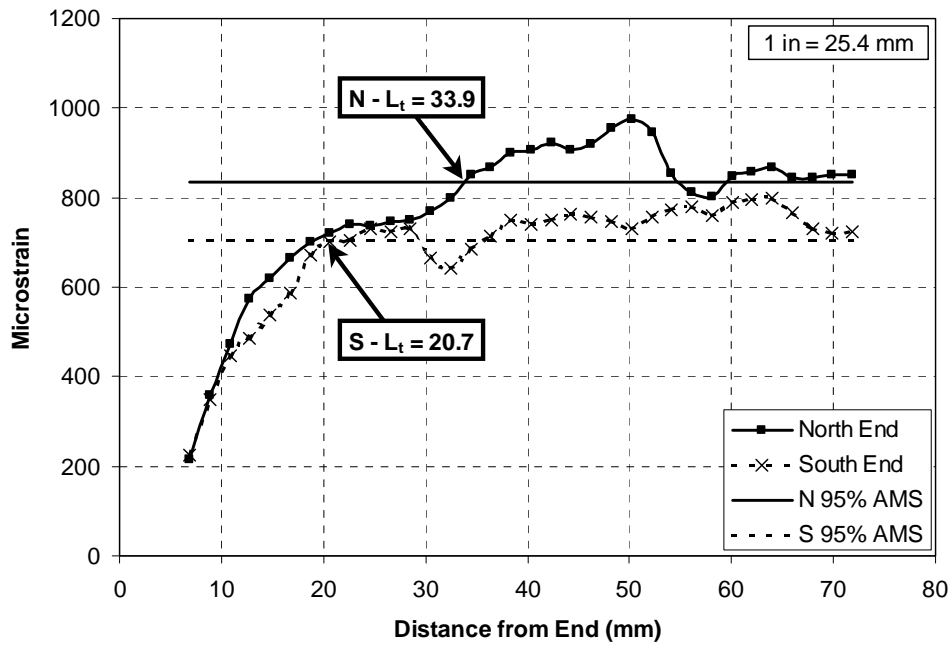
Figure C.5: Strain Profiles for LW6000-2
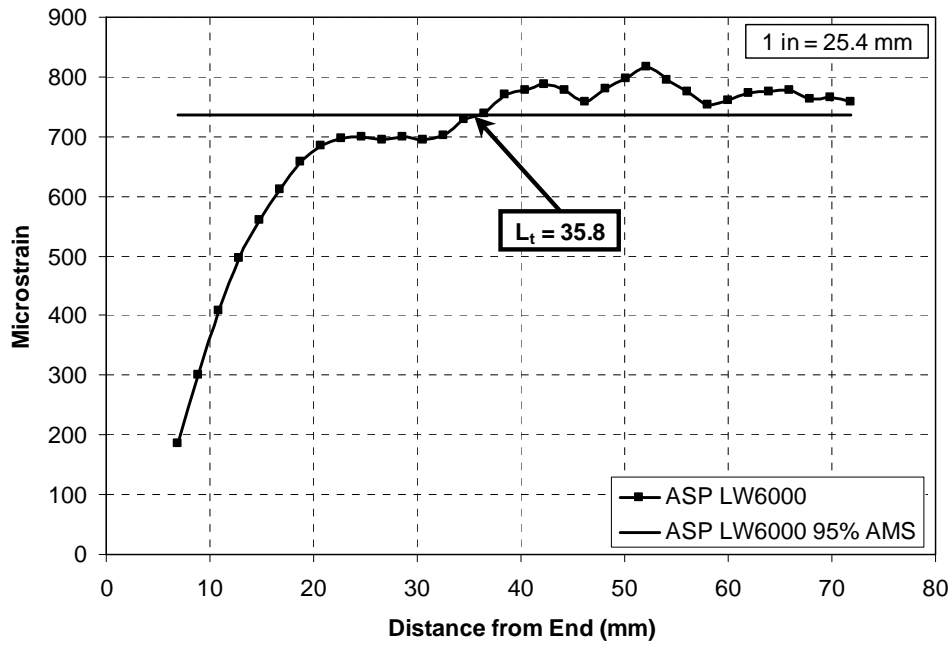
Figure C.6: Average Strain Profile for LW6000

138
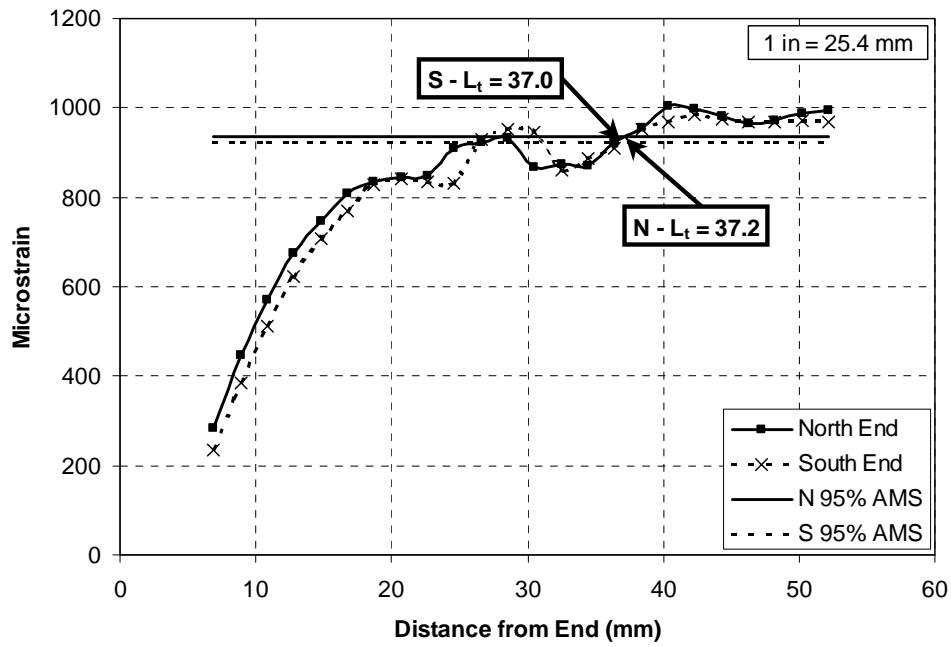
Figure C.7: Strain Profiles for LW8000-20
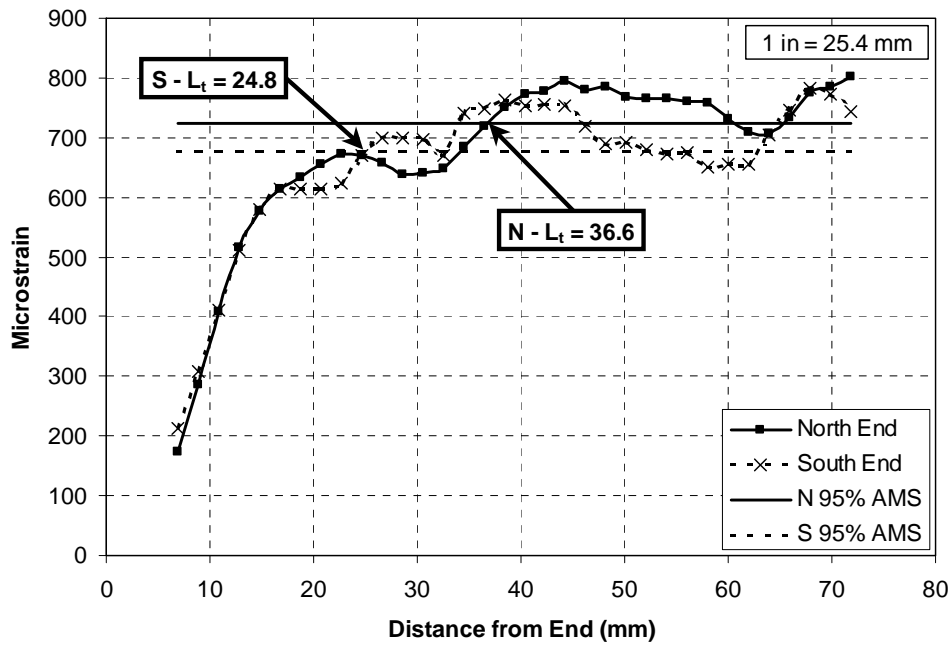
Figure C.8: Strain Profiles for LW8000-1

139
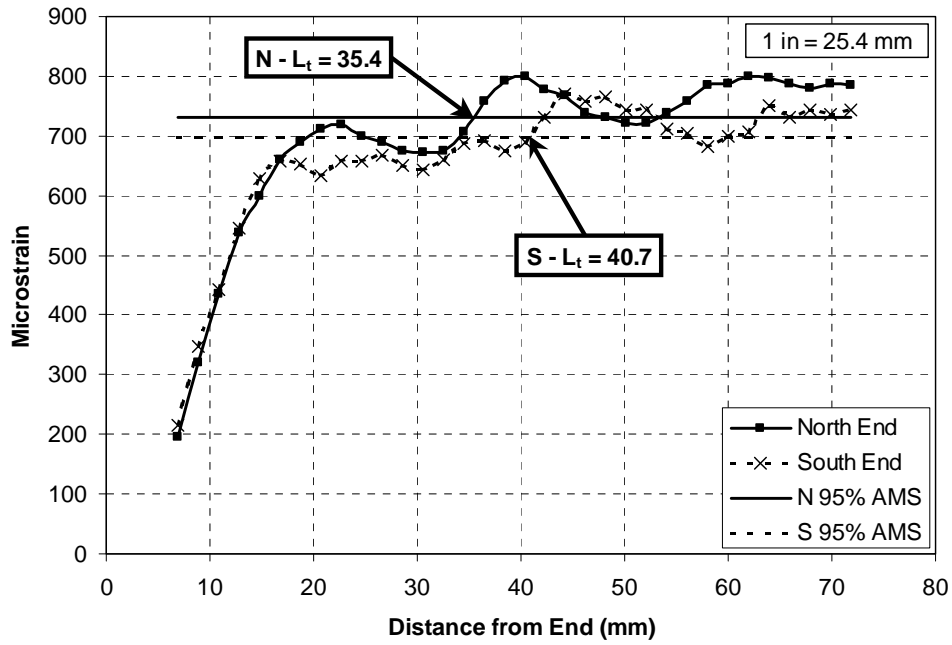
Figure C.9: Strain Profiles for LW8000-2
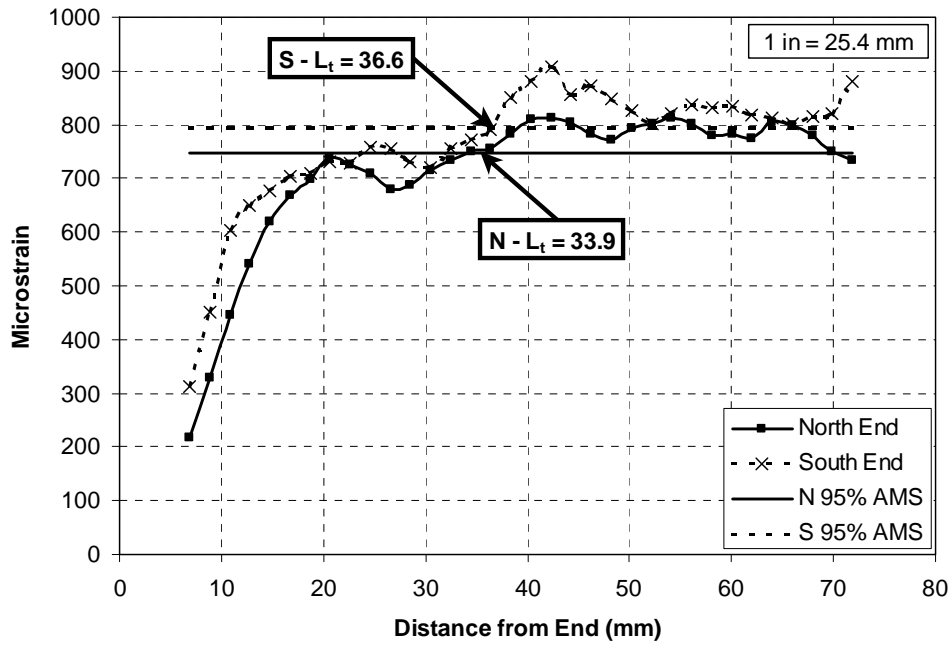
Figure C.10: Strain Profiles for LW8000-3

140
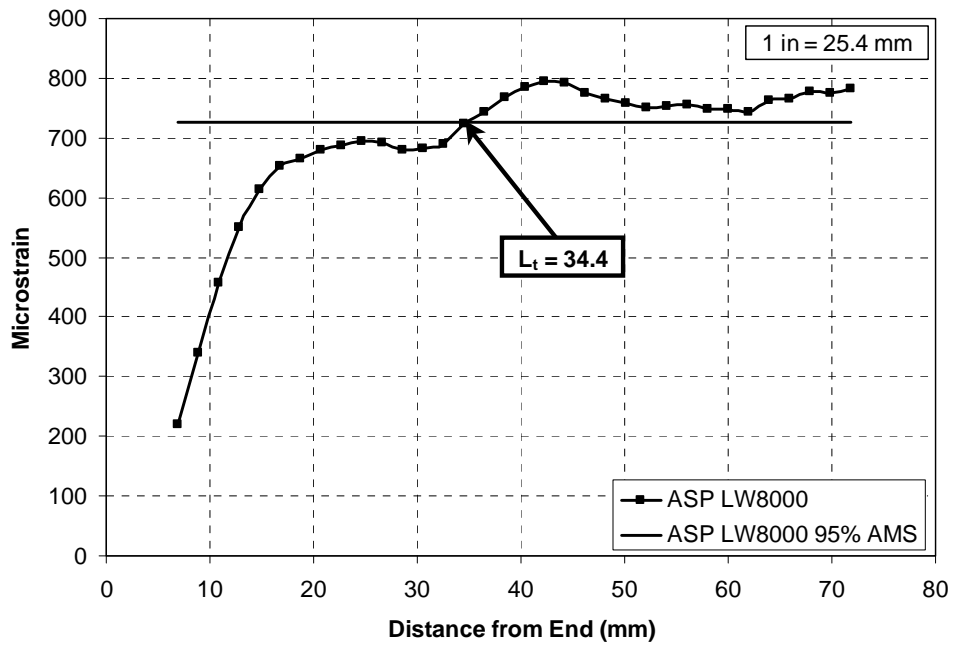
Figure C.11: Average Strain Profile for LW8000

Appendix D: Load vs. Deflection Charts
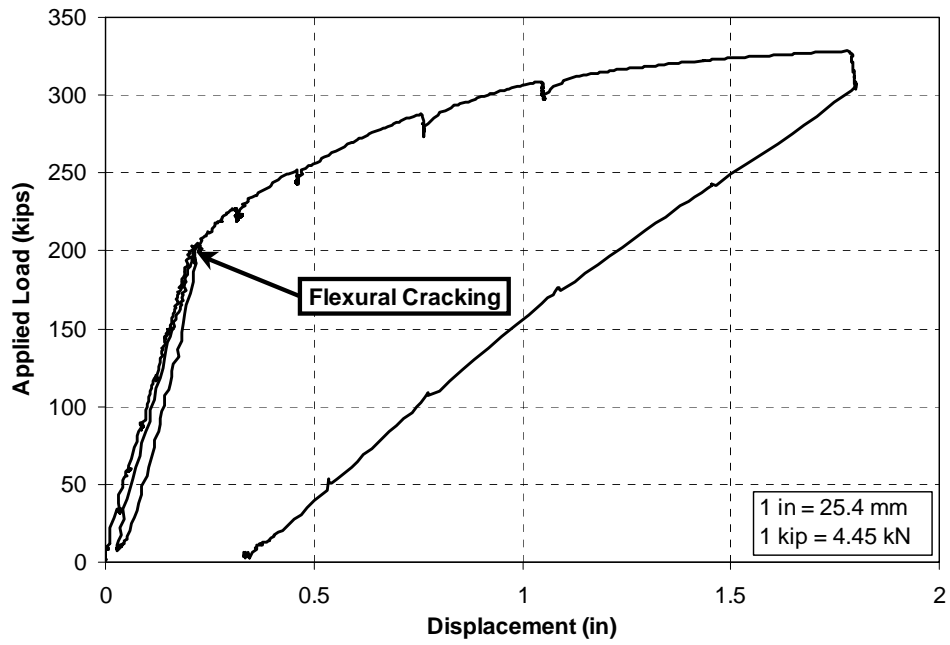
Figure D.1: Load vs. Deflection for NW6000-1-N-80
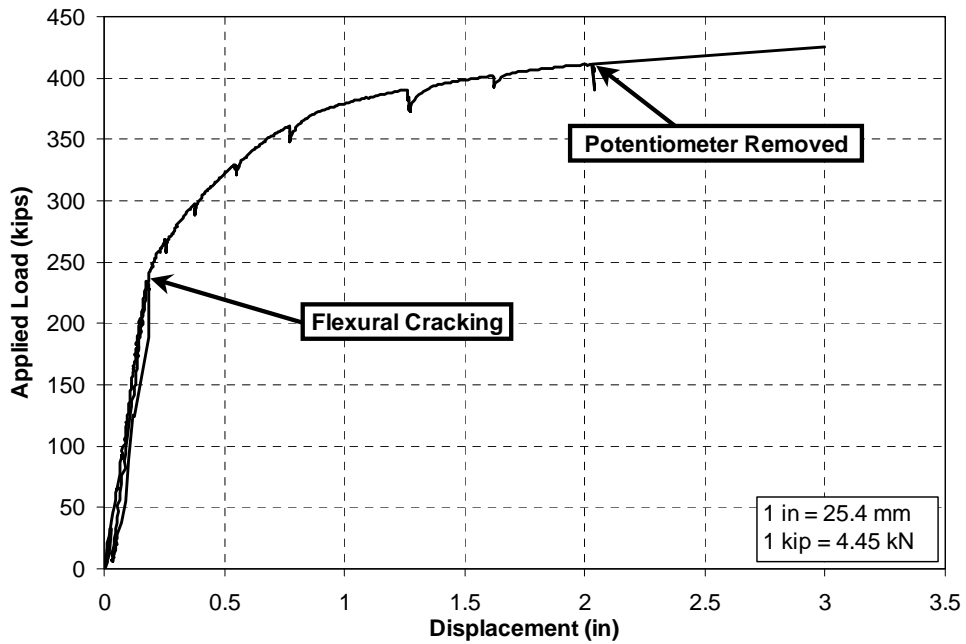
Figure D.2: Load vs. Deflection for NW6000-1-S-60

143
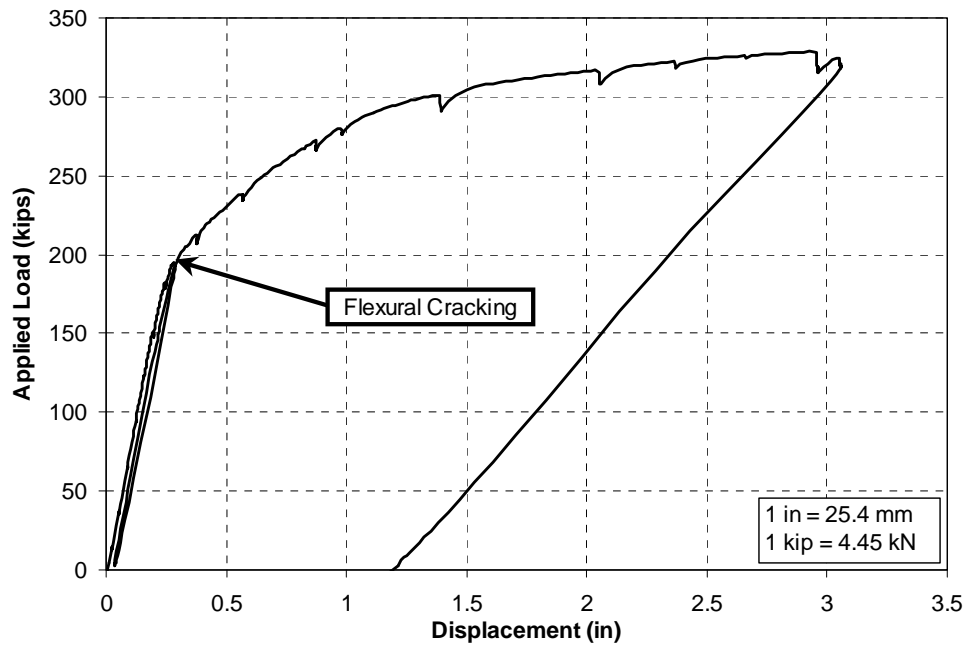
Figure D.3: Load vs. Deflection for LW6000-1-N-80
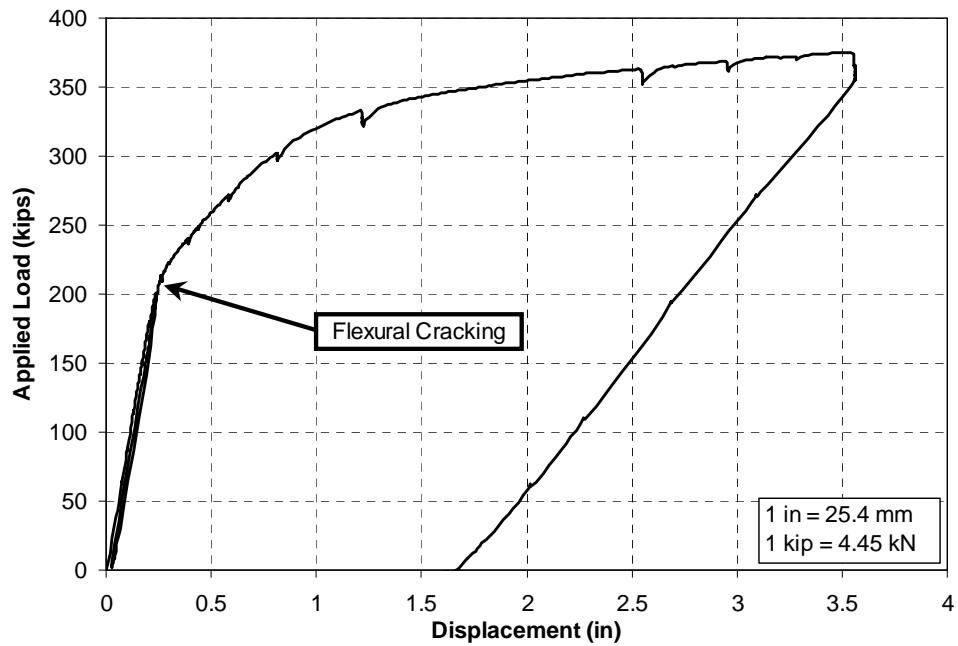
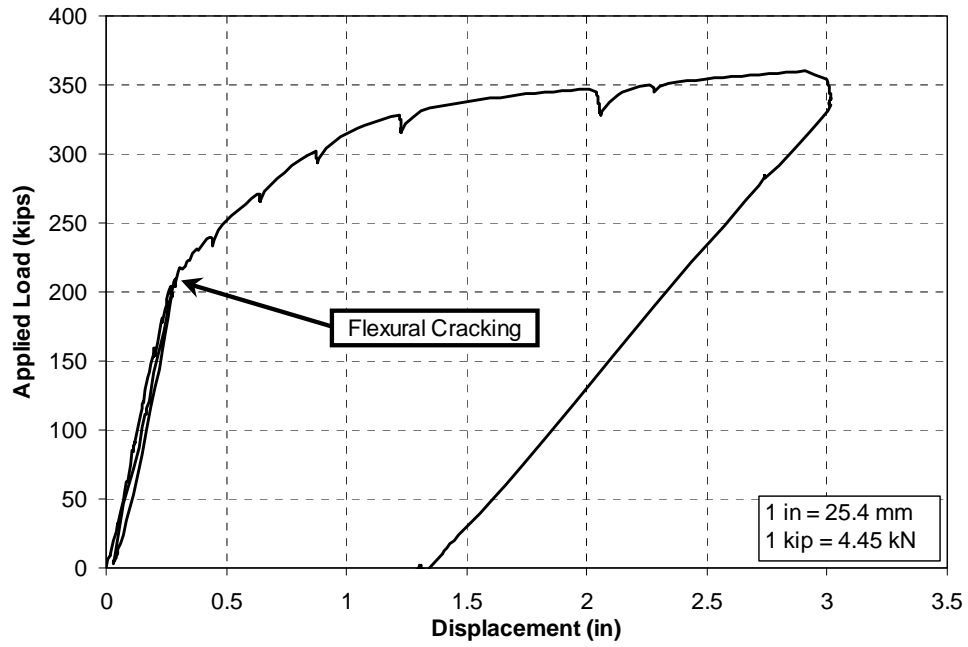**Figure D.4: Load vs. Deflection for LW6000-1-S-70**

144

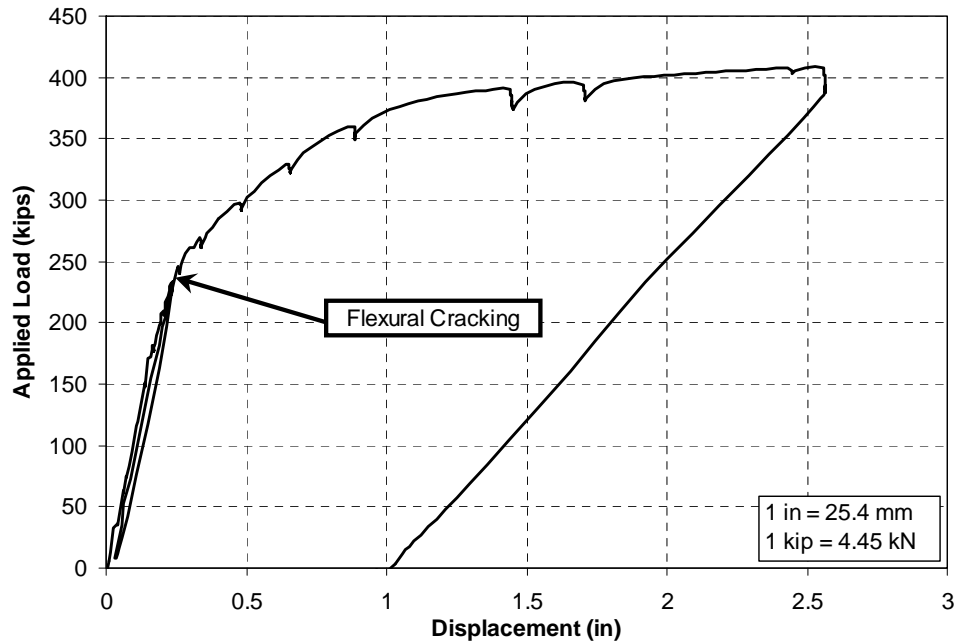**Figure D.5: Load vs. Deflection for LW6000-2-N-70**

Figure D.6: Load vs. Deflection for LW6000-2-S-60

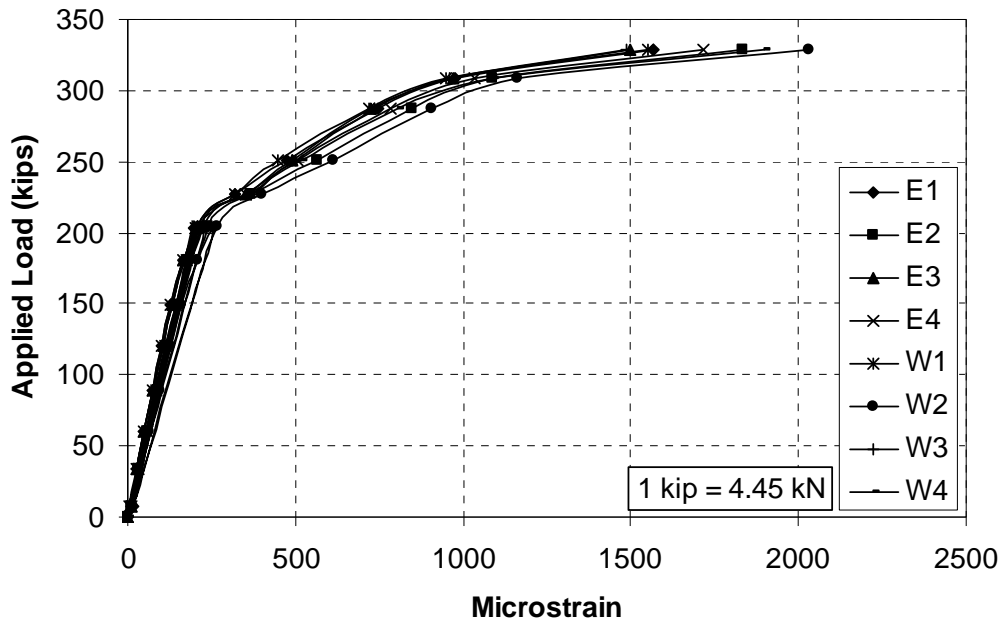**Appendix E: Strain Gauge Data from Deck**

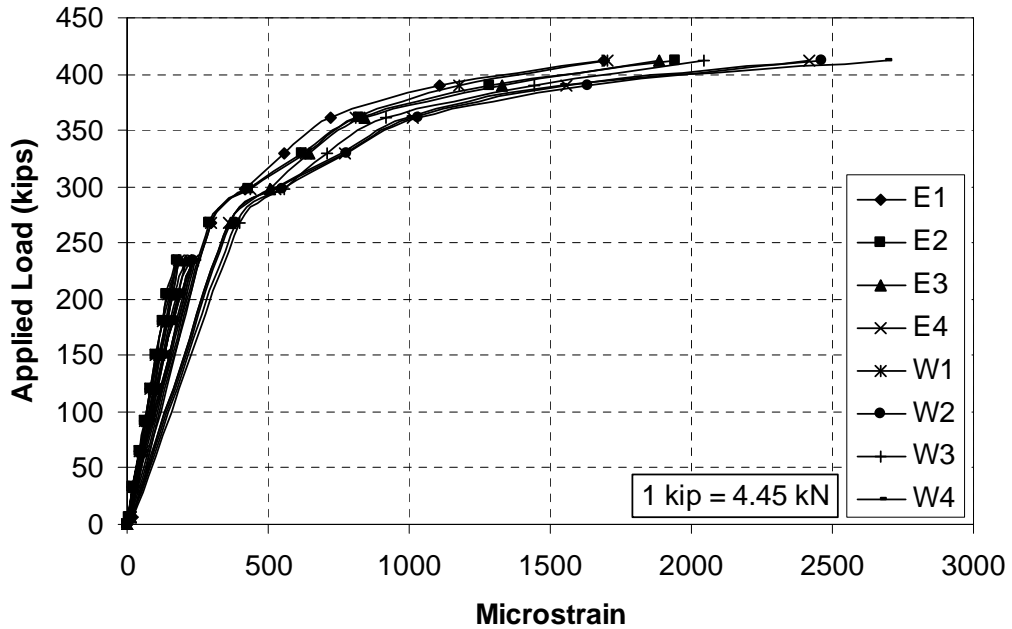**Figure E.1: Microstrain vs. Applied Load for NW6000-1-N-80**

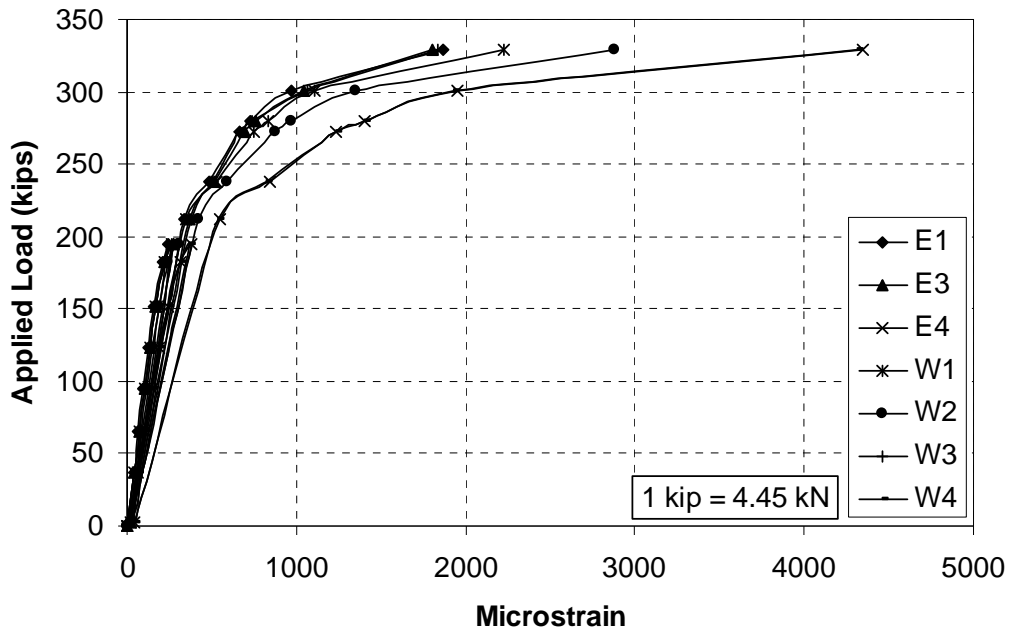**Figure E.2: Microstrain vs. Applied Load for NW6000-1-S-70**

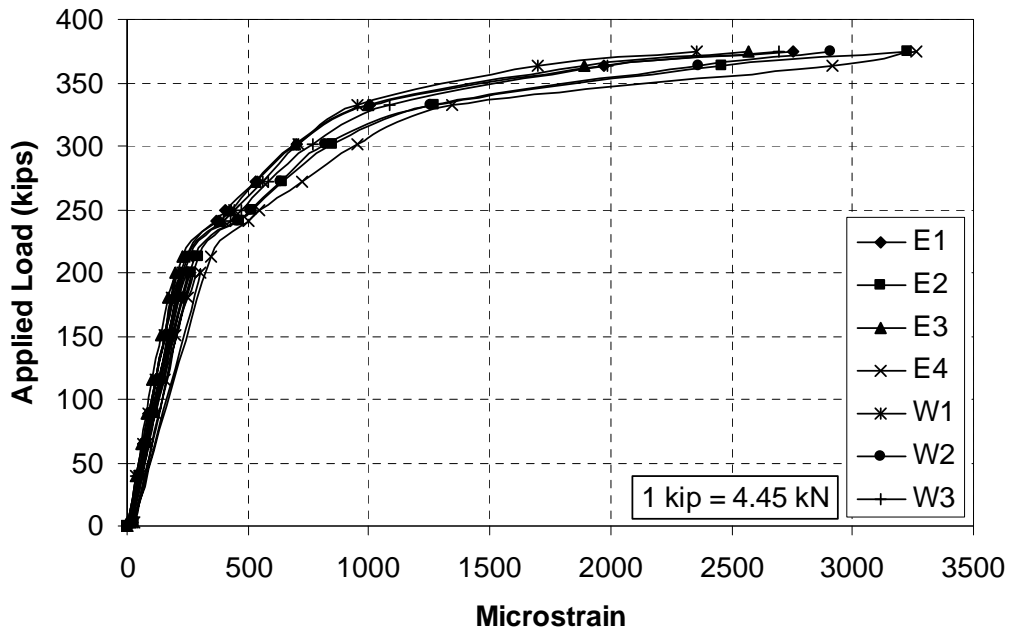**Figure E.3: Microstrain vs. Applied Load for LW6000-1-N-80**

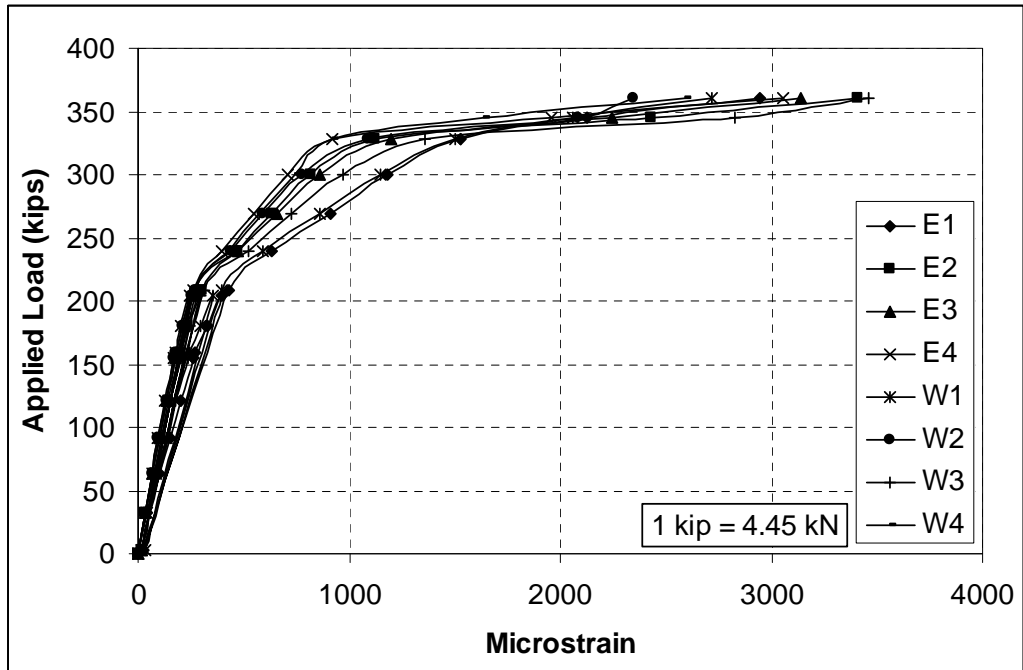**Figure E.4: Microstrain vs. Applied Load for LW6000-1-S-70**

148

Figure E.5: Microstrain vs. Applied Load for LW6000-2-N-70
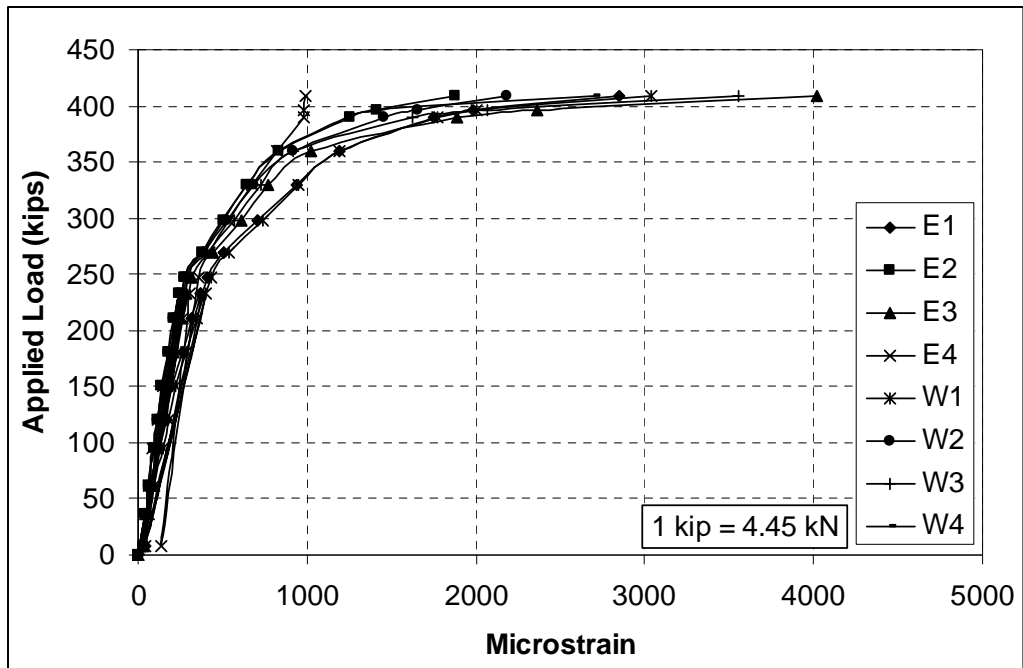

Figure E.6: Microstrain vs. Applied Load for LW6000-2-S-60

149

References

1. AASHTO. 1998. *AASHTO LRFD bridge design specifications: Customary U.S. units*. 2nd ed., Washington, D.C.: American Association of State highway and Transportation Officials (AASHTO).

2. ACI Committee 318. 1999. *Building code requirements for structural concrete (318-99) and commentary (318R-99)*. Farmington Hills, Michigan: American Concrete Institute (ACI).

3. Ahmad, S. H., and Barker, R. 1991. Flexural behavior of reinforced high-strength lightweight concrete beams. *ACI Structural Journal* Jan.-Feb.: 69-77.

4. Ahmad, S. H., and Batts, J. 1991. Flexural behavior of doubly reinforced high-strength lightweight concrete beams with web reinforcement. *ACI Structural Journal* May-June: 351-358.

5. Ahmad, S. H., Xie, Y., and Yu, T. 1995. Shear ductility of reinforced lightweight concrete beams of normal and high strength concrete. *Cement & Concrete Composites* 17: 147-159.

6. Balazs, G. L. 1993. Transfer lengths of prestressing strand as a function of draw-in and initial prestress. *PCI Journal* 38(2): 86-93.

7. Barnes, R. W. 2000. Development length of 0.6-inch prestressing strand in standard I-shaped pretensioned concrete beams. Dissertation, The University of Texas at Austin.

8. Barnoff, R. M., Orndorff, J. A. Jr., Harbaugh, R. B. Jr., and Rainey, D. E. 1977. Full scale test of prestressed bridge with precast deck planks. *PCI Journal* Sept.-Oct.: 66-82.

9. Base, G. D. 1958. Some tests on the effect of time on Transmission length in pretensioned concrete. *Magazine of Concrete Research* 9(26): 73-82.

10. Bieschke, L. A., and Klingner, R. E. 1982. The effect of transverse strand extensions on the behavior of precast pretensioned panel bridges. Research Report 303-1F. Austin: Center for Transportation Research, The University of Texas at Austin..

11. Breen, J. E. 1999. Class Notes for CE 383S: Structural Concrete Bridges. The University of Texas at Austin.

12. Bridges, C. P., and Fish, R. C. 1996. Design of structural lightweight concrete for the Folsom Bridge. Caltrans: International Symposium on Lightweight Concrete Bridges.

13. Buckner, C. D. 1994. *An Analysis of Transfer and Development Lengths for Pretensioned Concrete Structures.* Report No. FHWA-RD-94-049. McLean, Virginia: Federal Highway Administration.

14. Buckner, C. D. 1995. A review of strand development length for pretensioned concrete members. *PCI Journal* 40(2): 84-99.

15. Collins, M. P., and Mitchell, D. 1991. *Prestressed concrete structures*. Englewood Cliffs, NJ: Prentice-Hall, Inc.

16. Dokken, R. A. 1996. Napa River Bridge: 20 years later. CalTrans: International Symposium on Lightweight Concrete Bridges.

17. Fang, I.-K., Worley, J. A., Burns, N. H., and Klingner, R. E.1986. Behavior of Ontario-type bridge decks on steel girders. Research Report 350-1. Austin: Center for Transportation Research, The University of Texas at Austin.

18. Federal Highway Administration (FHWA). 1985. Criteria for designing lightweight concrete bridges. Report No. FHWA/RD-85/045. T.Y. Lin International.

19. FIP Report on Prestressing Steel 2. 1978. Anchorage and application of 7-wire strands. FIP 5/4. London

20. Guyon, Y. 1953. *Prestressed concrete*. New York, NY: John Wiley and Sons.

21. Hanson, N. W., and Kaar, P. H. 1959. Flexural bond tests of pretensioned prestressed beams. *ACI Journal, Proceedings* 55(7): 783-802.

22. Heffington, J. A. 2000. Development of High Performance Lightweight Concrete Mixes for Prestressed Bridge Girders. Thesis, The University of Texas at Austin.

23. Hoyer, E., and Friedrich, E. 1939. Beitrag zur frage der haftspannung in eisenbetonbauteilen (Contribution to the question of bond stress in reinforced concrete elements). *Beton und Eisen* 38 (March 20).

24. Imbsen, R. A., and Tracy, T. G. 1996. Lightweight concrete design study for the Alameda Street Viaduct. Caltrans: International Symposium on Lightweight Concrete Bridges.

25. Janney, J. R. 1963. Report of stress transfer length studies on 270k prestressing strand. *PCI Journal, Proceedings* 8(1): 41-45.

26. Jobson, H. L. 1997. Transfer and development length of fully bonded 15.2 mm (0.6 in) diameter prestressing strand in standard AASHTO Type I concrete beams. Thesis, The University of Texas at Austin.

27. Kaar, P. H., LaFraugh, R. W., and Mass, M. A.1963. Influence of concrete strength on strand transfer length. *PCI Journal* 8(5): 47-67.

28. Khaloo, A. R., and Kim, N. 1999. Effect of curing condition on strength and elastic modulus of lightweight high-strength concrete," *ACI Materials Journal* July-Aug: 485-490.

29. Kowalsky, M. J., Priestly, N. M.J., Seible, F. 1996. Shear, flexural and dynamic behavior of lightweight concrete bridge systems. Caltrans: International Symposium on Lightweight Concrete Bridges.

30. Lin, T. Y., and Burns, N. H. 1981. *Design of prestressed concrete structures*. Third Edition, New York, NY: John Wiley & Sons.

31. Manzanarez, R. 1996. The new Benicia-Martinez bridge project: A lightweight concrete segmental structure. Caltrans: International Symposium on Lightweight Concrete Bridges.

32. Martin, L. D., and Normal L. S. 1976. Development of prestressing strand in pretensioned members. *ACI Journal, Proceedings* 73(8): 453-456.

33. Mitchell, D., Cook, W. D., Khan, A. A., and Tham, T. 1993. Influence of high strength concrete on transfer and development length of prestressing strand. *PCI Journal* 38(3): 52-66.

34. Mor, A. 1992. Steel-concrete bond in high-strength lightweight concrete. *ACI Materials Journal* Jan.-Feb: 76-82.

35. Nilson, A. H. 1978. *Design of prestressed concrete*. 2nd Edition, New York, NY: John Wiley & Sons.

36. PCI. 1999. *PCI design handbook: precast and pretensioned concrete*. 5th ed., Chicago: Precast/Prestressed Concrete Institute.

37. Price, B. 1994. BP invests heavily in lightweight concrete for North Sea. Concrete 28(6): 9-13.

38. Russel, B. W., and Burns, N. H. 1993. Design guidelines for transfer, development and debonding of large diameter seven wire strands in pretensioned concrete girders. Research Report 1210-5F. Austin: Center for Transportation Research, The University of Texas at Austin.

39. Russell, B. W., and Burns, N. H. 1996. Measured transfer lengths of 0.5 and 0.6 in. strands in pretensioned concrete. *PCI Journal* 41(5): 44-65.

40. Shahawy, M. A., Isa, M., and Batchelor, B. 1992. Strand transfer lengths in full-scale AASHTO prestressed concrete girders. *PCI Journal* 37(3): 84-96.

41. Swamy, R. N., and Ibrahim, A. B. 1975. Flexural behavior of reinforced and prestressed Solite structural lightweight concrete beams. *Building Science* 10: 43-56.

42. Thorkildsen, E., Kowalsky, M., Priestly, N. M.J. 1996. Use of lightweight concrete in seismic design of California bridges. Caltrans: International Symposium on Lightweight Concrete Bridges.

43. Ujil, J. A. 1983. Tensile stresses in the transmission zones of hollow-core slabs prestressed with pretensioned strands. Report No. 5-83-10. Delft: Delft University of Technology.

44. Yang, Y. C., Holm, T. A. 1996. A 1996 perspective on the 1985 FHWA/T.Y. Lin report 'Criteria for designing lightweight concrete bridges. CalTrans: International Symposium on Lightweight Concrete Bridges.

45. Zia, P., Preston, H. K., Scott, N. E., and Workman, E. B. 1979. Estimating prestress losses. *Concrete International* June: 32-38.

46. Zia, P. and Mostafa, T. 1997. Development length of prestressing strands. *PCI Journal* 22(5): 54-65.

47. Zia, P. 1998. A feasibility study of high-strength lightweight concrete for highway bridge applications. Report of North Carolina State University Study, American Concrete Institute Convention Paper. Houston, Texas, March 24, 1998.

Vita

Robert Thomas Kolozs was born and has accomplished many things since this time, the latest of which happens to be this thesis.

Permanent address: 26812 Ave. Domingo
                      Mission Viejo, CA 92691

This thesis was typed by the author.